UNIVERSITY OF OKLAHOMA

GRADUATE COLLEGE

INCORPORATING GRILLAGE MODEL DERIVED LOAD DISTRIBUTION FACTORS INTO RATINGS OF PRESTRESSED CONCRETE BRIDGES

A THESIS

SUBMITTED TO THE GRADUATE FACULTY

in partial fulfillment of the requirements for the

Degree of

MASTER OF SCIENCE

By

AFNAN ALI
Norman, Oklahoma
2018

INCORPORATING GRILLAGE MODEL DERIVED LOAD DISTRIBUTION FACTORS INTO RATINGS OF PRESTRESSED CONCRETE BRIDGES

A THESIS APPROVED FOR THE
SCHOOL OF CIVIL ENGINEERING AND ENVIRONMENTAL SCIENCE

BY

_____
Dr. Royce W. Floyd, Chair

_____
Dr. Jeffery S. Volz

_____
Dr. P. Scott Harvey, Jr.

Dedicated to my parents and to all the incredible teachers.

Acknowledgements

Unfortunately, on the title page there could be only one name but there are people and organizations who contributed to make this work possible directly or indirectly. To start with I would like to mention my mom and dad for making the biggest sacrifice by letting me fly away about 8,200 miles away from home. I would like to thank my advisor, Dr. Floyd, I think of him more as a mentor. He is definitely the humblest and most supportive professor I came across in America and Pakistan. I would also thank my committee members Dr. Jeff Volz and Dr. Scott Harvey, for providing their critical review on my thesis. I would also like to mention Dr. Cameron Murray for providing assistance with modeling and for sharing his work. The Oklahoma Department for Transportation made this study possible by contributing financially. I would also thank Shakeel Ahmed and Jason Martwig for giving me the opportunity to intern at their office in the bridge engineering department which helped me with the critical thinking required to complete this thesis. Finally, my friends, Trevor Looney and Trupti Chaure for providing their support during my studies. I would also mention Connor Casey who taught me laboratory work.

Table of Contents

List of Tables

List of Figures

Abstract

Characterization and evaluation of bridges is a laborious task. A large number of bridges in Oklahoma are potentially deficient for shear due to differences between the current codes and those used to design the bridges. A robust method is needed to evaluate the sufficiency of these bridges. One potential consideration for accurate evaluation of bridges is consideration of composite behaviour and resulting load distribution. Load distribution among the girders of a bridge's superstructure is dependent on many parameters such as girder spacing, material properties, skew angle, stiffening lateral elements (diaphragms), etc. The American Association of State Highway and Transportation Officials (AASHTO) LRFD Bridge Design Specifications contain load distribution factor equations for most of the common bridge types. The methods presented in AASHTO are simple, empirical, conservative, and intended to be applicable for a large sample of bridges. The work presented in this thesis is part of on-going work on the shear behavior of prestressed concrete girder bridges and focuses on how to accurately model transverse load distribution relationships and determine accurate load distribution factors for use in bridge design and load rating. The analysis is primarily based on the 2D grillage modeling method using finite element analysis. Different configurations of superstructures are examined by varying parameters such as girder type, span length, deck thickness, girder spacing, and presence of diaphragms to determine the parameters most affecting load distribution. Results from this study are also compared to a 3D finite element plate model for specific cases to evaluate whether a 2D model sufficiently captures bridge behavior for taller girder sections. It was observed that girder spacing has the largest impact on the load distribution factor among

all the parameters considers in this study. The impact of diaphragms was more evident in plate models, particularly, when the girder spacings were larger. It was found that AASHTO LRFD equations produce values for shear load distribution factor at least 1.9% to 22.5% larger than those from grillage models.

Chapter 1: Introduction

1.1: Background

The health of bridge infrastructure in the United States is deteriorating as indicated by the ASCE Infrastructure Report Card C+ bridge rating and 9.1% of the nation's bridges rated as structurally deficient. There are 188 million rides on these deficient bridges each day. Specifically, for Oklahoma, the grade is D+ with 15% of the state's bridges rated structurally deficient (Infrastructure Report Card, 2017). Additionally, many bridges with current acceptable ratings are nearing the end of their design lives. The average age of bridges in the United States is 43 years and 55% of bridges are older than 40 years (Infrastructure Report Card, 2017). In 1998 the typical bridge design life was increased to 75 years from a previous value of 50 years, meaning that more than half of the in-service bridges in the United States will be at the end of their design life in the next 10 years. Replacing the deficient bridges and those at the end of their design life is a very expensive and demanding operation.

In addition to the effects of aging, the design loads used in the past were smaller compared to the current HL-93 loading used in the latest edition of the AASHTO LRFD Bridge Design Specifications (afterwards referred to as AASHTO LRFD), and the calculation of shear demand was different than what is used currently (AASHTO, 2014). In some cases, ratings of older bridges may indicate deficiencies related to shear and potentially require load posting or replacement. It is important to have an accurate understanding of both the capacity and demand for older bridges to produce the most accurate rating possible.

Load rating methods typically use load distribution factor from AASHTO LRFD for calculating shear demand, which are based on girder spacing for AASHTO I-Girders. A

previous study at the University of Oklahoma by Dr. Cameron Murray focused on AASHTO Type-II girders (Murray, 2017). A scale bridge was tested to failure and the experimental results were used to verify the accuracy of a 2D finite element based grillage modeling procedure. The model was then used to examine additional variables and all results were compared to AASHTO load distribution factors. Diaphragms provided an important contribution to the failure mechanism of the scale bridge tested by Murray, but had limited effect on the distribution factors determined using the grillage models. Girder spacing had the greatest effect on the difference between grillage model derived distribution factors and those from the AASHTO LRFD specifications (Murray, 2017). However, Murray's work only considered one girder type and relatively short span bridges.

1.2: Overview of Research Conducted

The parametric study described in this thesis involved examination of factors which may influence the load distribution factors for girder types other than AASHTO Type-II girders, as well as to further examine a simplified method of modelling to determine accurate load distribution factors. This study expanded on the previous work for AASHTO Type-II girders by examining Type-III and Type-IV I-beams and BT-63 and BT-72 bulb tee sections. All of these girder types except BT-63 are currently used by the Oklahoma Department of Transportation (ODOT). Additionally, 3D finite element based plate models were developed to examine torsional effects, which may not be captured effectively using 2D grillage models.

1.3: Objectives and Anticipated Results

This parametric study is the extension of work done by Dr. Cameron Murray related to shear load distribution in precast, prestressed concrete girder bridges (Murray, 2017). In his study the results from a scaled bridge superstructure tested in the lab were compared with 2D grillage model results, and several variables with potential to affect shear load distribution were examined for AASHTO Type-II girder bridges using the model. This current study examined the same variables for additional AASHTO girder types and examined effects of using a 3D plate model instead of a 2D grillage model on the results. The objectives of the study were to:

1. Determine the effects of girder type, span length, presence of diaphragms, deck thickness and girder spacing on the shear load distribution factors for AASHTO Type II, Type III, and Type IV I-girders, and AASHTO/PCI BT-63 and BT-72 bulb tees.
2. Develop relatively simple modeling procedures to provide accurate distribution factors for load rating of bridges constructed with these girder types.
3. Compare load distribution factors determined from 2D grillage models with the 3D plate models for selected cases.
4. Identify and utilize the conservatism available in the AASHTO LRFD equations when load rating a bridge so that the capacity of the bridge is compared with as accurate an estimate of the applied loads as possible.

The results obtained from this study are expected to show that the relatively simple grillage models can be used to produce accurate load distribution factors for all girder types. The study will also result in a detailed procedure for creating and utilizing the

grillage models for load distribution analysis along with guidance for identifying important variables to consider for each girder type.

Chapter 2: Literature Review

2.1: History of Prestressed Concrete

Prestressed concrete has been around since the late 19th century, when an engineer from California, P. H. Jackson, patented a system that used a tie rod to construct beams and arches from individual blocks. Early attempts to use prestressed concrete were not successful because of low residual stresses; high strength steel was needed. Prestressed concrete continued to develop in Europe, particularly through the inventiveness of Eugene Freyssinet, who proposed methods to overcome prestress losses using high strength and ductile steel. Prestressed concrete was first widely used during World War II and thereafter to rebuild the infrastructure of Europe (Nawy, 2003). Today, prestressed concrete is widely use around the world for a number of applications.

2.2: Introduction to Prestressed Concrete

Concrete is strong in compression and weak in tension. The tensile capacity of concrete is between 8 and 14 percent of the compressive strength (Nawy, 2003) which leads to flexural cracks in concrete at early stages of loading. In order to prevent the cracking of concrete, a concentric or eccentric prestressing force in the longitudinal direction of the beam is applied to counter tensile stresses from bending. The initial prestressing force applied to the concrete reduces over time due to the effects of elastic shortening, concrete creep, concrete shrinkage, and steel relaxation. There are limitations on what stresses can be applied to a concrete beam from the prestress force, and to control these stresses

prestressing strands are often harped, draped, or debonded. All of these items must be considered when designing the beam section and when determining shear capacity.

2.3: Response of Prestressed Beam in Shear

Prestressed concrete beams under shear loads behave differently than reinforced concrete beams due to the presence of the prestress force. Similar to reinforced concrete beam behavior, applied shear stresses cause principal tensile stresses at critical locations which can exceed the tensile strength of concrete. The stress that causes cracking and the angle of the resulting shear cracks differ from a reinforced concrete beam due to the compressive stresses resulting from the prestress force. In both the reinforced and prestressed cases, shear failures occur without warning and the diagonal cracks developed are much wider than flexural cracks. This section examines previous work to better understand the behavior of prestressed concrete in shear. The crack patterns can be used to determine the path of shear flow and subsequently classifying beams according to their cracking patterns. The crack patterns are used to classify the mode of failures. Beam and loading configurations control the type of shear failure. These failures have been described by Sozen et al. (1959) in his experimental study for prestressed concrete. In one of the recent study by Naji et al. (2016), the modes of failure are classified on the basis of bond failure and these failure types are summarized in the following sections.

2.3.1: Bond Shear Failure

Bond shear failure is the most common type of failure observed in bond loss failures. This type of failure commonly occurs when the span to depth ratio is less than 3. In this failure mode the inclined cracks start from the bottom flange and web close to the

support. The anchorage of the prestressing strand is affected by these cracks which results in loss of concrete-strand bond and strand slippage (Naji et al., 2016).

2.3.2: Bond Flexure Failure

Girders with bond flexure failure exhibit linear-elastic behavior until cracking is initiated. Cracking may not cause the slippage of strands but after cracking the moment of inertia of the girder reduces and subsequently strand slippage occurs. Slippage of strand occurs when a crack passes through the strand near the support. Cracks are further widened due to slip of strands which leads to crushing of the girder flange. This type of failure occurs when span to depth was greater than 2.5 (Naji et al., 2016).

2.3.3: Flexure Bond Failure

In flexure bond failure, small amount of slip occurs and behavior is similar to that of typical flexural failure. Though not technically a shear failure, it can be induced by high shear loadings near the support. This type of failure occurs when span to depth ratio is greater than 2.5 (Naji et al., 2016).

2.3.4: Bond-Shear/Flexure

This bond-shear/flexure failure occurs when the span to depth ratio is equal to or less than 2.5. Failure occurs due to both shear and flexure acting on the girder compression zone. This kind of failure initiates with the start of flexure and/or shear cracking which leads to bond loss (Naji et al. 2016).

2.4: 2D Grillage Modeling

Most of the modern day small to medium span bridges are constructed using a beam-and-slab structural system. The majority of beam-and-slab bridges have many beams spanning longitudinally between abutments or bents with a relatively thin slab cast over all of the

beams. Transverse beams, called diaphragms, are used to connect the longitudinal members in the transverse direction. For longitudinal bending, the slab acts as a top flange of the beams. In the transverse direction, the slab acts as a one-way slab to transfer forces to the beams. This kind of superstructure can be effectively modelled as a two-dimensional structure using an equivalent grillage model. It is important to predict the load distribution accurately so that the bridges are designed for the load that will be applied and same is true with load rating of bridges. The grillage model breaks the bridge into a series of longitudinal members (beams) and transverse members (sections of slab and diaphragms) for analysis.

According to Hambly (1991), the stiffness of the slab is very low compared to the stiffness of beams, so the slab bends with higher curvature transversely than longitudinally. Most of the concrete I-beams in these bridges have much less torsional stiffness than bending stiffness, so the design of these bridges can be safely simplified by ignoring the effects of the torsion on the beams due to slab bending. However, a grillage model can be configured to include the effects of torsional stiffness. When the superstructure is analyzed with a torsionless grillage model, the bending moments in the beams are found to be slightly higher than when including the effects of torsion. Torsional effects cannot be safely ignored if the beam has higher torsional stiffness such as a box beam (Hambly, 1991).

2.5: Past Analytical Studies on Load Distribution

2.5.1: Background on the Development of Load Distribution Equations in AASHTO 1994 Edition

In 1994, introduction of the AASHTO-LRFD bridge design specifications brought a major change from the method used to determine load distribution in the AASHTO Load Factor Design (LFD) Standard Specifications (Zokaie, 2000), which had been in place for more than 50 years at that time. This change resulted from the NCHRP 12-26 project entitled "Distribution of Live Load on Highway Bridges" started in 1985 (Zokaie and Imbsen, 1992). AASHTO LFD formulas were based on S/D in which "S" is the spacing of the girders and "D" is a factor dependent on the bridge type. These S/D formulas were valid for typical bridges with girder spacing near 6 ft and span length of near 60 ft.

In the NCHRP 12-26 project a large sample of data was taken from National Bridge Inventory File. Information included all the details of the bridge configurations. Different parameters were compared with one another and any correlation was determined. An example of one case stated was that the deck thickness is related to girder spacing: if higher girder spacing is provided then deck thickness will be larger. A new parameter, K_g which is dependent on the moment of inertia, cross-sectional area and eccentricity of composite beams, was introduced to represent the longitudinal stiffness of the bridge and to reduce the number of parameters. Bridges having difference sectional properties, but similar K_g, were analyzed using plate elements for the deck slab to capture the effect of eccentricity. The final distribution factors were not affected by the change in properties if the longitudinal stiffness was similar. Equations were given to provide for wider range of applicability, and which produced results within 5% of detailed analyses. The models

that were used to develop the formulas had uniform spacing, girder moment of inertia, and skew. Continuous bridge models had equal spans and effects of diaphragms were not included in the models (Zokaie, 2000).

If the bridge is beyond the range of applicability of the developed equations, as mentioned in Zokaie et al. (2000), then a more detailed analysis may be required. Load distribution for the exterior girders was found to be most sensitive to the distance between the exterior girder and the truck load on the overhanging part of the deck. The shear force at the obtuse corner of a skewed bridge was found to be greater when compared to a non-skewed bridge of same size (Zokaie, 2000).

2.5.2: Comparison of Finite Element Models with AASHTO 1998 Edition

In another study by Barr et al. (2001), twenty-four different variations of 3D finite element (FE) models were developed for bridge superstructures to compare load distribution factors from models and three codes (AASHTO LRFD 1998, AASHTO Standard Specification 1996, and Ontario Bridge Highway Design Code 1992). The finite element models were developed to investigate the effects of lifts (haunches), intermediate diaphragms, end diaphragms, continuity, skew angle, and load type. The effects of haunches, intermediate diaphragms, end diaphragms, and continuity were missing from the study used to develop the equations in AASHTO LRFD 1998, but were incorporated in the study by Barr et al. (2001). FE models were developed using SAP2000, with shell elements used for the deck and frame elements for the girders. The addition of haunches was found to reduce the load distribution factor for exterior girders by 17% and by 11% for interior girders. Intermediate diaphragms were found to have negligible effects on load distribution factor. End diaphragms were found to affect the midspan moment for

skewed and non-skewed bridges. If the bridge was skewed, the midspan moment was reduced due to end diaphragms and if present the reduction in rotation of the loaded decreased at the cost of an increase in rotation of the adjacent girders. This behavior was observed when the diaphragms were tortionally stiff. The load distribution factor was found to be inversely proportional to the degree of skew angle for skewed bridges. Based on their results Barr et al. (2001) determined that if the load distribution factors from FE models were used instead of those from AASHTO LRFD, then girder release strength could have been reduced from 7.4 ksi to 6.4 ksi or the bridge could alternatively, have been designed for 39% higher live loads (Barr et al., 2001).

2.5.3: Comparison of Finite Element Models with AASHTO 2004 Edition

A study by Yousif and Hindi (2007) compared load distribution factors calculated using the AASHTO LRFD (AASHTO, 2004), 2D grillage models (frame elements), and 3D FE (shell and frame elements) models. AASHTO LRFD load distribution factors have range of applicability which is defined in terms of span length, slab thickness, girder spacing, and longitudinal stiffness. All AASHTO LRFD prestressed concrete girder sections (Type I-VI) were covered in this study by Yousif and Hindi (2007). The live load used in the analysis was the vehicular live load and lane load as specified by AASHTO LRFD 2004. Studies in the past have shown that load distribution factors from AASHTO LRFD may give either conservative results or unconservative results for specific bridge parameters (Yousif and Hindi, 2007). Therefore, the study covered FE models of different bridge configurations within the limits specified by AASHTO to examine a wide range of variables and improve the applicability of the load distribution factor (Yousif and Hindi, 2007). The torsional constant proposed by Eby et al. (1993) was used for the

girders as it correlated with experimental data with a minor error of ±3%. The torsional constant plays a significant role in the determination of load distribution factor. The 2004 AASHTO LRFD gave load distribution factor in a range with a maximum of approximately 55% more than FE analysis and a minimum 20% less than from the FE model. Yousif and Hindi (2007) observed that the AASHTO LRFD equations seemed to give reasonable results using parameters within the intermediate zone of the applicable range and tended to deviate at the extreme ends of the range. The authors concluded that range of applicability on the load distribution factors should be reconsidered because in some cases the deviation was too conservative and in some cases the deviation was unsafe (Yousif and Hindi, 2007).

2.6: Comparison of 1D, 2D, and 3D Models

Turer and Shahrooz (2011) conducted a study to compare 1D beam element model, 2D grillage and 3D FE models for concrete deck on steel beams. 2D grillage and 3D FE models were developed for the same bridge configuration. Typically, a 1D model is used for analysis and gives quick and conservative results in most cases. Drawbacks that come with 1D beam analysis are oversimplified geometry, weakness in modelling in the transverse direction (i.e. diaphragm, cross bracing), and irregularities such as skew. A 2D model can mitigate the limitations of 1D models because it provides the capability to have elements in the transverse direction such as diaphragms or cross bracing. 3D models are superior to both 2D and 1D models in defining the geometric dimensions, continuity, material properties and support conditions. The 3D models have a high number of elements, usually in the thousands, depending on the size of mesh and take more time for

analysis than 2D and 1D models. Through their study the authors found that 2D models were merely a step behind 3D models in accuracy (Turer and Shahrooz, 2011).

2.7: Load Distribution Factors for Integral Abutment Bridges

The purpose of the study by Dicleli and Erhan (2009) was to give load distribution factor formulas of moment and shear for single-span integral abutment bridges (IABs). IABs have many economical and functional advantages which make them popular in parts of the United States and Europe. However, design standards for IABs are not fully established. Most of the past research on IABs is focused on the performance of IABs under thermal loads. In AASHTO LRFD 2007 the load distribution factor equations for IABs are based on jointed bridges where the superstructure is separated from the abutments through expansion joints, whereas IABs have monolithic construction where the superstructure and the abutment act together. The continuity of the superstructure-abutment system improves the distribution of live load moment among the girders, particularly for short spans. live load distribution factor equations from AASHTO LRFD 2007 do not give good results for IABs according to Dicleli and Erhan (2009).

Dicleli and Erhan performed analyses to better understand load distribution in IABs by developing 2D frame models and 3D FE models for different configurations of span length, number of design lanes, deck thickness, girder size, and girder spacing. Variations in substructure components, specifically abutments, piles, backfill and foundation soil properties were found to have negligible effects on the distribution of live load effects among the girders of IABs. Load distribution factors for girder moments and exterior girder shear of IABs determined using the models were generally smaller than those calculated for simply supported bridges using the AASHTO LRFD 2007 equations.

However, interior girder shear factors from the models were consistent with AASHTO LRFD 2007. Correction equations for AASHTO LRFD 2007 and new equations to calculate live load distribution factors were proposed by the authors (Dicleli and Erhan, 2009).

2.8: Field Test of Concrete Girder Bridges for Live Load Distribution and Continuity

Bridges having a superstructure that behaves as simply supported for dead loads and continuous for live load is common practice among different state departments of transportation (DOTs). This is usually accomplished by having a cast-in-place concrete deck over precast prestressed concrete girders. Bridges tested in the study by Eamon et al. (2016) had simply supported girders with diaphragms cast between the girders and a continuous deck cast above them. At each support of a continuous bridge, negative moment will occur causing tension at the top of the section and compression at the bottom due to continuity. Tension at top will be resisted by deck reinforcement and compression by the diaphragm concrete. However, the degree of continuity achieved in practice is the area of concern relative to determining load distribution. It is unconservative to assume that the support is purely continuous as well as to assume it is entirely uncontinuous. An assumption that the joint is completely uncontinuous will be conservative for positive moment, but will be unconservative for negative moment. Similarly, assuming completely continuous joints will be conservative for negative moment at the support but unconservative for positive moment at the middle of the girder (Eamon et al., 2016).

In the study by Eamon et al. (2016) two bridges in Lansing, MI were load tested in place to evaluate the distribution of moments and shear forces. The resulting load distribution

factors were compared with AASHTO LRFD 2012 load distribution factors. Bridges were loaded per the Michigan DOT criteria and experimental load distribution factors were compared with AASHTO LRFD load distribution factors. It was evident from the results that load distribution factor for positive moment of exterior girders with a single truck in a single lane were very conservative, and that negative moment for an exterior girder with two lanes loaded resulted in unconservative load distribution factors for these bridges (Eamon et al., 2016).

As for the effects of joint continuity, it was concluded that for positive moment a simple span assumption produced a moment 7% higher than observed for the actual structure, whereas maximum positive moment produced by assumption of a purely continuous structure was 16% lower than that of actual structure. For negative moments, the actual structure experienced only 28% of the moment calculated for the full continuous condition (Eamon et al., 2016).

In another study by Cross et al. (2009) focused on continuous bridges, tests on 12 bridges in Illinois were performed to validate the bearing forces calculated using AASHTO LRFD 2008 and AASHTO LFD Standard Specifications 2002. The static, rolling, and dynamic short-term (1 day) tests conducted were targeted at determining experimentally the shear load distribution factor. FE models were developed to compare to the experimental results. Both FE analysis and experimental results showed that in some cases the shear load distribution factor specified by the LFD specifications were exceeded. The results showed that the AASHTO LRFD specifications closely approximated the shear load distribution factor determined by the FE analysis and testing of bridges (Cross et al., 2009).

2.9: Studies on Impact of Diaphragm on Load Distribution

The contribution of diaphragms on the load distribution is controversial especially when the radius of the curvature of the alignment of the bridge is infinity (i.e. a straight bridge). There is inconsistency among different state DOTs regarding the usage of diaphragms. The Texas Department of Transportation (TxDOT) bridge design manual says that intermediate diaphragms are not required for structure performance unless required for erection stability of girder sizes extended beyond their normal span limits (TxDOT, 2015). On the other hand, in Oklahoma Department of Transportation's (ODOT) standard drawings, end and intermediate diaphragms are present, and the Louisiana Department of Transportation and Development (LADOTD), as per their design manual, does not require diaphragms when the span length is less than 50 ft (LADOTD, 2002). Construction of intermediate diaphragms is an extra burden on the schedule and cost of the project. There are benefits described by the Garcia (1999) in his study about intermediate diaphragms, such as that diaphragms help with lateral load transfer, reduce deflection, provide support to girders during construction, and redistribute impact load if an over height truck hits the bottom of girder. However, it is difficult to predict the real stiffness contribution of diaphragms to load distribution due to typically weak connections between the diaphragm and girder (Cai et al., 2007).

2.10: Summary

Most of the past research in the area of lateral load distribution factors has been focused on the distribution of moment. It is observed that the past researchers have confidence in the plate and grillage models which were used in the study described in this thesis. Even in the study by Eamon at el. (2016) which used AASHTO LRFD 6th Ed. (AASHTO,

2012) showed that AASHTO equations are very conservative for some cases and in some cases AASHTO LRFD gives smaller load distribution factors than results from field tests indicate. The load distribution factor equations are the same in AASHTO LRFD 6th Ed. (2012) and AASHTO LRFD 7th Ed. (2014) (the current version). Therefore, a study involving AASHTO I-Girders (which are commonly used by ODOT), shear load distribution, 2D grillage models and comparison with 3D plate models is warranted to ensure safe use of grillage models for the load rating of shear critical bridges in the state of Oklahoma in the future.

Chapter 3: Procedure

The following chapter describes how shear load distribution factors were calculated using AASHTO LRFD 7th Ed. for comparison to the model results (AASHTO, 2014). This chapter explains how the different bridge superstructures considered in this research were modelled using the grillage method and plate model in detail. It also discusses the load cases which would result in the critical load distribution factors.

3.1: Selection of Bridge Configurations

One of the primary objectives of the study was to determine which parameters have the most influence on the load distribution factor for shear. The parameters considered were deck thickness, span length, presence of diaphragms, girder type, and girder spacing. The selection of the different span lengths was dependent on the type of girder. Typical span lengths were chosen from standard bridge drawings available on the Oklahoma Department of Transportation (ODOT) website (ODOT, 2016). In the state of Oklahoma, the most common type of bridge structure, besides culverts, is cast-in-place decks over precast concrete I-girders. The current study focused only on precast concrete I-girder

and bulb-tee girder bridges. The girders selected for the study were Type-III, Type-IV, BT-63 and BT-72. All these girders are used by ODOT except BT-63. ODOT uses Type-IV and BT-72 for longer spans skipping BT-63 in the progression of sizes, but this girder section is used by surrounding states and may be used by ODOT in the future. The deck thicknesses and girder spacing were selected based on the values typically used in the industry. All the ODOT standard bridges include end and midspan diaphragms, but to study the impact of the diaphragm on shear load transfer, the bridge superstructure without diaphragms was also considered in this study. Table 1 summarizes the configurations used for models developed for this study. All the models fall within the range of applicability defined in AASHTO LRFD for the equations of load distribution factors (AASHTO, 2014). For all cases a four girders bridge was considered with a width varying based on the girder spacing.

Table 1. Bridge Grillage Models (deck thickness (in.) on interior of table)

Girder	Spacing (ft)	Length (ft)						
		45		60		75		
Type-III	6	7	9	7	9	7	9	Diaphragm
		7	9	7	9	7	9	No Diaphragm
	9	7	9	7	9	7	9	Diaphragm
		7	9	7	9	7	9	No Diaphragm
	12	7	9	7	9	7	9	Diaphragm
		7	9	7	9	7	9	No Diaphragm
Girder	**Spacing (ft)**	**Length (ft)**						
		75		90		105		
Type-IV	6	7	9	7	9	7	9	Diaphragm
		7	9	7	9	7	9	No Diaphragm
	9	7	9	7	9	7	9	Diaphragm
		7	9	7	9	7	9	No Diaphragm
	12	7	9	7	9	7	9	Diaphragm
		7	9	7	9	7	9	No Diaphragm
Girder	**Spacing (ft)**	**Length (ft)**						
		105		120		135		
BT-63	6	7	9	7	9	7	9	Diaphragm
		7	9	7	9	7	9	No Diaphragm
	9	7	9	7	9	7	9	Diaphragm
		7	9	7	9	7	9	No Diaphragm
	12	7	9	7	9	7	9	Diaphragm
		7	9	7	9	7	9	No Diaphragm
Girder	**Spacing (ft)**	**Length (ft)**						
		120		135		150		
BT-72	6	7	9	7	9	7	9	Diaphragm
		7	9	7	9	7	9	No Diaphragm
	9	7	9	7	9	7	9	Diaphragm
		7	9	7	9	7	9	No Diaphragm
	12	7	9	7	9	7	9	Diaphragm
		7	9	7	9	7	9	No Diaphragm

3.1: Shear Load Distribution Factor using AASHTO LRFD

The idea of determining the most critical moment and shear for use in designing the bridge superstructure has been around since the 1930's and this topic is still a primary

point of concern (Suksawang et al., 2013). The latest bridge design code is the AASHTO LRFD 7th Edition (afterwards referred to as AASHTO LRFD) which was released in 2014 with interims in 2015 and 2016 (AASHTO, 2014). AASHTO LRFD has different load distribution factor equations for single and two or more design lanes. In this study girder spacings of 6.0 ft, 9.0 ft, and 12.0 ft were used to study the effect of girder spacing on load distribution using a four girder bridge. Section 3.6.1.1.1 of AASHTO LRFD defines the width of design lane as 12.0 ft (AASHTO, 2014). Single and multiple lanes were considered on the bridge deck for each of the models to make comparisons with AASHTO LRFD single lane and multilane load distribution factor equations. Load cases were created to determine the most critical location of load. For instance, for a single lane loaded, load cases were defined by placing the HS-20 design truck defined in the AASHTO LRFD close to the deck railing and then moving the truck load in the transverse direction in 1.0 ft increments until the truck load was in the middle of bridge (AASHTO, 2014). Since all bridge models were symmetric more load cases were not required.

Section 3.6.1.2.2 of AASHTO LRFD defines the design truck load for a typical bridge. There are two kinds of vehicles defined in this section: design tandem and design truck. For smaller spans the design tandem shown in Figure 1, and defined as a pair of 25.0 kip axles spaced 4.0 ft apart with a transverse spacing between wheels of 6.0 ft, usually governs. The design truck shown in Figure 2, designated HS-20, normally controls for medium and longer spans. It is defined by three axles, an 8.0 kip front axle and 32.0 kip intermediate and end axles. The spacing between the front and the intermediate axle is fixed at 14.0 ft and the spacing between intermediate and end axle shall be varied between 14.0 ft and 30.0 ft to produce extreme force effects. Transverse spacing of wheels for HS-

20 truck is also 6.0 ft. A lane load of 0.64 klf is assigned to every 12 ft design lane defined. For this study the lane load does not affect the distribution of load on girders and therefore the lane load was not considered.

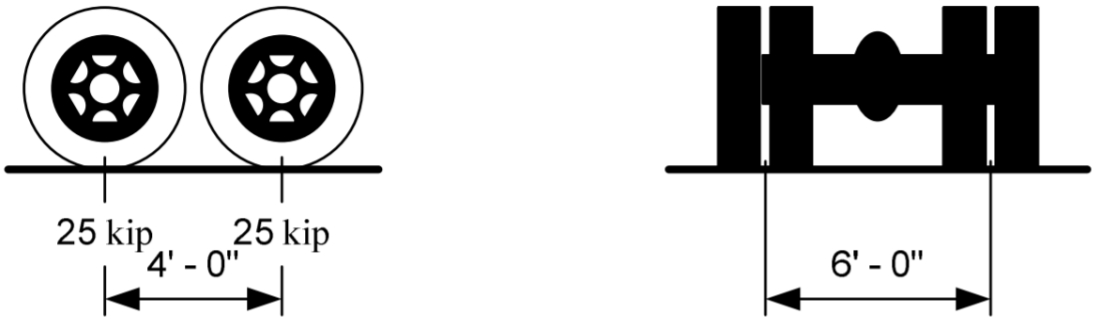

Figure 1: Characteristics of Design Tandem Load (Swanson and Miller, 2007)

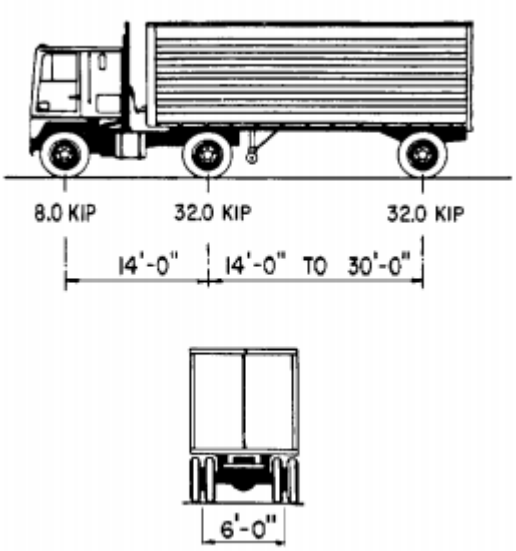

Figure 2: Characteristics of HS-20 Truck (AASHTO, 2014)

Determination of lateral load distribution for shear in AASHTO LRFD depends on the bridge type. Precast concrete girders are categorized as type-k in AASHTO LRFD Table 4.6.2.2.1-1, which is used to select the proper interior beam live load shear distribution factor equation from Table 4.6.2.2.3a-1 (AASHTO, 2014). For an interior beam shear load distribution factors are determined using:

$$0.36 + \frac{S}{25.0} \quad For\ one\ Design\ Lane\ Loaded \tag{1}$$

$$0.2 + \frac{S}{12} - \left(\frac{S}{35}\right)^{2.0} \quad For\ two\ or\ more\ Design\ Lanes\ Loaded \tag{2}$$

The range of applicability for equations 1 and 2 defined by AASHTO is:

$$3.5 \leq S \leq 16.0$$

$$4.5 \leq t_s \leq 12.0$$

$$20 \leq L \leq 240$$

$$N_b \geq 4$$

where:

S = Spacing of beams (ft)

L = Span length (ft)

t_s = Thickness of concrete deck slab (in)

N_b = Number of beams

For exterior beams AASHTO LRFD Table 4.6.2.2.3b-1 gives the procedure for determining shear load distribution factors as:

$$Lever\ Rule\ to\ be\ used\ for\ one\ Design\ Lane\ Loaded$$

$$g = eg_{interior}, For\ two\ or\ more\ Design\ Lanes\ Loaded$$

$$e = 0.6 + \frac{d_e}{10} \tag{3}$$

The range of applicability for equation 3 defined by AASHTO LRFD is:

$$-1 \leq d_e \leq 5.5$$

where:

d_e = horizontal distance from the centerline of the exterior web of exterior beam at deck level to the interior edge of curb or traffic barrier (ft)

e = correction factor

$g_{interior}$ = live load distribution factor for interior beams

g= live load distribution factor for exterior beams

For a three-girder bridge the level rule should be used for the interior beam as well. The load distribution factor for the interior and exterior beam determined using the lever rule is dependent on the spacing of the girders.

If the bridge bents are skewed, then the load distribution factors are multiplied by the skew correction factors from Table 4.6.2.2.3c-1 in AASHTO LRFD (2014) which are beyond the scope of this work.

The load distribution factors are then multiplied by the notional truck loadings, either the HS-20 design truck or the design tandem load, whichever produces the largest effects, to determine the load acting on a single girder. The load distribution factors obtained from equations 1 and 2 already include the multiple presence factor, as mentioned in AASHTO LRFD C3.6.1.1.2; therefore, the factors obtained from these equations must be divided by the multiple presence factors from AASHTO LRFD Table 3.6.1.1.2-1 (shown in Table 2) for comparison with the distribution factors obtained from grillage or plate models.

Table 2. Multiple Lane Presence Factors (AASHTO, 2014)

Number of Loaded Lanes	Multiple Presence Factors
1	1.2
2	1
3	0.85
>3	0.65

3.2: Load Cases Used for Grillage and Plate Models

As discussed in Section 3.1, AASHTO LRFD provides two sets of equations for load distribution factors, i.e. for one design lane loaded and two or more design lanes loaded. In this study the one and two lanes loaded cases were considered. The maximum width of the superstructure used in this study was 40 ft and the number of lanes as per AASHTO LRFD 7th Ed., section 3.6.1.1.1 is calculated by taking the width of the roadway divided by 12 ft. The maximum number of design lanes in this study could, therefore, have been 3 design lanes for 40 ft wide bridge deck, but it is difficult to study the effects of lateral load distribution when the entire width of the bridge is loaded. This problem was evident when the 22 ft width bridge deck was loaded with two trucks, which is discussed in detail in Section 4.4. There are different equations for exterior and interior girders as well; therefore, the goal was to determine the critical load case for exterior girders when the specific bridge configuration was loaded with one and two design lanes and interior girders when the bridge was loaded with one or two design lanes. In this study the girder spacing was varied and values of 6 ft, 9 ft and 12 ft were considered. The critical load case may be different for different girder spacings. An overhang of 2 ft was considered for all of bridge configurations in this study and the roadway width was considered to be the distance between exterior girders. For the span lengths used in this study, which are provided in Table 1, truck tandem loads did not govern and all loadings were based on the HS-20 design truck.

3.2.1: Critical Location of Design Truck in the Longitudinal Direction

The program used in this study for the analysis, STAAD.Pro, has the capability to move the load in the longitudinal direction, which is helpful when the goal is to determine the

maximum moment for two or more design lanes. To determine the case of maximum shear, the truck needs to be located as shown in Figure 3. The spacing between the 32 kips axles can be between 14 ft and 30 ft as shown in Figure 2. In this case the 14 ft spacing would give maximum shear at support, which is why a spacing of 14 ft was used for all load cases for all models. It should be noted that for some bridge configurations the one lane loaded case governs because of the multiple presence factor given in Table 2.

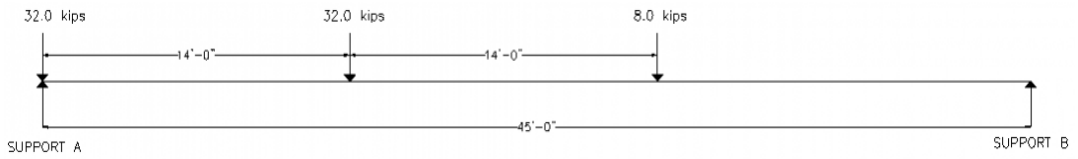

Figure 3: Location of Truck in Longitudinal Direction

3.2.2: Critical Location of Truck in Transverse Direction

Determining the critical location of the design truck in the transverse direction required a number of iterations. It should be kept in mind that all the bridge geometries considered in this research were symmetric. Determination of the critical transverse load location was broken into four categories discussed in the following sections.

3.2.3: One Lane Loaded Case for Exterior Girder

This case was the easiest case to predict the critical load location, which is when the truck is placed right over the exterior girder as shown in Figure 4. When the truck was moved closer to the interior girder the load on the exterior girder reduced. The truck was placed on the exterior girder, and because of the discontinuity from the bridge edge on one side this location, produced the critical case for the exterior girder with one lane loaded. This location was applicable for each girder spacing.

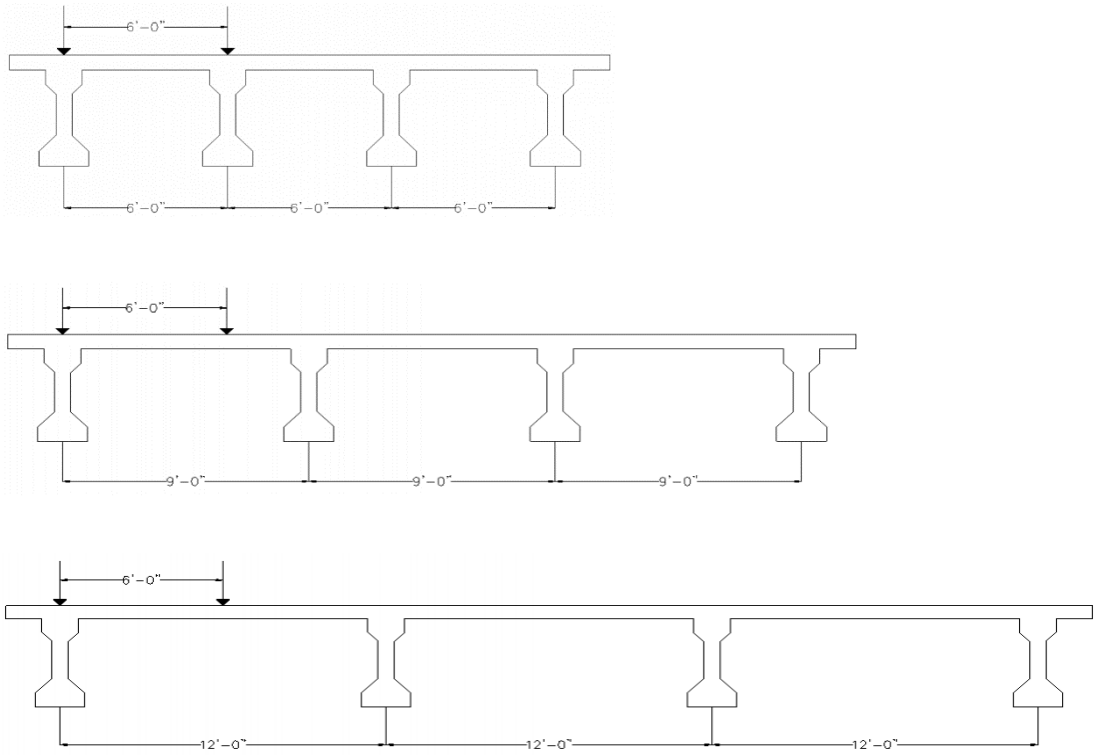

Figure 4: Critical Lateral Location of Design Truck for Exterior Girder, One Lane Loaded Case

3.2.4: One Lane Loaded Case for Interior Girders

For this case the truck was placed on the bridge cross-section as shown in Figure 4 and then it was moved in the transverse direction in 1 ft increments to determine which location would cause the maximum shear on the interior girder. It was found that the truck placed centered on the interior girder (Figure 5) resulted in maximum shear on the interior girder for all girder spacing values used in this study.

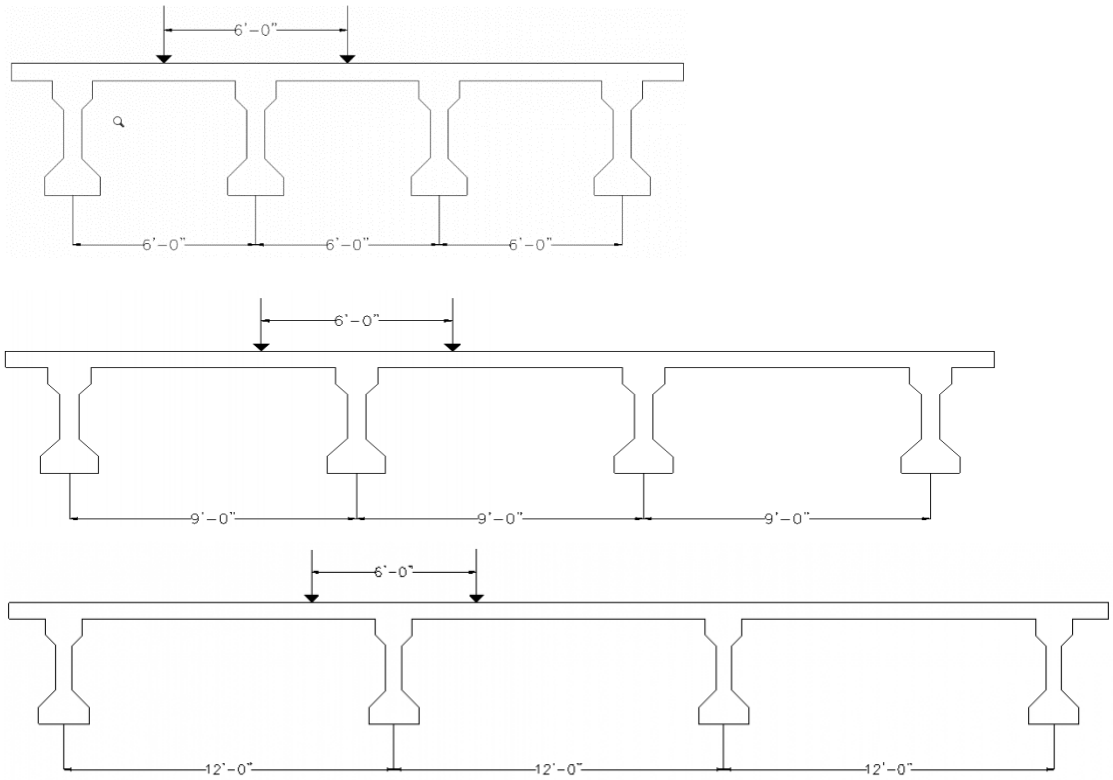

Figure 5: Critical Location of Design Truck for Interior Girder, One Lane Loaded Case

3.2.5: Two Lanes Loaded Case for Exterior Girder

When two or more trucks are placed side by side on the bridge deck the lateral spacing between them should be 4 ft based on the distribution of the design truck within the design lane shown in Figure 6. Two trucks placed side by side with one on the exterior girder, as shown in Figure 7, resulted in the highest shear on the exterior girder.

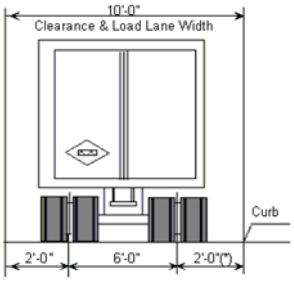

Figure 6: Lane Load Width of HS-20 Truck (MoDOT, 2007)

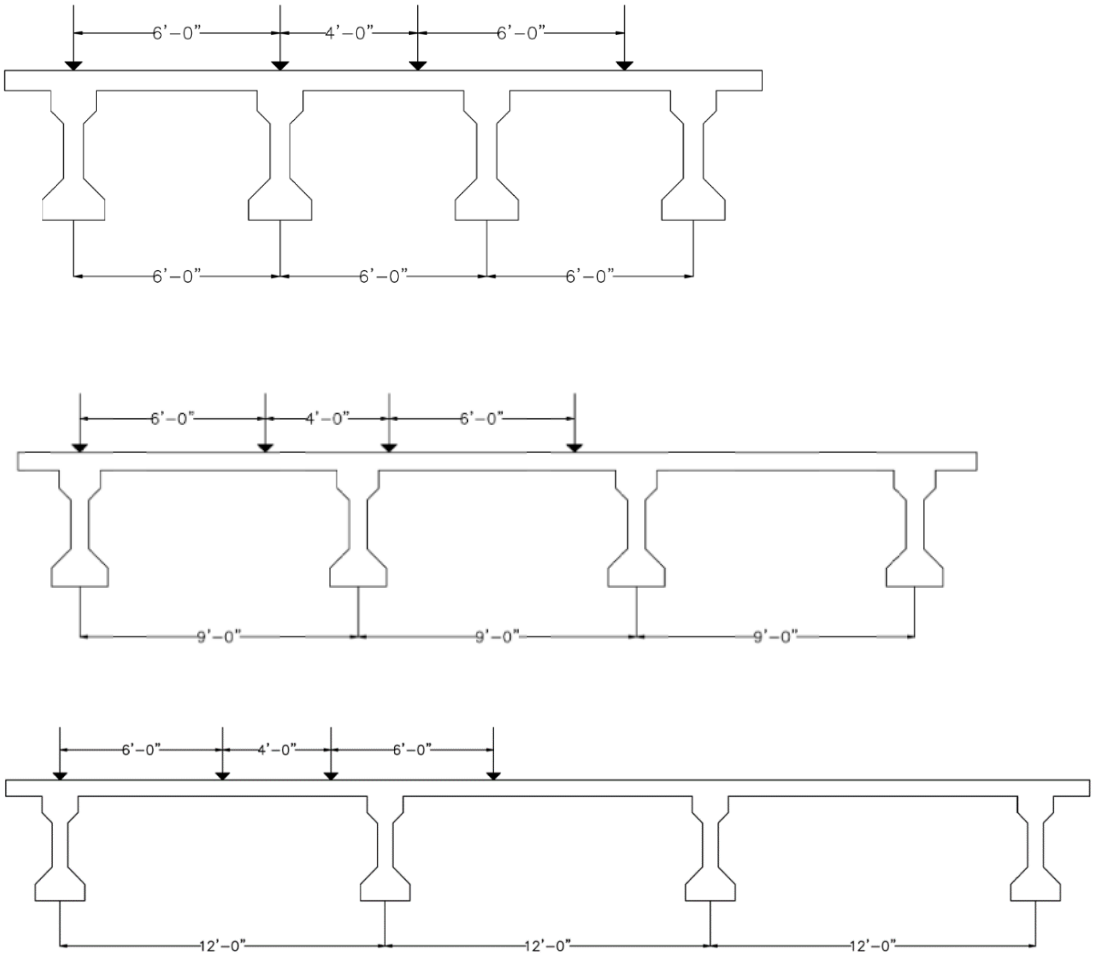

Figure 7: Critical Location of Design Truck for Exterior Girder, Two Lanes Loaded Case

3.2.6: Two Lanes Loaded Case for Interior Girder

For girder spacings of 6 ft and 9 ft the critical load placement for the two design lanes loaded case for an interior girder was the same as shown in Figure 7. When the girder spacing was 12 ft the critical load case was as shown in Figure 8.

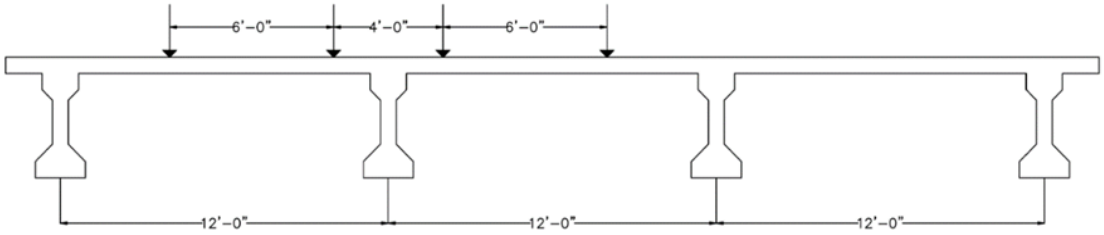

Figure 8: Critical Location of Truck for Interior Girder, Two Lane Loaded Case

3.3: Grillage Model of Bridge Superstructure using STAAD.Pro

The grillage modeling method simulates the superstructure of the bridge by having discrete members coinciding with the centroid of the bridge beams, resulting in a 2-dimensional (2D) model. The grillage modeling technique used to examine the behavior of the bridge superstructure in the current research was validated using experimental results by a former graduate student at OU (Murray, 2017). 2D grillage model results have also been compared with 3D model results and were found to be satisfactory by other researchers (Turer and Shahrooz, 2011).

The grillage model was assembled by discretizing the bridge into longitudinal grillage members (prestressed girders), and transverse members (slabs and diaphragms). The width of slab used to determine properties for the interior girders was selected based on the tributary width, specified by AASHTO LRFD Section 4.6.2.6 to determine the effective slab included with each girder. Exterior girder tributary slab widths were chosen in a similar way, but terminating at the edge of the slab. In the transverse direction, the slab (including diaphragms if present) was divided into a series of discrete sections. For

superstructures with diaphragms, the diaphragm was defined by its section properties including the slab section based on tributary width. For superstructures without diaphragms the members in the transverse direction were defined using the respective section properties of each slab element's tributary width. The major steps in developing a grillage model were developing the geometry, assigning member properties, assigning supports, and applying loads, which are all explained in the following sections. The different variations of bridge configuration for grillage models considered in this study are shown in Table 1. All grillage models were built and analyzed using the finite element analysis program STAAD.Pro (Version: 20.07.11.90) made by Bentley Systems.

3.3.1: Defining the Geometry

All elements of the superstructure were defined using line elements. The longitudinal elements (beams) were defined by having a line element at the centroid of the beam cross-section. The diaphragm elements, if required, were also defined like the longitudinal elements by having a line element along the centroid of the cross-section. The deck was broken into the flanges of the diaphragms or slab elements in the transverse direction and as part of the beams in longitudinal direction. Line elements were broken at every intersection of beam, slab and diaphragm to connect the elements. A dummy beam was assigned at the edges of the deck with negligible stiffness to connect the ends of the transverse elements. A typical grillage model layout with the different elements identified is shown in Figure 9. A sensitivity study of mesh spacing was done by Peterson-Gauthier et al. (2013) where transverse grillage spacings of half and twice what was typically used were considered. In general, a finer mesh gave results which were about 1% closer to a 3D finite element model and the grillage model

with double spacing gave the results which were 1% farther away (Peterson-Gauthier et al., 2013). In this study there were 9 transverse beam used to define deck, end diaphragm and mid diaphragm. The width and spacing of these transverse elements varied with span length. Typically, it is suggested to use a 1.5:1 ratio with the beam spacing to determine transverse line element spacing (ICE Manual of Bridge Engineering, 2008).

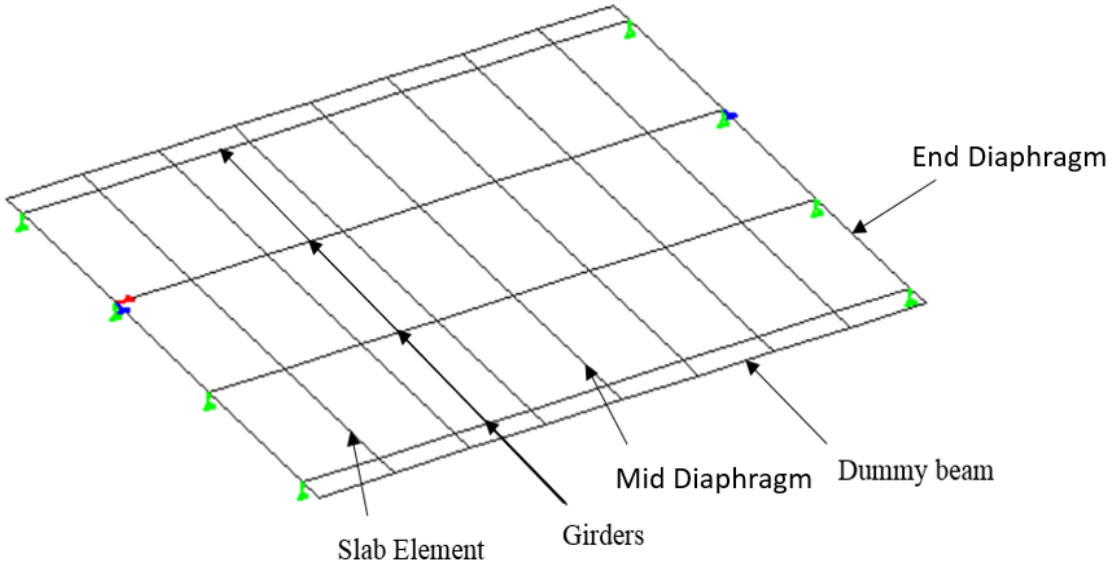

Figure 9: Typical Grillage Model

3.3.2: Member Properties:

Sectional properties determined for each element, such as area, moment of inertia, and torsional constant, were used to define the element properties in STAAD.Pro. As discussed in Section 3.3.1, girder flange widths were determined using the tributary width from AASHTO LRFD Section 4.6.2.6 and the beam line elements were given section properties based on this composite section. Concrete material properties such as compressive strength and elastic modulus were also defined as part of this step. The girder cross-sections were simplified into smaller rectangular elements to enable the user to

calculate the girder section properties with ease. An example for a Type III girder is shown in Figure 10. The torsional stiffnesses of the individual rectangles were summed to obtain the torsional stiffness of the section (ICE Manual of Bridge Engineering, 2008).

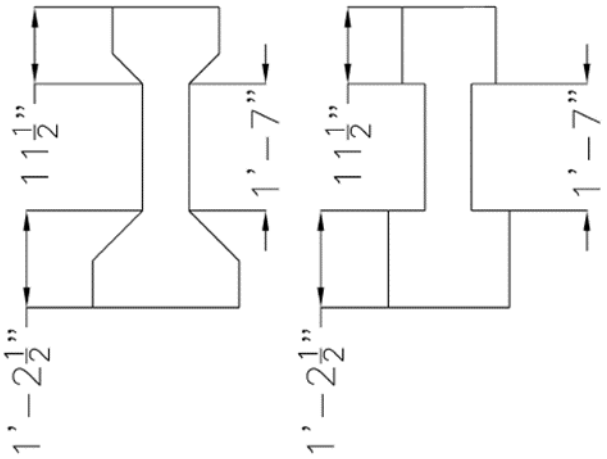

Figure 10: Type-III Girder Section and its Equivalent Section

To determine the torsional stiffness of the rectangular sections, the equations described by Ghali and Neville (1997) were used in this study.

$$J = ba^3\left[\frac{1}{3} - 0.21\frac{a}{b}\left(1 - \frac{a^4}{12b^4}\right)\right] \quad (4)$$

Where:

J = Torsional stiffness (in^4)

a = Width of the rectangular section (in.)

b = Depth of the rectangular section (in.)

3.3.3: Assign Loads

Deck systems with four longitudinal I-girders were used to provide enough deck width to capture the effects of load distribution. The HS-20 truck load was applied at critical

locations described in Section 3.2 for the three girder spacings used in this study: 6 ft (deck width = 22 ft), 9 ft (deck width = 31 ft) and 12 ft (deck width = 40 ft). The 40 ft deck width sections had a maximum of 3 lane widths (based on a 12 ft wide design lane from AASHTO LRFD 3.6.1.1.1) which could be placed on the deck simultaneously. The other two deck widths used had a maximum of two loaded design lanes. The HS-20 truck load predefined in STAAD.Pro was used for all loadings.

3.3.4: Assign Support

All the supports in the model were restrained in vertical direction. Because the bearing conditions of in-service bridges are typically elastomeric pads and the scale bridge test used to verify the model included elasticity of the support (elastomeric bearing pads), an elastic modulus was assigned to the supports. The stiffness of the support used was 300 kips/in. and was selected based on the work of Murray (2017) who examined other values based on Hambly (1991).

3.3.5: Determine Distribution Factors

After running the analysis for the critical load case, the reactions at the support were extracted from the post-processing mode in STAAD.Pro. The reactions obtained from the model were then filtered and sorted to obtain the critical numbers. Reactions obtained for a particular case were also added up and compared with the applied loads to check the quality of the model. The reaction at a particular beam support was then divided with the sum of reactions at that end of the bridge to get the load distribution factor for that particular support.

3.4: Plate Model of Bridge Superstructure using STAAD.Pro

In grillage models the slab is taken as a frame element and the centroids of the slab and girders coincide resulting in a 2D model. Such discrepancies between the model and an actual bridge can be overcome by developing 3D models. There are different ways to develop 3D models of a bridge superstructure. Several of these were summarized in a study by Sotelino and Chung (2006). They characterized the geometry using the different combinations of elements shown in Table 3. Plate elements were used for the deck and beam elements combined with shell elements were used for the girder as shown in Figure 11. The model type 4 in Table 3 was found to be the most economical model and was found to be capable of accurately predicting the flexural behavior of the bridge girders including deflection, strain, and lateral distribution (Sotelino and Chung, 2006).

Table 3: Types of 3D FE Models Described by Sotelino and Chung (2006)

Model Type	**Girder Web**	**Girder Flanges**
1	Shell Element	Shell Element
2	Shell Element	Beam Element
3	Beam Element	Shell Element
4	Beam Element	

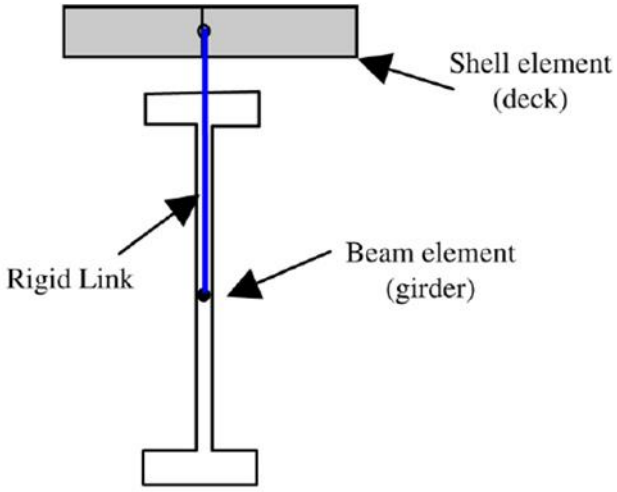

Figure 11: Representation of an Element of Plate Models (Sotelino and Chung, 2006)

For the models considered in this study, all the applied forces on the deck were out-of-plane forces. Therefore, the plate element was selected for the deck and line element was selected for the girders. An example plate model is shown in Figure 12. In the program (STAAD.Pro) this plate element has both membrane (in-plane effect) and bending (out-of-plane effect) attributes which provides the capabilities required for modeling the expected behavior. Bending effects can be shut off by defining the element as plane stress. A four noded quadrilateral plate element with the thickness defined was considered for the plate model. Initially, models were developed with and without offsets between the centroid of the deck and centroid of the girder. There was a difference in the results between models when girder spacing was 12 ft, but the difference was negligible in case of 6 ft spacing. It was decided to proceed with an offset between the centroid of deck and centroid of the girder in an attempt to more

accurately represent the actual bridge. Offsets were also provided for the diaphragms. The beam sections used in the study were not predefined in the program.

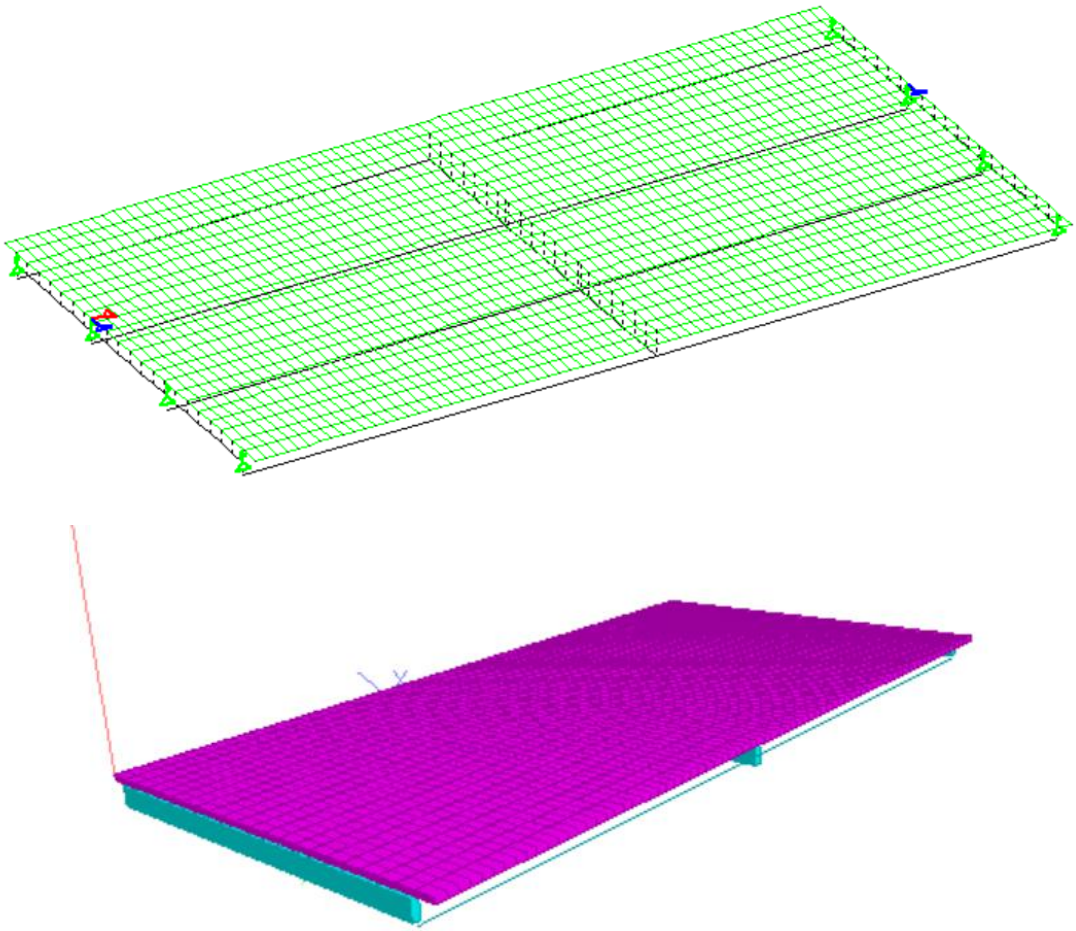

Figure 12: Wireframe and Extruded View of Plate Model

Therefore, prismatic sections were defined in the program, which is why the girders are only shown as lines in the extruded view in Figure 12. The mesh size used for the deck and girders were defined such that the nodes for each coincide with one other. Application of loads and analysis of the data to determine load distribution factors were conducted in the same fashion as for grillage models. To make the comparison between plate and grillage models only Type-III and BT-72 girder were considered, and only

certain parameters were included. For instance, the girder spacing of 9 ft was skipped, whereas 6 ft and 12 ft were considered to reduce the number of models and subsequently time required for data analysis. All the parameters considered for the plate model and its comparison with the grillage model are summarized in Table 7 of chapter 4.

Chapter 4: Results and Discussion

This chapter discusses the results obtained from grillage and plate models. Comparisons are made between shear load distribution factor obtained from AASHTO LRFD 7th Ed. (2014) equations and those from the grillage and plate models. The credibility of the grillage model used in this research was proven by the study conducted by Dr. Murray, a former student at OU (Murray, 2017). The reactions obtained from the experiment conducted by Dr. Murray are also compared with results from a plate model having the same configuration used in the experiment. The grillage models place the centroid of all model elements at the same elevation, thereby limiting the representation of torsional effects. The plate models were developed to study the change in load distribution factor when the centroid of the girders and diaphragm do not coincide with the centroid of the deck, as in an actual bridge. Finally, the comparisons are made between plate models and grillage models for the Type-III and BT-72 girders only, to bound the range of girder heights examined.

4.1: Comparison of AASHTO LRFD and Grillage Models

This section discusses the results obtained from the grillage modeling, which are compared with the load distribution factor calculated using equations available in AASHTO LRFD. All of these distribution factor equations already include the multiple

presence factor. Therefore, all the results obtained from AASHTO LRFD equations were divided with the respective multiple presence factor to ensure the correct comparison with the grillage models. In general, the AASHTO LRFD equations produced larger load distribution factors compared to the grillage models mentioned in Table 1 in Chapter 3. Though the AASHTO LRFD equations were generally found to produce larger distribution factors compared to the grillage models, in few of the cases the load distribution factor from the model was found to be greater than the value given by the AASHTO LRFD equations.

The percentage difference between the distribution factor calculated using the AASHTO LRFD equation and the distribution factor determined from the grillage model was calculated using following equation.

$$Percentage\ Difference = \frac{X_{AASHTO} - X_{grillage}}{X_{AASHTO}} \quad (5)$$

Where,

X_{AASHTO} = Distribution factor calculated using AASHTO equations

$X_{grillage}$ = Distribution factor determined using grillage models

4.2 Type-III Girders

4.2.1: Effects of Girder Spacing

The girder spacing is the most important factor influencing the load distribution factor based on the results of this study. The equations in AASHTO LRFD only consider this one variable, i.e. the spacing of girder. Figures 13, 14, 15 and 16 compare the load distribution factors calculated from the AASHTO LRFD equations and those determined from grillage models for Type-III girders. Each figure includes three panels for different span lengths and there are four set of figures for each girder type, as

comparisons were made between one and two lanes load cases for the interior and exterior girders. It is obvious from Figures 13, 14, 15 and 16 that the load distribution factor increased with an increase in girder spacing for all cases examined. It can be understood that if the girders are far apart then transfer of the load to the adjacent girder would be less and the girder closest to the truck would take the most load. The distribution factor calculated using the AASHTO LRFD equations for each case showed good agreement with the parametric models examined. It can also be noticed that trends of distribution factor given by the AASHTO LRFD equations are linear for interior girders and bilinear for exterior girders, whereas, all the results from grillage models have a bilinear trend.

Figures 17, 18, 19 and 20 show the difference between the AASHTO LRFD distribution factors and those determined from the grillage models. These figures show that the AASHTO LRFD equations produces larger distribution factor compared to the grillage models for all cases. For the one lane loaded interior girder case it can be seen in Figure 17 that the AASHTO LRFD equation gives 16.3% to 21% higher distribution factor than the grillage model when girders are spaced at 6 ft. For the 9 ft and 12 ft girder spacing the difference between AASHTO LRFD equations and grillage model reduces to about 3.8% to 15.5% for all configurations considered for the Type-III girder. It can be seen from Figure 18 that for the exterior girder with one lane loaded case the AASHTO LRFD equations result in 4.9% to 11.2% higher load distribution factors than the grillage models for all configurations considered. Specifically, for the 6 ft, 9 ft, and 12 ft spacings the range is 4.9% to 5.3%, 5.7% to 11.2% and 5.8% to 7.5%, respectively.

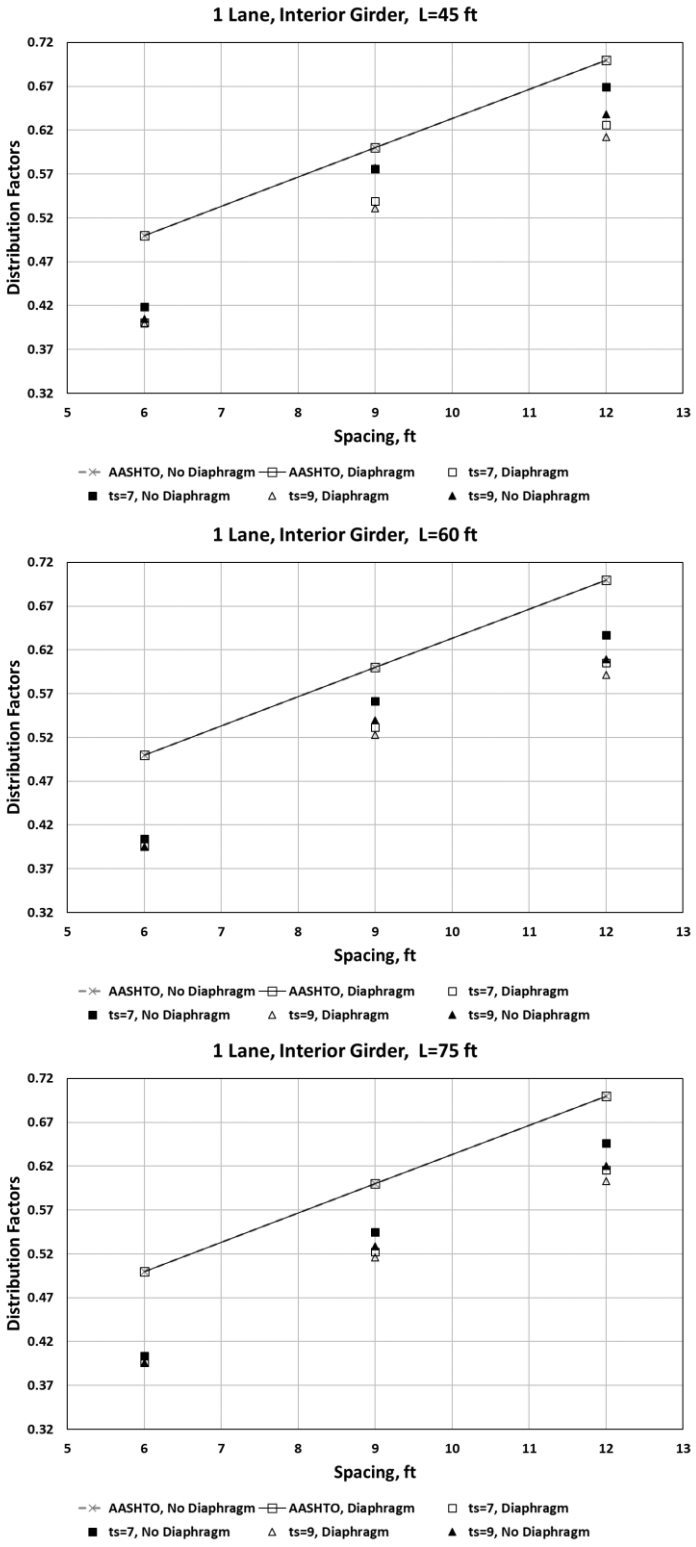

Figure 13. Distribution Factors for the Interior Girders, One Lane Loaded Versus Girder Spacing, Type-III

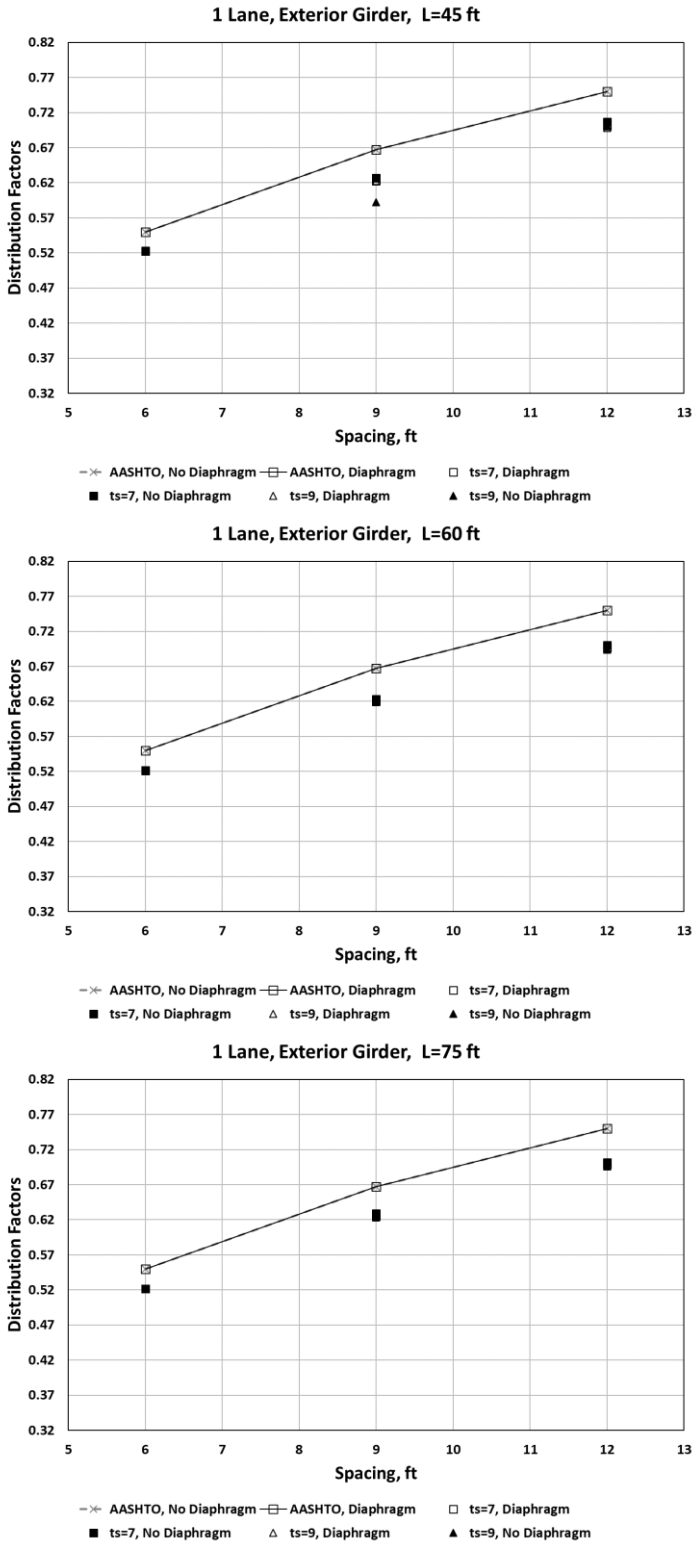

Figure 14. Distribution Factors for the Exterior Girders, One Lane Loaded Versus Girder Spacing, Type-III

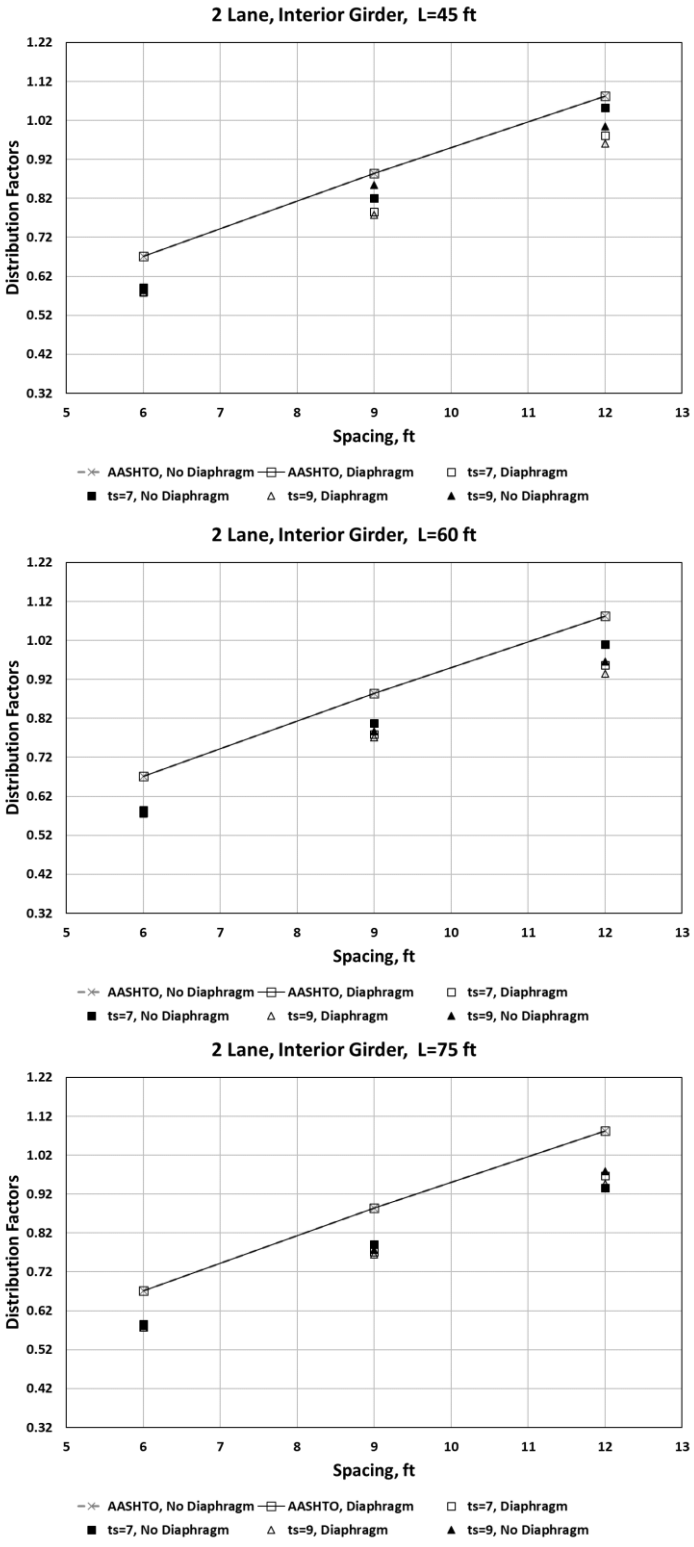

Figure 15. Distribution Factors for the Interior Girders, Two Lanes Loaded Versus Girder Spacing, Type-III

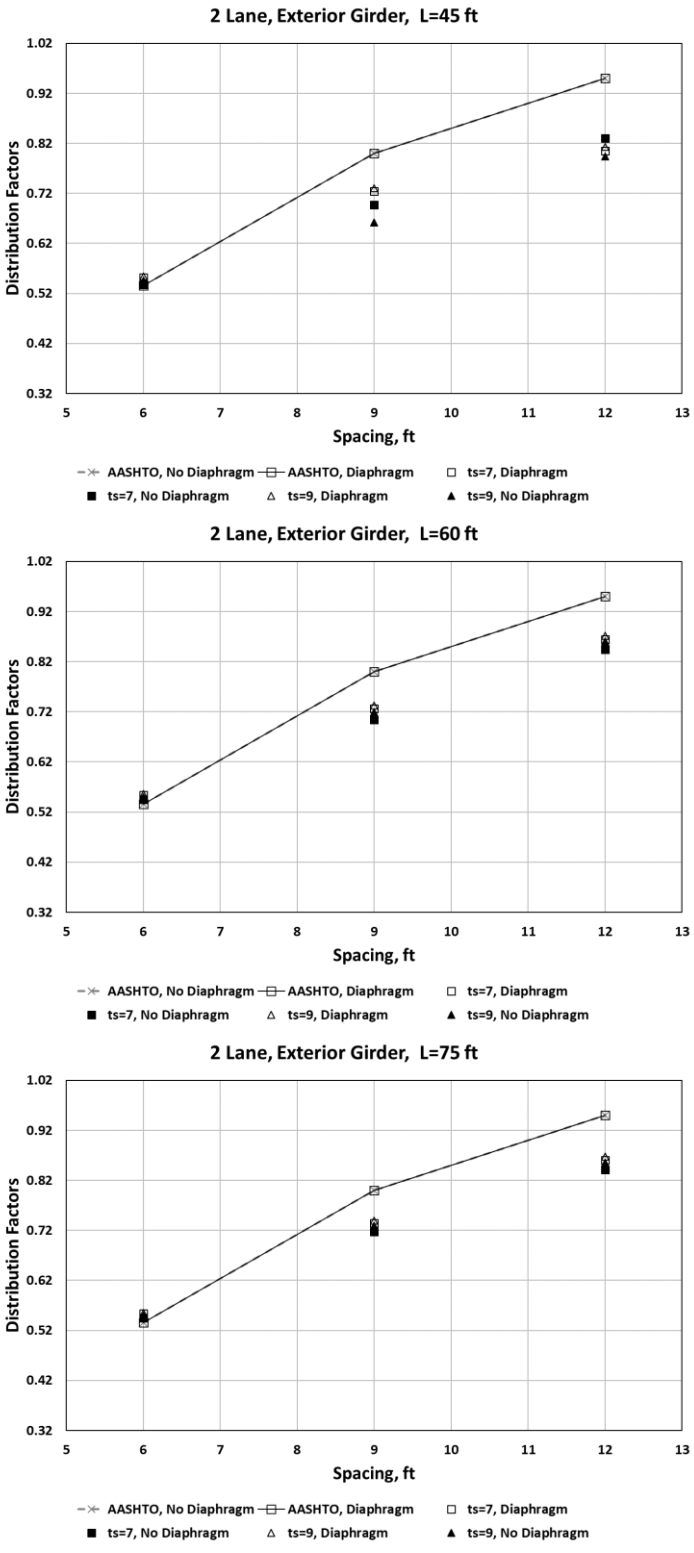

Figure 16. Distribution Factors for the Exterior Girders, Two Lanes Loaded Versus Girder Spacing, Type-III

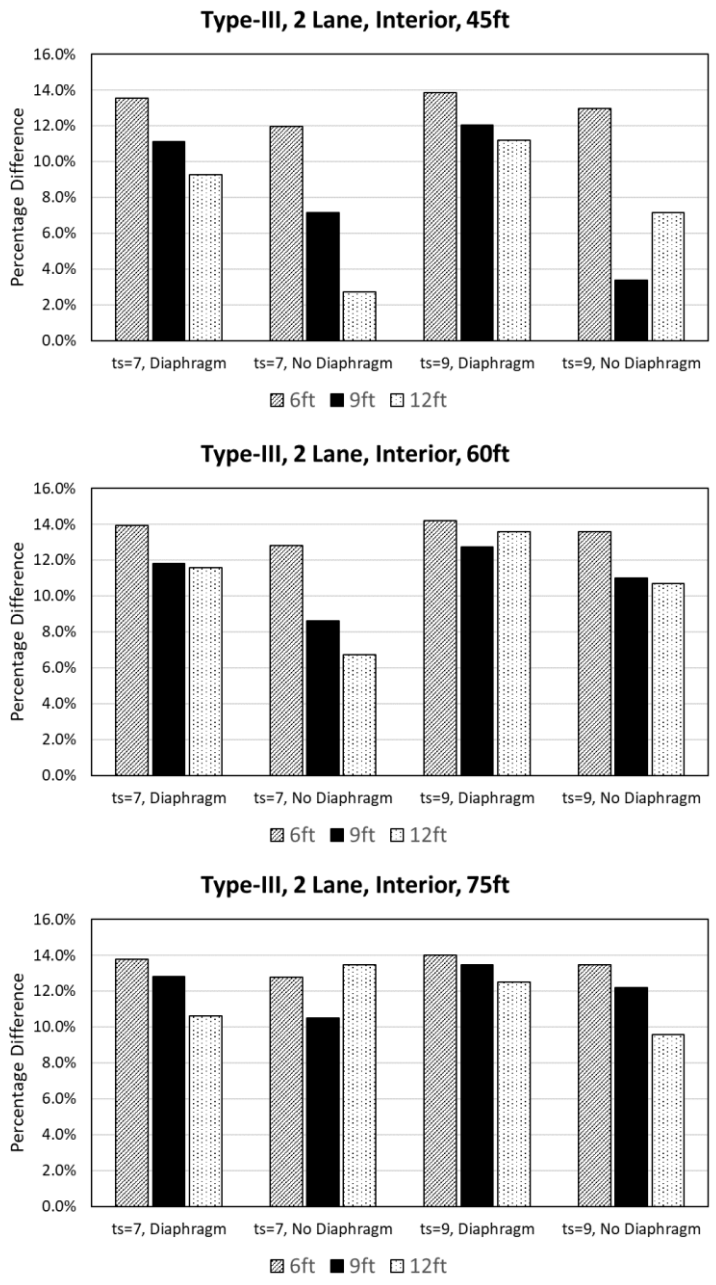

Figure 17. Percentage Difference Between AASHTO Equations and Grillage Models, for Two Lanes Loaded and Interior Girder, Type-III

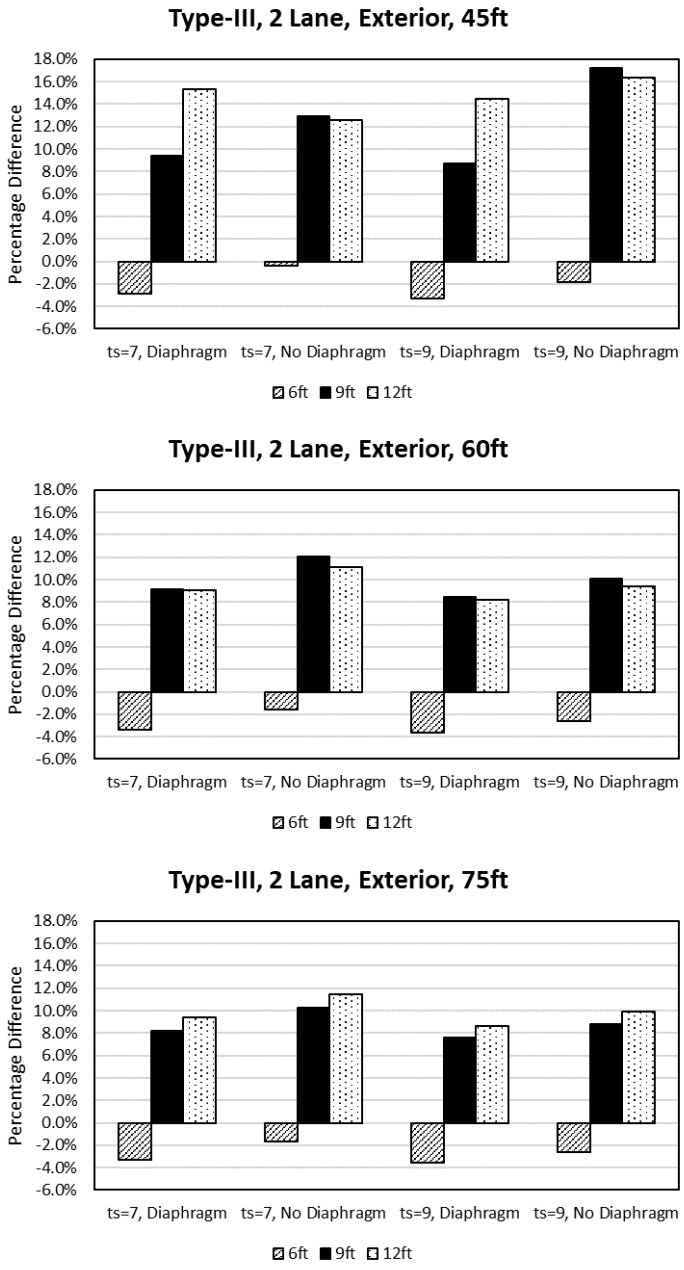

Figure 18. Percentage Difference Between AASHTO Equations and Grillage Models, for Two Lanes Loaded and Exterior Girder, Type-III

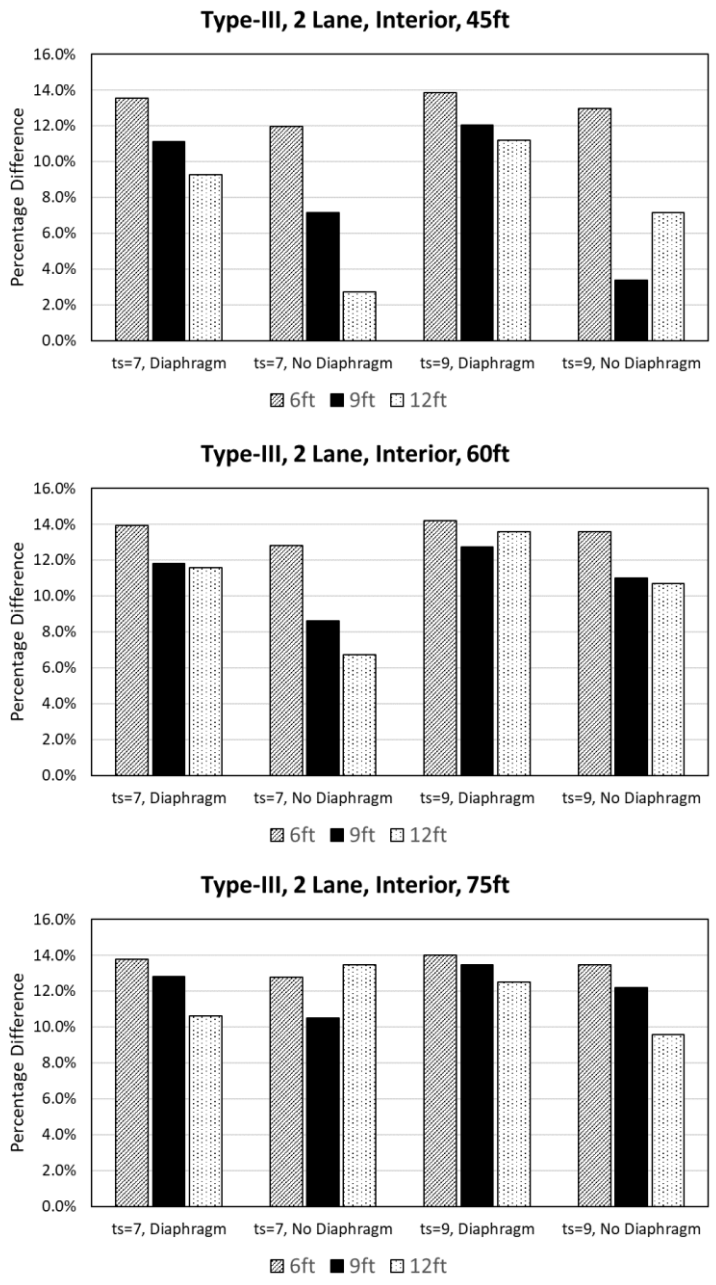

Figure 19. Percentage Difference Between AASHTO Equations and Grillage Models, for Two Lanes Loaded and Interior Girder, Type-III

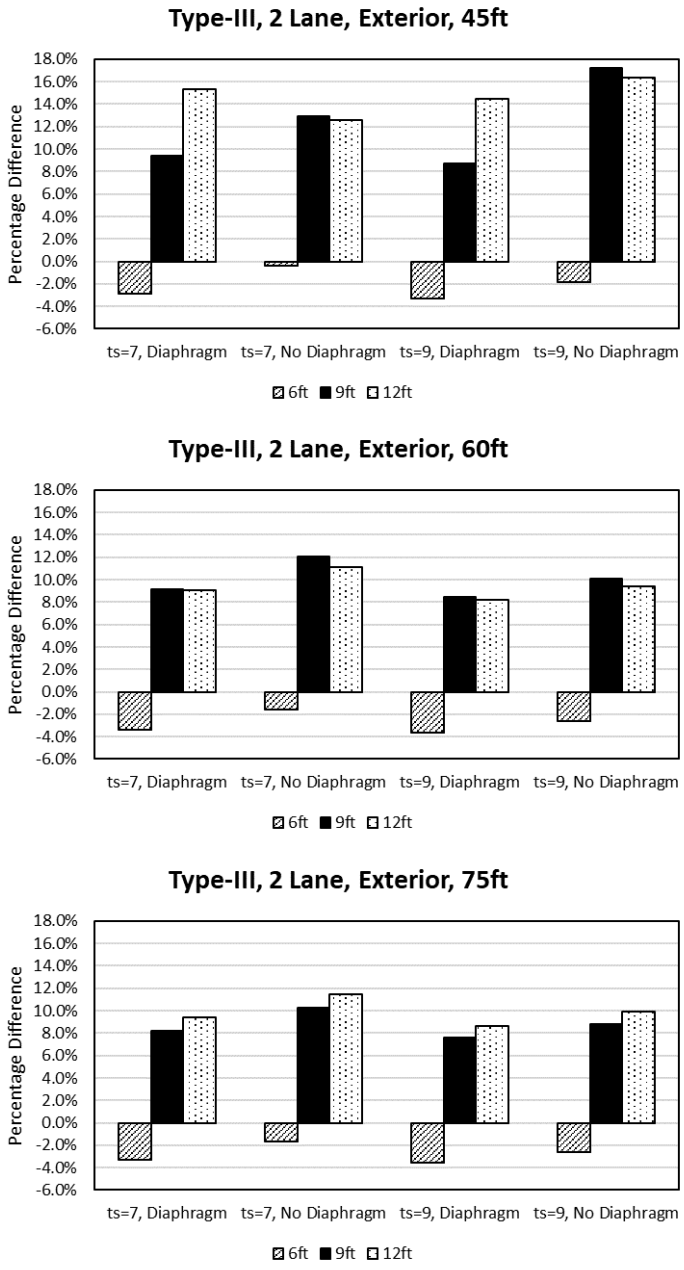

Figure 20. Percentage Difference Between AASHTO Equations and Grillage Models, for Two Lanes Loaded and Exterior Girder, Type-III

Similarly, the case when two lanes are loaded for interior girders (Figure 19) the AASHTO LRFD equations give distribution factors 3.8% to 15.5% higher than the grillage models for 9 ft and 12 ft girder spacing, but for 6 ft girder spacing the AASHTO LRFD equation factors were larger by 11.9% to 14.2%. The difference between the AASHTO LRFD equation and grillage model factors for the two lanes loaded cases can be seen for interior and exterior girders in Figures 19 and 20 respectively. For most cases considered, the AASHTO LRFD factors were larger than those from the grillage models. It should be noted that the when the bridge was loaded with two trucks on either end of the bridge in the transverse direction with minimum spacing of 4 ft between the trucks, the grillage models gave a larger distribution factor than the AASHTO LRFD equations for the 6 ft girder spacing. However, these differences were by a maximum of only 4% for all configurations considered for Type-III girders as shown in Figure 20.

4.2.2: Effects of Diaphragms

The AASHTO LRFD equations do not take the effect of the presence of transverse diaphragms into account. In general, the grillage models show that the effect of diaphragms is not significant, which supports their having not been included in the AASHTO LRFD equations. Nevertheless, the grillage models showed that diaphragms help in transfer of load to the adjacent girders. The load case for calculating maximum load distribution for exterior girders and one lane loaded is shown in Figure 21. This was the critical case for all the Type-III girder bridge configurations for exterior girders and the one lane loaded condition. It was observed that the reaction at the support of the interior girder was slightly higher when an end diaphragm was present and less when

there was no diaphragm for all the models. This behavior was more evident in plate models. This resulted in a smaller distribution factor for the exterior girder when a diaphragm was included. The difference between the reactions in cases of diaphragm and no diaphragm was small, which is why the effects cannot be seen clearly in graphs where comparisons are made. Similar trends can be seen in Figures 17, 18, 19 and 20 that the percentage difference between the AASHTO LRFD and grillage model distribution factors for no diaphragm cases are smaller than for the diaphragm cases. This is because of the better transfer of load to adjacent girders with end diaphragms. It should be noted that a higher percentage difference shows that the load distribution factor determined using grillage model was smaller than the AASHTO LRFD factor and vice versa.

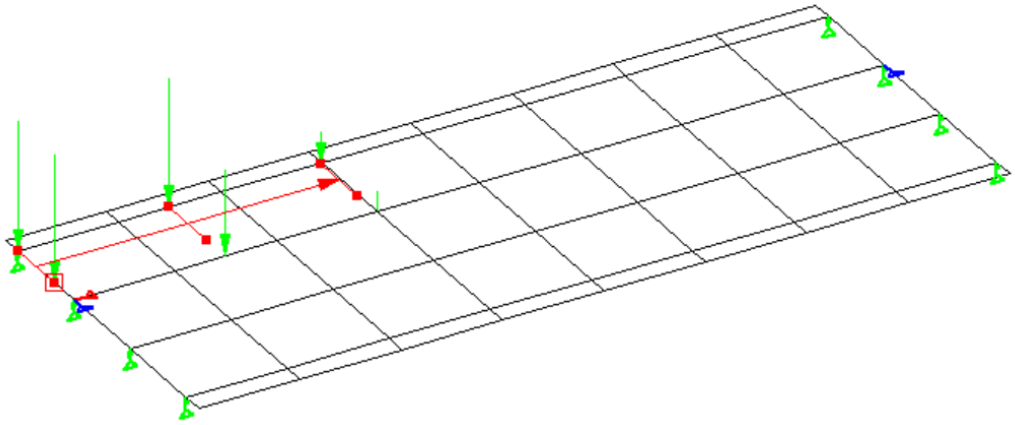

Figure 21. Grillage Model, Showing the Critical Load Case for Exterior Girder One Lane Loaded Condition

4.2.3: Effects of Deck Thickness

As discussed earlier, the AASHTO LRFD shear distribution factor equations for concrete I-beams only consider girder spacing as a variable. The grillage model results showed that for the values examined, deck thickness had very little effect on the load

distribution. Some of the results given in Figures 17 to 20 are so close that it is difficult to differentiate between them visually. Generally, it was observed that the 9 in. thick deck resulted in slightly higher distribution factors than the 7 in. thick deck. For all of the models of Type-III girders examined, the distribution factor for the 9 in. thick deck cases was 2% - 4% higher than the load distribution factor for the 7 in. deck.

4.2.4: Effects of Span Length

The effect of span length for all the configurations considered can be divided into two types. The first type is bridges without diaphragms. The grillage model results for bridges without diaphragms show little or no effect of span length on the load distribution factor. The support reactions increased with an increase in span length, as expected, since the loads are placed close to one end of the bridge span such that with a longer span the other end of the bridge takes a smaller portion of the total truck load. The load distribution factors remained relatively constant since the load distribution factor is a ratio of the force taken by an individual girder to that of the entire reaction. The second type is bridges with diaphragms. All the models with diaphragms have three diaphragms: one at the center of the span and one at each end. It was observed that shorter spans, which have less distance between the end and intermediate diaphragm, gave slightly better load distribution (smaller distribution factors) than for the bridges with the longer spans in which the distance between the intermediate and the end diaphragm is much greater. This was more evident for larger girder spacings. It can be observed from Figure 17 where, if the bars for the 12 ft spacing are compared with one another, it can be seen that percentage difference is higher for the 45 ft span and reduces for the 60 ft and 75 ft spans. It should be noted that the equations in AASHTO are

developed for much wider range of bridges that what was considered in this study and are only dependent on the spacing of girders unless the lever rule is applied. This could be the reason behind the larger load distribution factors for the AASHTO equations compared to the grillage models.

4.2.5: Quantitative Comparison of Load Distribution Factors

Figures 22 and 23 show linear trendlines of distribution factors for Type-III girders relative to girder spacing for the four different load cases. All the variations investigated for each load case for Type-III girders are merged in one graph. For the interior girder one lane loaded case, shown in Figure 22, the AASHTO LRFD equation is linear with a slope of 0.0333, therefore, the coefficient of determination for the linear fit of the AASHTO distribution factors is 1.0. A linear trendline plotted for the different variations examined with grillage models gave an acceptable coefficient of determination 0.9454, indicating that a linear trend was an appropriate model. The AASHTO LRFD equation for an interior girder with two lanes loaded, is a quadratic. However, the slope of the quadratic is very small and linear trendline gives reasonable coefficient of determination. The same is true for the exterior girder with two lanes loaded since the distribution factor is based on the interior girder case. For all cases, a linear trendline gave a good fit of the data and the lowest coefficient of determination was 0.9454, indicating that spacing has a significant impact on load distribution factors. For all the cases, the grillage model gave less steep trendlines than the AASHTO LRFD equations except for the one lane loaded interior girder case where the slopes for AASHTO LRFD and grillage models were 0.0333 and 0.0371, respectively. The highest percentage difference in slope of 29.4% was found for the two lanes loaded

exterior girder. The cases where the slope of the trendline for the grillage model data was less than for the AASHTO equations indicates that spacing has less of an impact on grillage model load distribution factors than for AASHTO LRFD distribution factors.

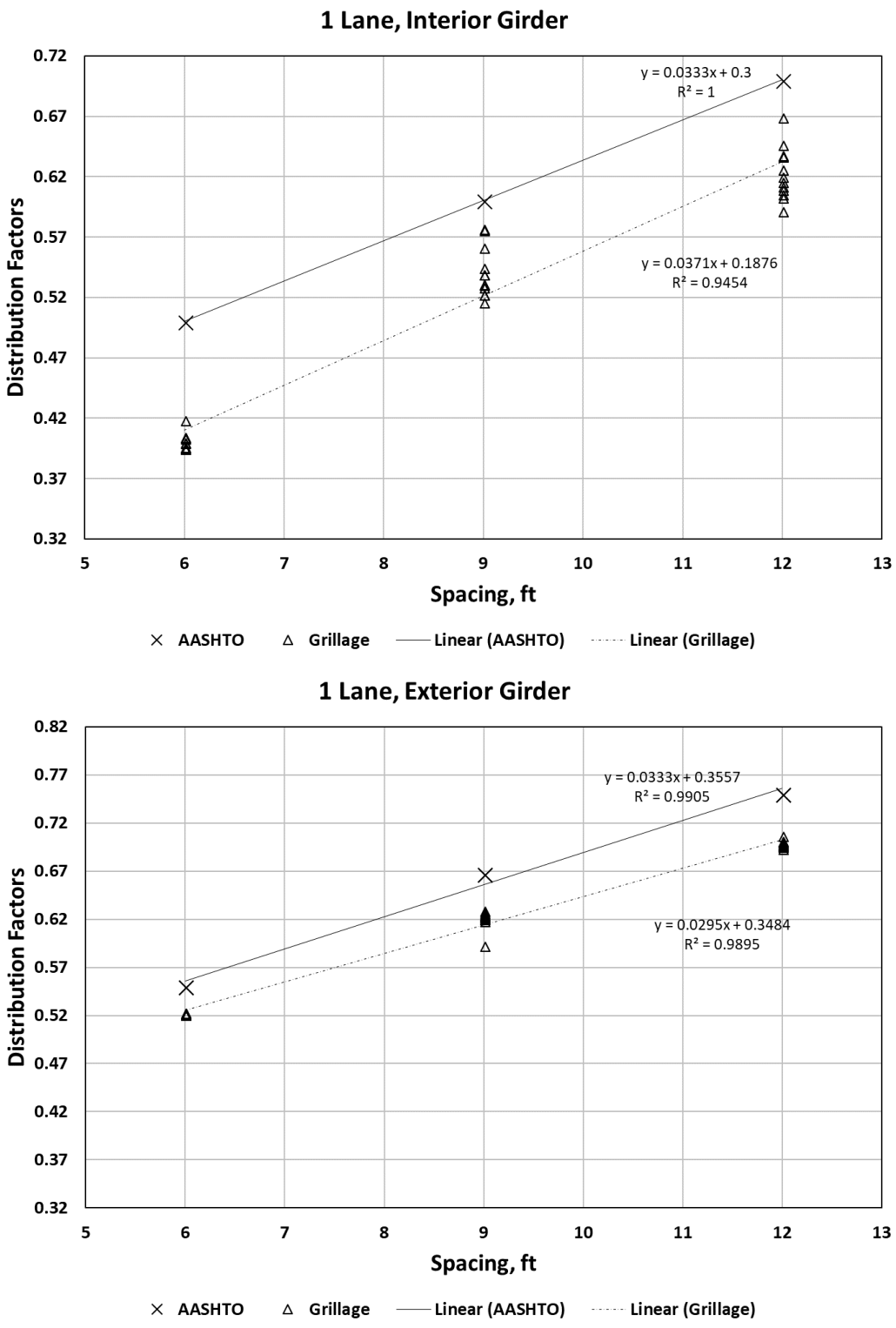

Figure 22: Linear Trendlines for Effect of Girder Spacing on Distribution Factors for Type-III Girders, One Lane Loaded Case

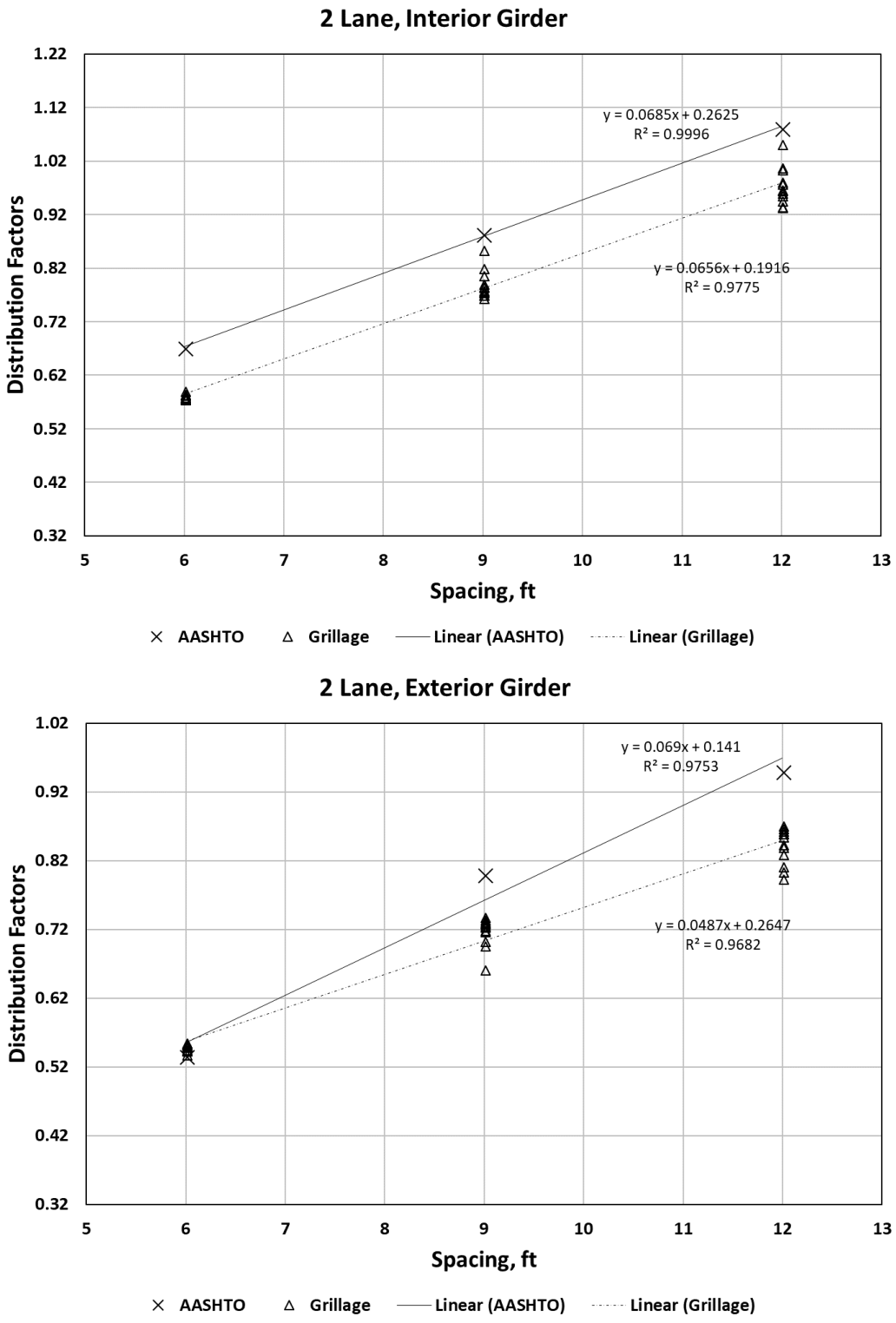

Figure 23: Linear Trendlines for Effect of Girder Spacing on Distribution Factors for Type-III Girders, Two Lanes Load Case

4.3: Type-IV Girders

4.3.1: Effects of Girder Spacing

Figures 24, 25, 26 and 27 compare the load distribution factors calculated from the AASHTO LRFD equations and those determined from grillage models for Type-IV girders. Each figure includes three panels for different span lengths and. there are four figures as comparisons are made for one and two lanes load cases for the interior and exterior girders. Figures 28, 29, 30 and 31 show the difference between the AASHTO LRFD distribution factors and those determined from the grillage models. These figures show that the load distribution factors from the AASHTO LRFD equations are larger than the grillage model factors for all cases. For the one lane loaded interior girder case it can be seen in Figure 28 that the AASHTO LRFD equation gives 18.2% to 21.6% higher distribution factor than the grillage model when girders are spaced at 6 ft. For the 9 ft and 12 ft girder spacing the difference between AASHTO LRFD equations and grillage models reduces to a range of 9.6% to 21.4% for all configurations considered for the Type-IV girder. It can be seen from Figure 29 that for the exterior girder with one lane loaded case the AASHTO LRFD equations resulted in at least 5.3% higher load distribution factors than the grillage model for all configurations considered. Similarly, for the case when two lanes are loaded for interior girders, as shown in Figure 30, the AASHTO LRFD equations give distribution factors 7.0% to 14.7% higher than the grillage models for the 6 ft, 9 ft and 12 ft girder spacings. The difference between the AASHTO LRFD equation and grillage model factors for the two lanes loaded case can be seen for exterior girders in Figure 29. When comparison is made between Type-III and Type-IV girders, Type-IV girders had larger lower and upper

limits for the range of difference from the AASHTO LRFD distribution factors for one lane loaded interior and two lanes load interior cases. The corresponding ranges are inconsistent for exterior girders except for when the girder spacing 6 ft and two lanes are loaded, the grillage models gave higher load distribution factor than the AASHTO LRFD equations.

4.3.2: Effects of Diaphragms

It is difficult to differentiate between the diaphragm or no diaphragm cases in Figure 24, 25, 26 and 27. If Figures 28, 29, 30 and 31 are considered, it can be seen that most of the cases have 1% to 2% difference in the percentage difference when diaphragm and no diaphragm are compared and there are some odd cases where the difference goes up to 6%.

4.3.3: Effects of Deck Thickness

Just like for diaphragms, the effects of deck thickness on distribution factors are difficult to determine as the distribution factors for these cases are plotted very close to each other on the graphs in Figures 24, 25, 26 and 27. When the percentage differences were compared between the 7 in. and 9 in. thick deck cases, which is shown in Figure 28, 29, 30 and 31, a difference of 2% was observed which is not significant.

4.3.4: Effects of Span Length

There is the variation of about 1% to 4% in the percentage difference between the AASHTO LRFD and grillage model load distribution factors when different spans were considered for the two lanes loaded exterior, two lanes loaded interior and one lane loaded exterior load cases in Figures 29, 30 and 31. When the variation for the one lane

loaded interior case is observed in Figure 28, the variation of about 10% between span length of 75 ft, 90 ft, and 105 ft appears significant.

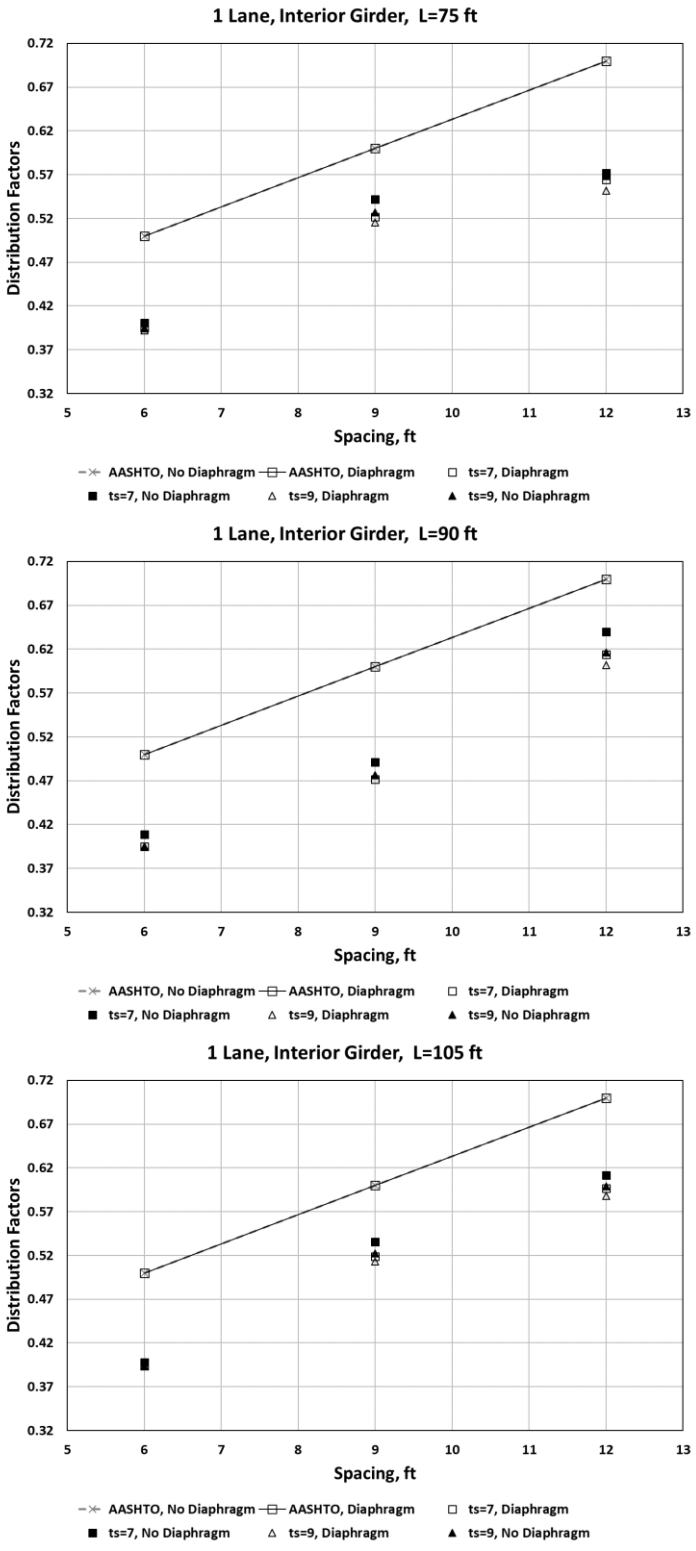

Figure 24. Distribution Factors for the Interior Girders, One Lanes Loaded Versus Girder Spacing, Type-IV

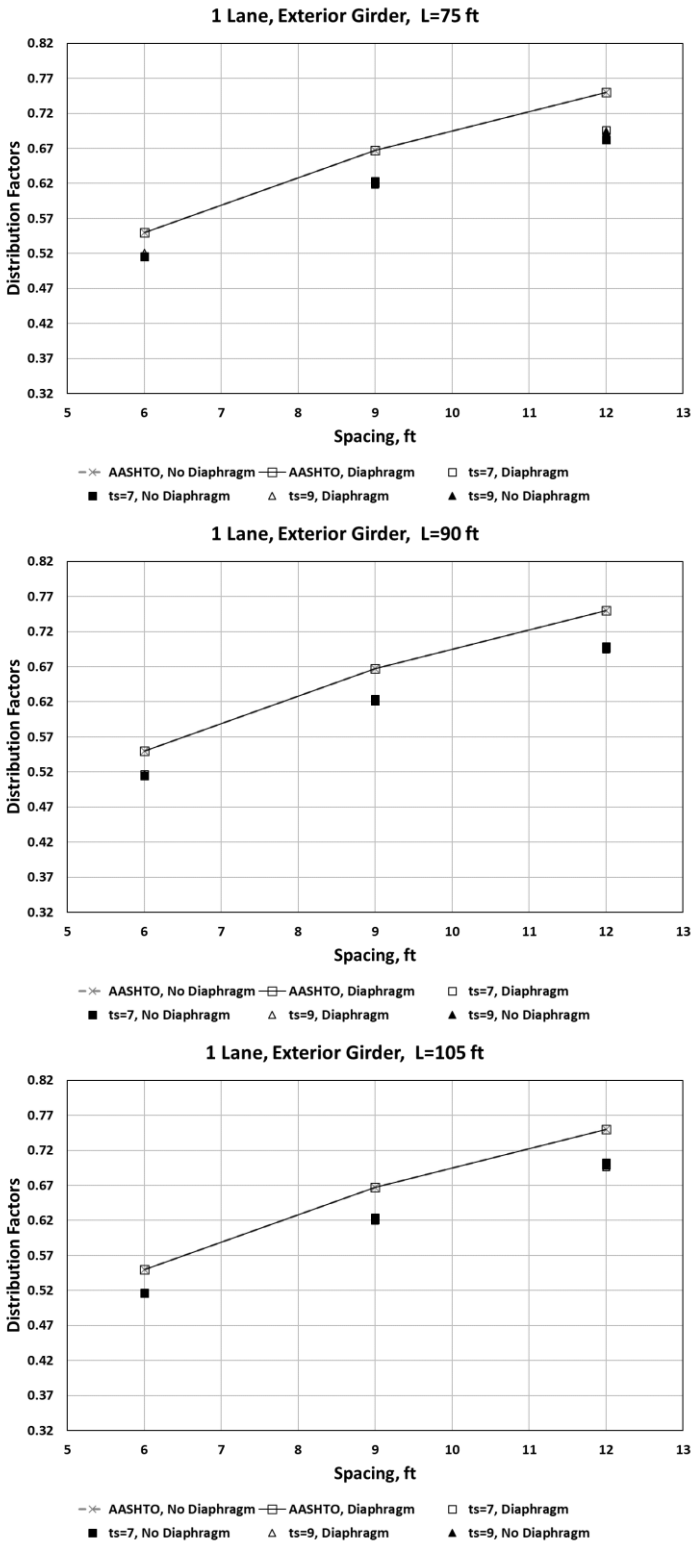

Figure 25. Distribution Factors for the Exterior Girders, One Lane Loaded Versus Girder Spacing, Type-IV

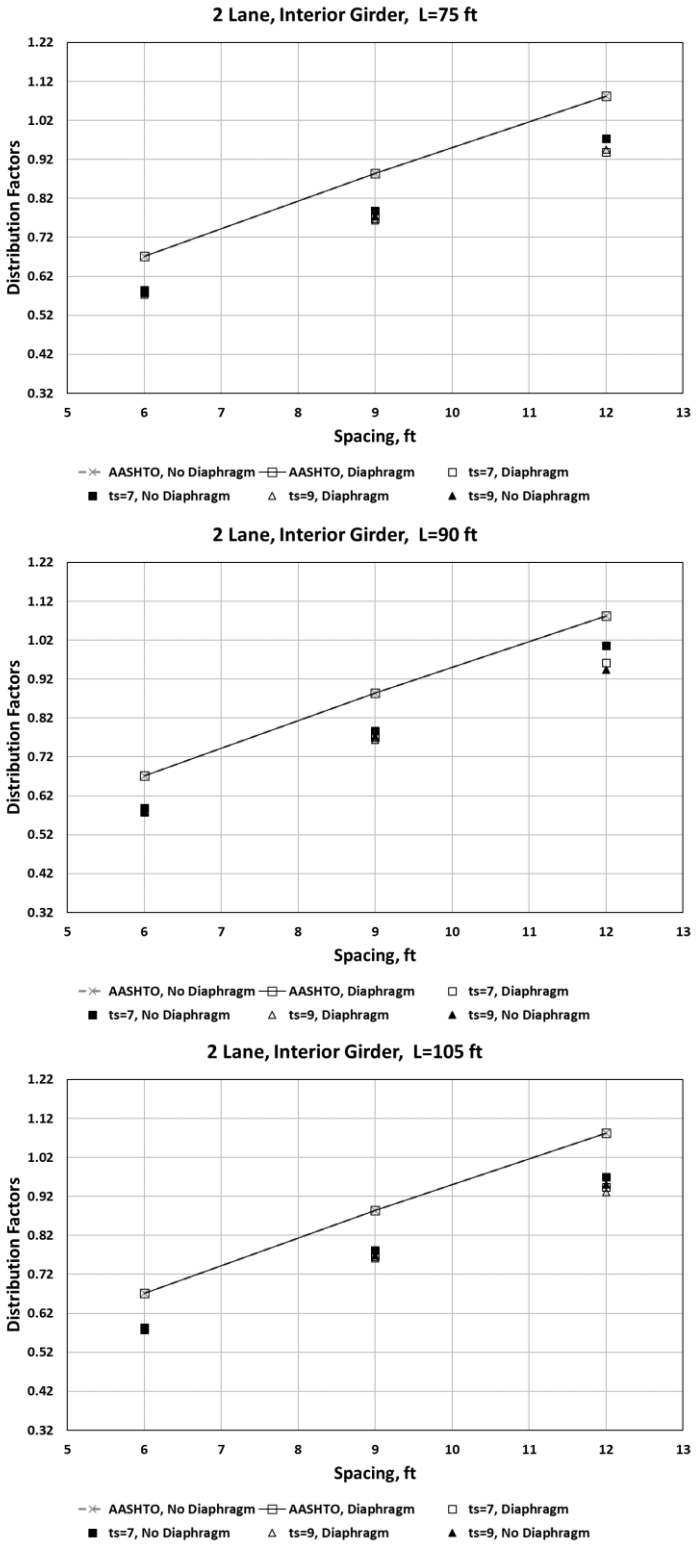

Figure 26. Distribution Factors for the Interior Girders, Two Lanes Loaded Versus Girder Spacing, Type-IV

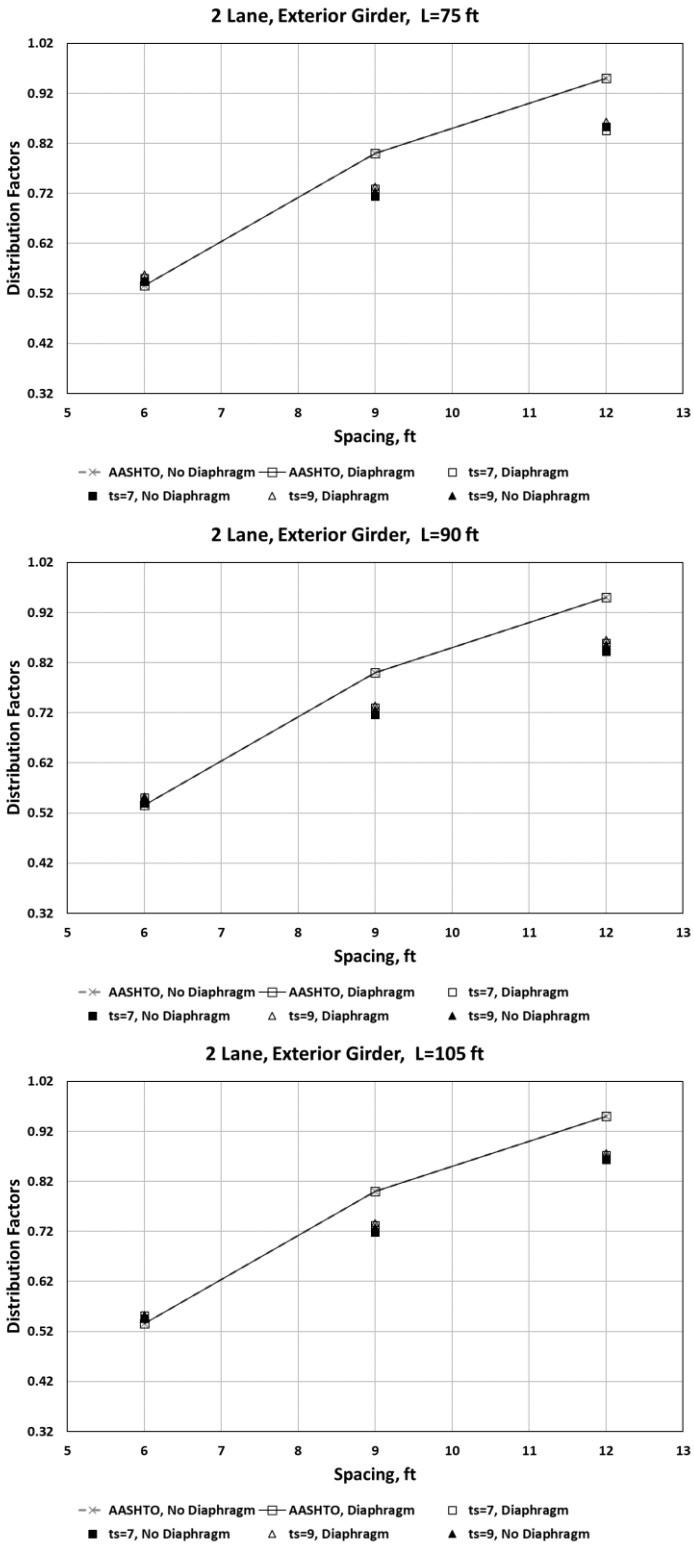

Figure 27. Distribution Factors for the Exterior Girders, Two Lanes Loaded Versus Girder Spacing, Type-IV

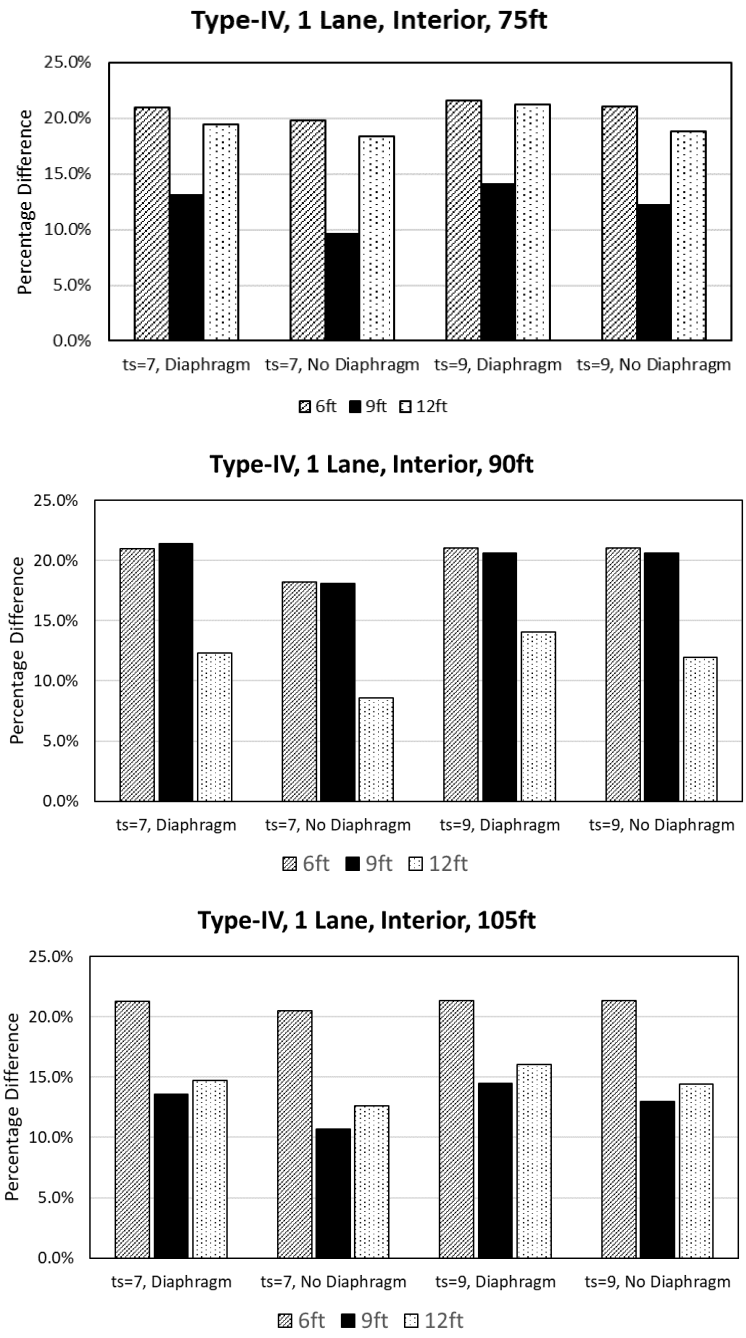

Figure 28. Percentage Difference Between AASHTO Equations and Grillage Models, for One Lane Loaded and Interior Girder, Type-IV

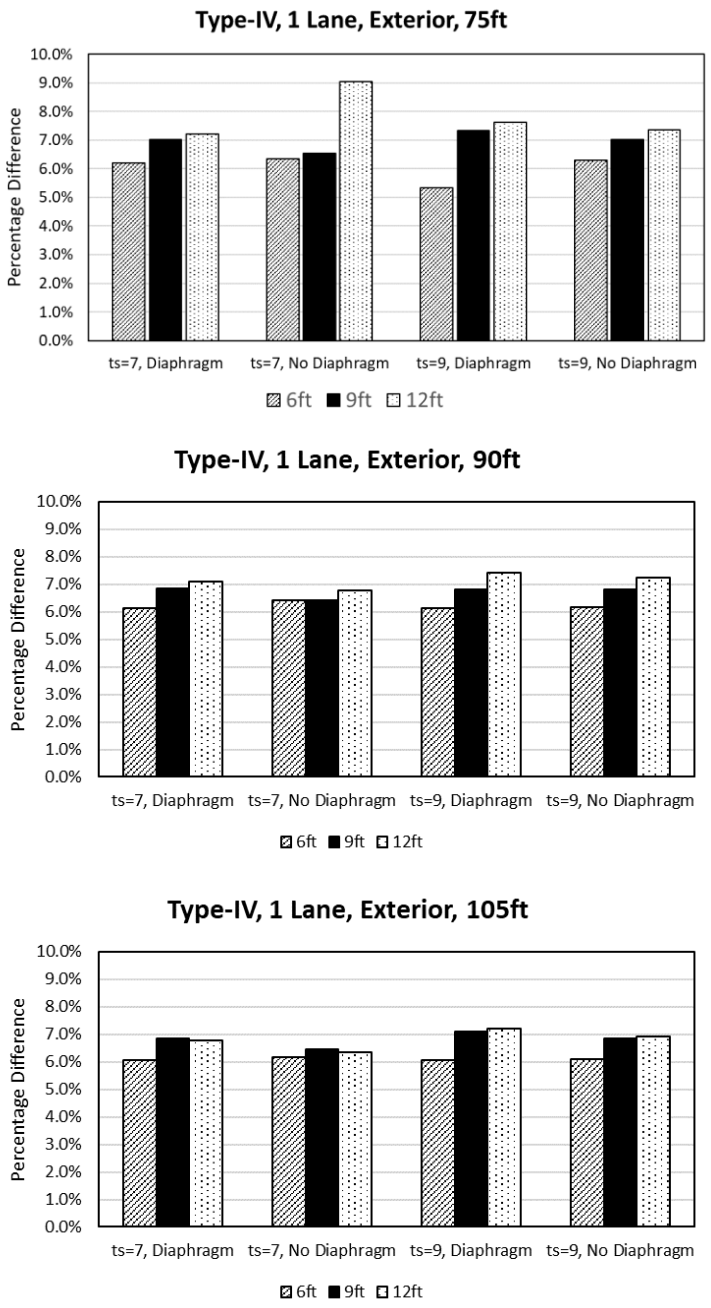

Figure 29. Percentage Difference Between AASHTO Equations and Grillage Models, for One Lane Loaded and Exterior Girder, Type-IV

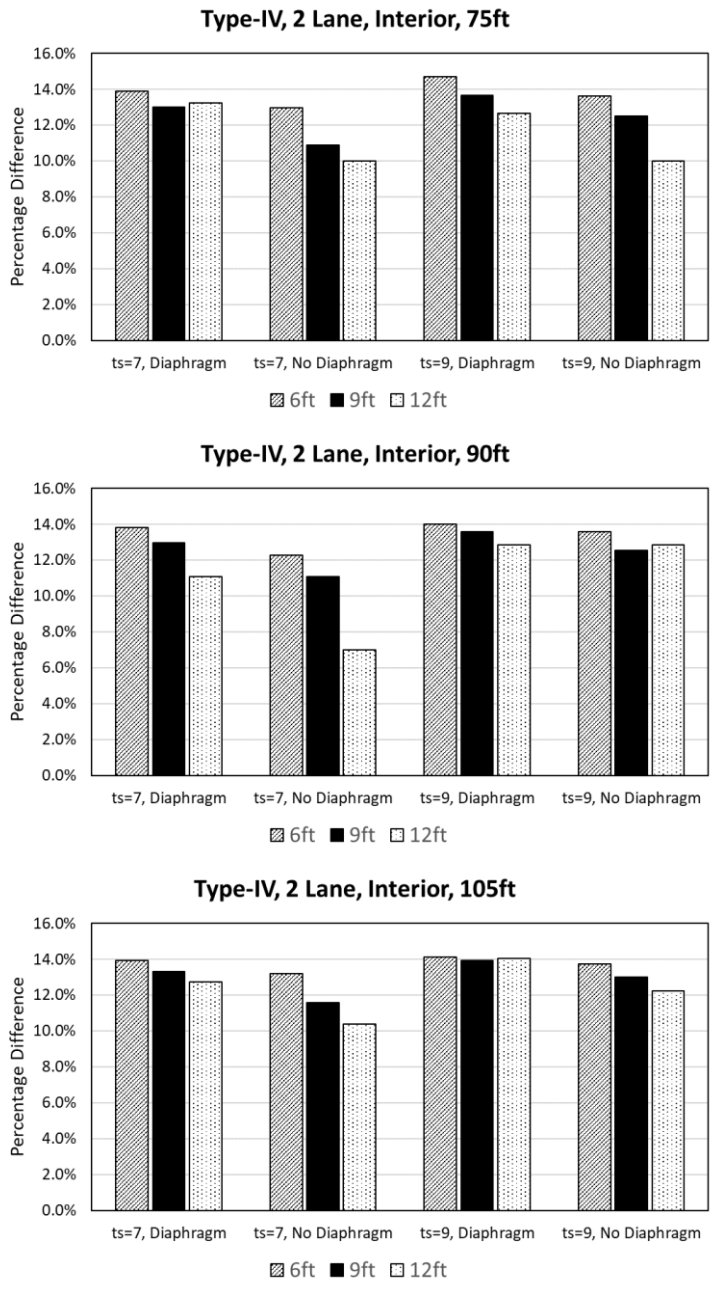

Figure 30. Percentage Difference Between AASHTO Equations and Grillage Models, for Two Lanes Loaded and Interior Girder, Type-IV

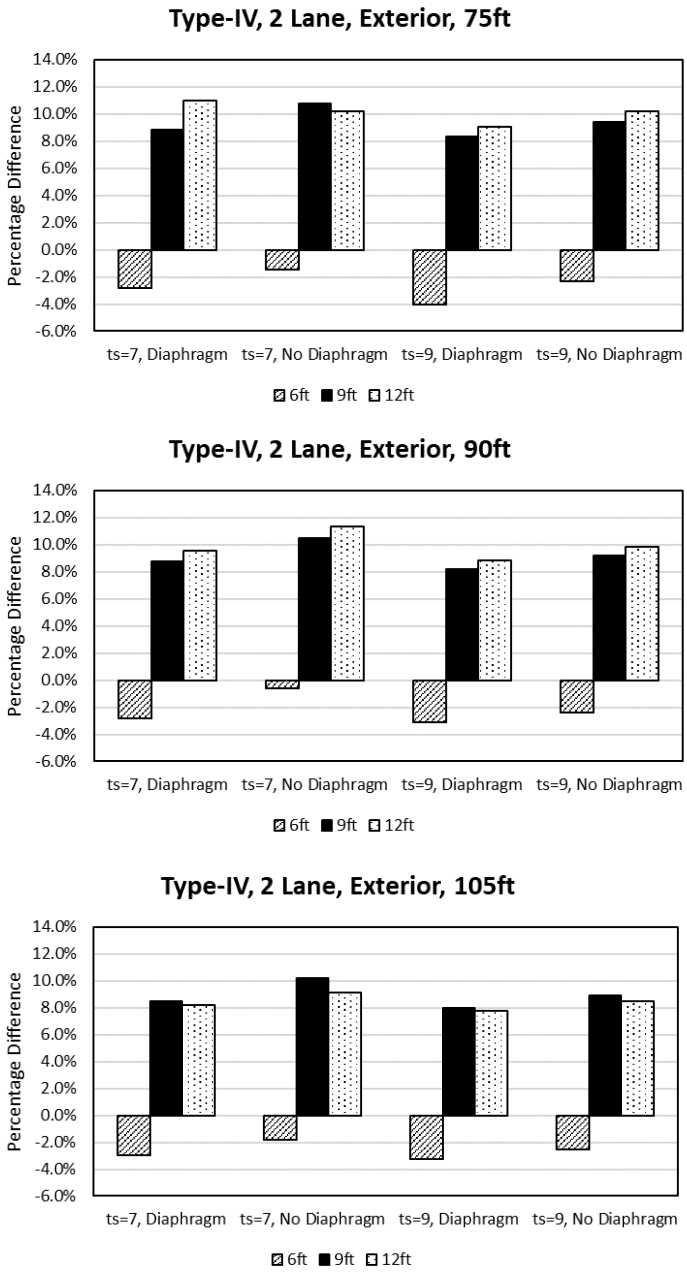

Figure 31. Percentage Difference Between AASHTO Equations and Grillage Models, for Two Lanes Loaded and Exterior Girder, Type IV

4.3.5: Quantitative Comparison of Load Distribution Factors

Figures 32 and 33 show linear trendlines for load distribution factors determined from AASHTO LRFD equations and grillage models relative to girder spacing. Discussion on the use of a linear trendline for the quadratic AASHTO equation is provided in Section 4.2.5. For all of the cases examined for Type-IV girders, trendlines for load distribution factors determined from grillage models were less steep than all of the AASHTO LRFD equations. The maximum difference of slope was 25%, which was for two lanes exterior girder load case. The minimum coefficient of determination was for the one lane loaded interior girder case, but was still found to be 0.9373 indicating that a linear trend was an appropriate model for the data. These results indicate that girder spacing had a large impact on load distribution factors and that the effect was less for grillage models than for the AASHTO equations.

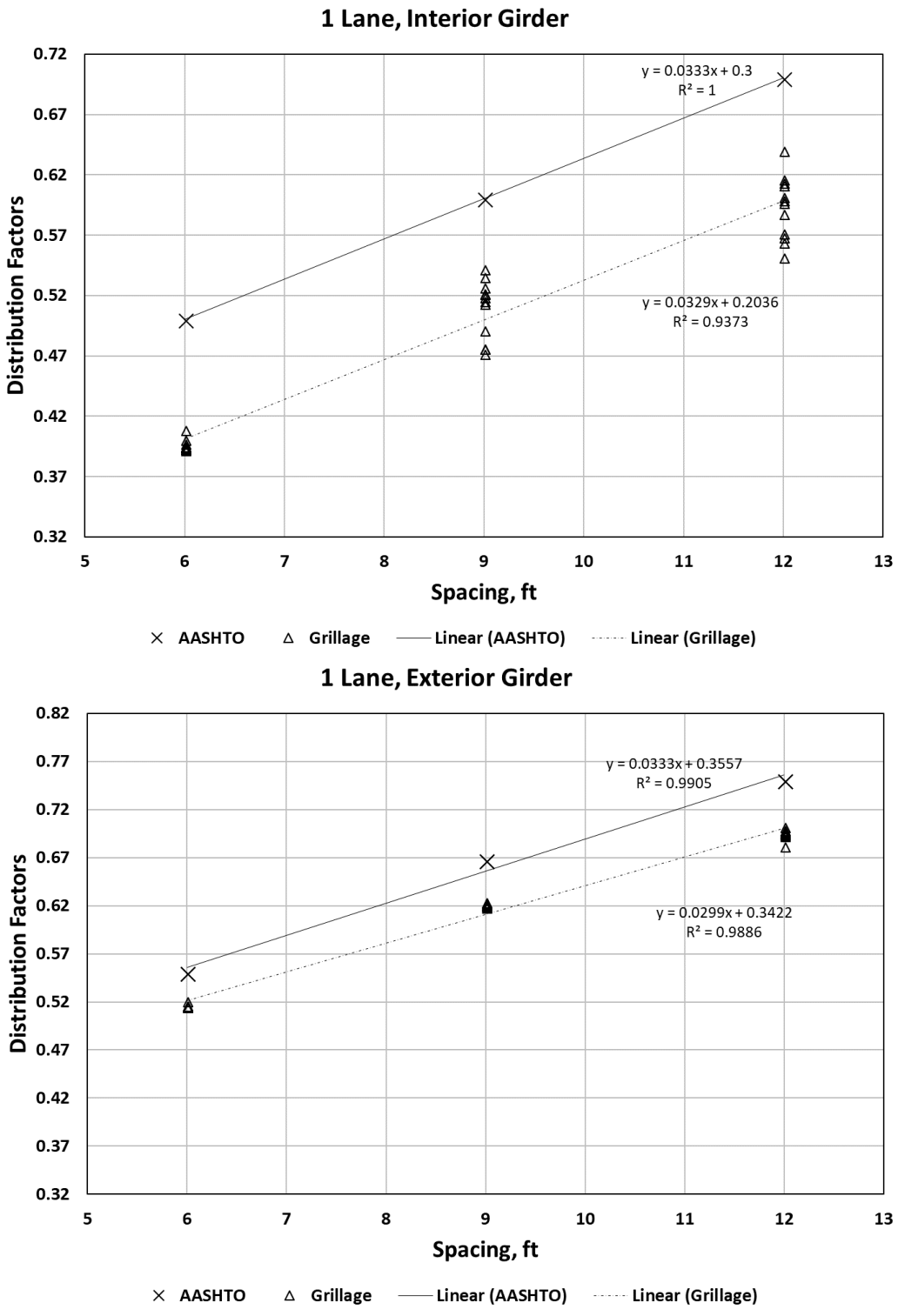

Figure 32: Linear Trendlines for Effect of Girder Spacing on Distribution Factors for Type-IV Girders, One Lane Loaded Case

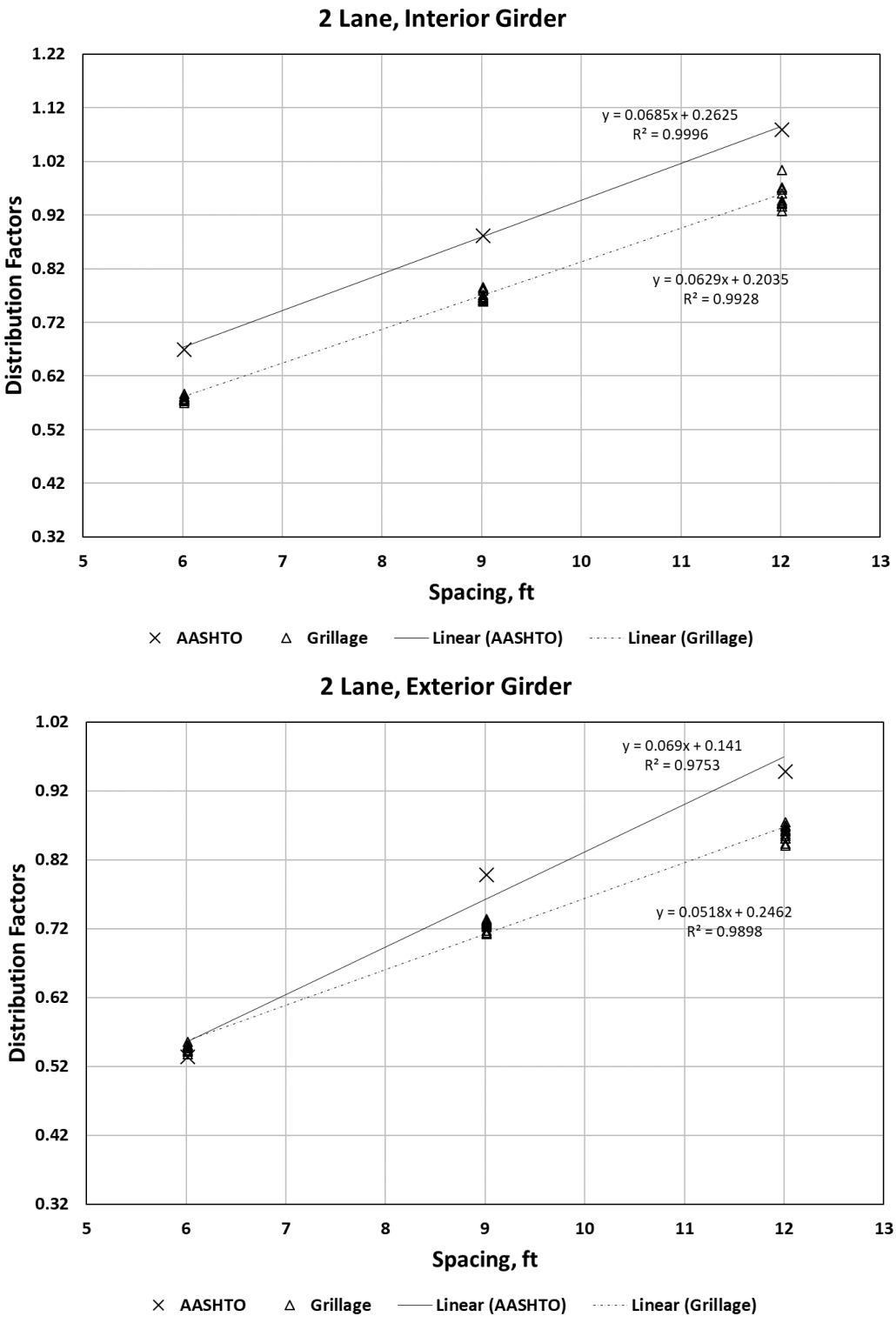

Figure 33: Linear Trendlines for Effect of Girder Spacing on Distribution Factors for Type-IV Girders, Two Lanes Loaded Case

4.4: BT-63 Girders

4.4.1: Effects of Girder Spacing

Geometrically, the Bulb Tee (BT) sections are different than the AASHTO I-girders (Type I, Type-II, Type-III, etc.). The BT sections have a larger depth to weight ratio than the typical AASHTO beams. For instance, a BT-72 has a depth of 72 in. and weight of 0.799 kip/ft while a Type-VI beam which has the same depth of 72 in. but the weight is 1.13 kip/ft (Nawy, 2009). When Figures 34, 35, 36 and 37 showing the distribution factors from the AASHTO LRFD equations and grillage models are considered, it can be seen that AASHTO LRFD equations give linearly related distribution factors for one lane and two lanes loaded interior girders and bilinearly related distribution factors for one lane and two lanes loaded exterior girders. The grillage models give bilinear relationships for all of the cases. The trends of spacing are different for the BT-63. The effect of girder spacing does not follow the same pattern as when Type-III and Type-IV girders are compared. In some cases, the 9 ft spacing gives greater deviation from AASHTO equations and in some cases 6 ft or 12 ft for similar configurations of the different girder types. This difference in trends could be the function of girder stiffness or potentially span lengths since as with the depth of the girders the span lengths are increasing, and all other variables such as deck thickness, presence of diaphragm and girder spacing are the same.

4.4.2: Effects of Diaphragms

The effects of diaphragm are similar to what was observed for Type-III and Type-IV girders. A difference of about 1% to 2% is observed between the percentage differences

between the grillage model and AASHTO distribution factors when the diaphragm and no diaphragm cases are compared as shown in Figures 38, 39, 40 and 41.

4.4.3: Effects of Deck Thickness

Similar to results observed for Type-III and Type-IV girders the effects of deck thickness are not noteworthy for BT-63 girders. Very little impact of about 1% to 2% is observed when the deck thickness is changed from 7 in. to 9 in.

4.4.4: Effects of Span Length

The percentage differences between the AASHTO and grillage model distribution factors, shown in Figures 38, 39, 40 and 41 suggest that there is only 1% to 2% change in the percentage difference when same configuration of bridge is compared with different span lengths. This difference could also be due to the change in location of intermediate diaphragm with change in span length, but a change in percentage difference can also be observed when different span lengths of no diaphragm cases are compared. Since the span lengths considered for BT-63 girders are very high compared to Type-III, the effect of intermediate diaphragm relative to span length observed for Type-III girders cannot be seen for BT-63 girders.

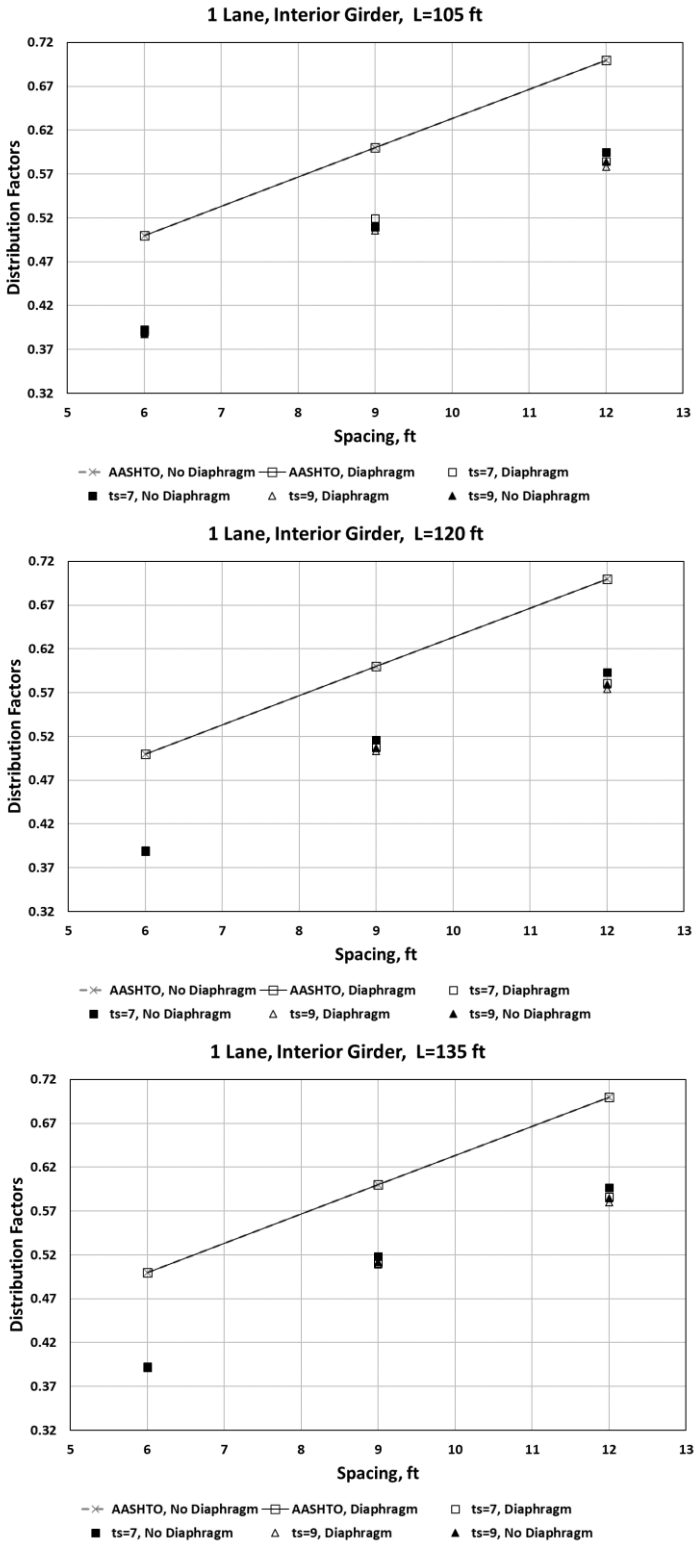

Figure 34. Distribution Factors for the Interior Girders, One Lane Loaded Versus Girder Spacing, BT-63

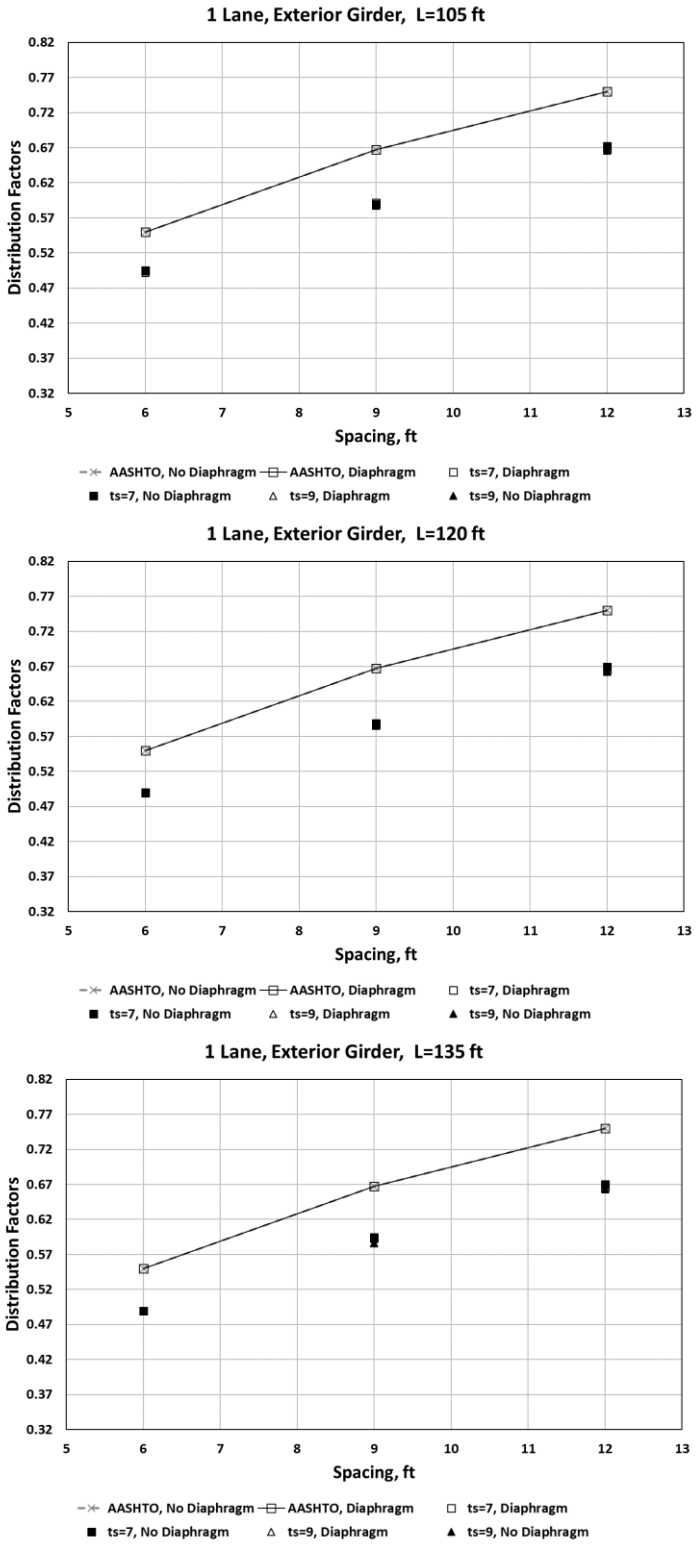

Figure 35. Distribution Factors for the Exterior Girders, One Lane Loaded Versus Girder Spacing, BT-63

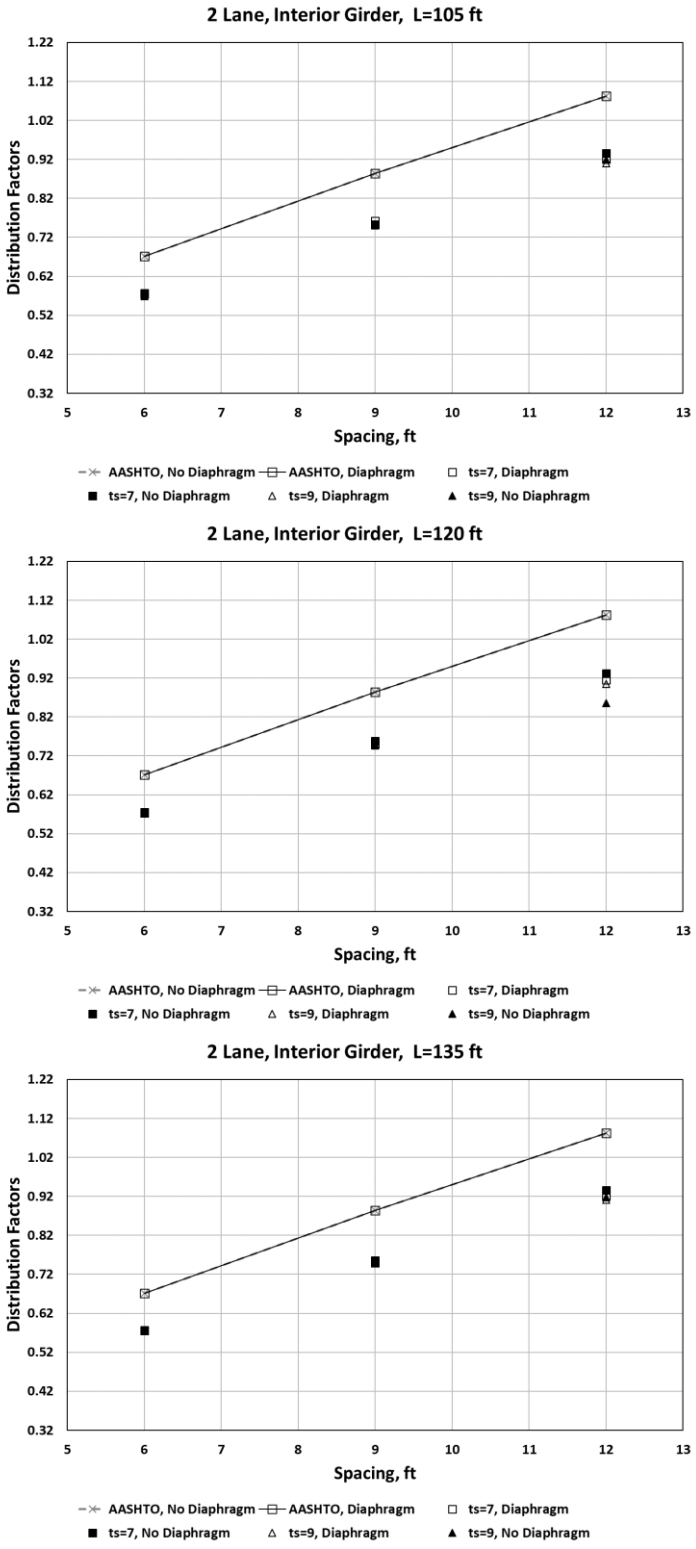

Figure 36. Distribution Factors for the Interior Girders, Two Lanes Loaded Versus Girder Spacing, BT-63

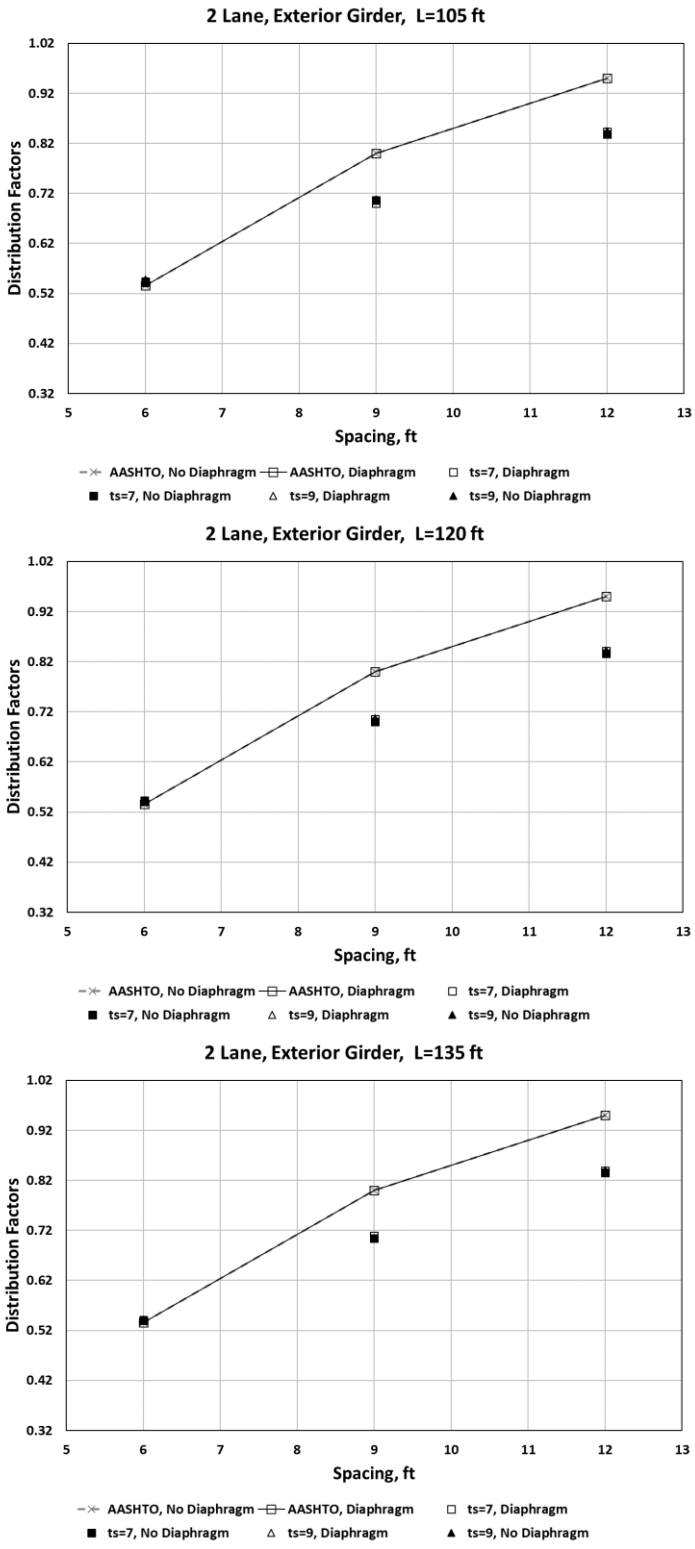

Figure 37. Distribution Factors for the Exterior Girders, Two Lanes Loaded Versus Girder Spacing, BT-63

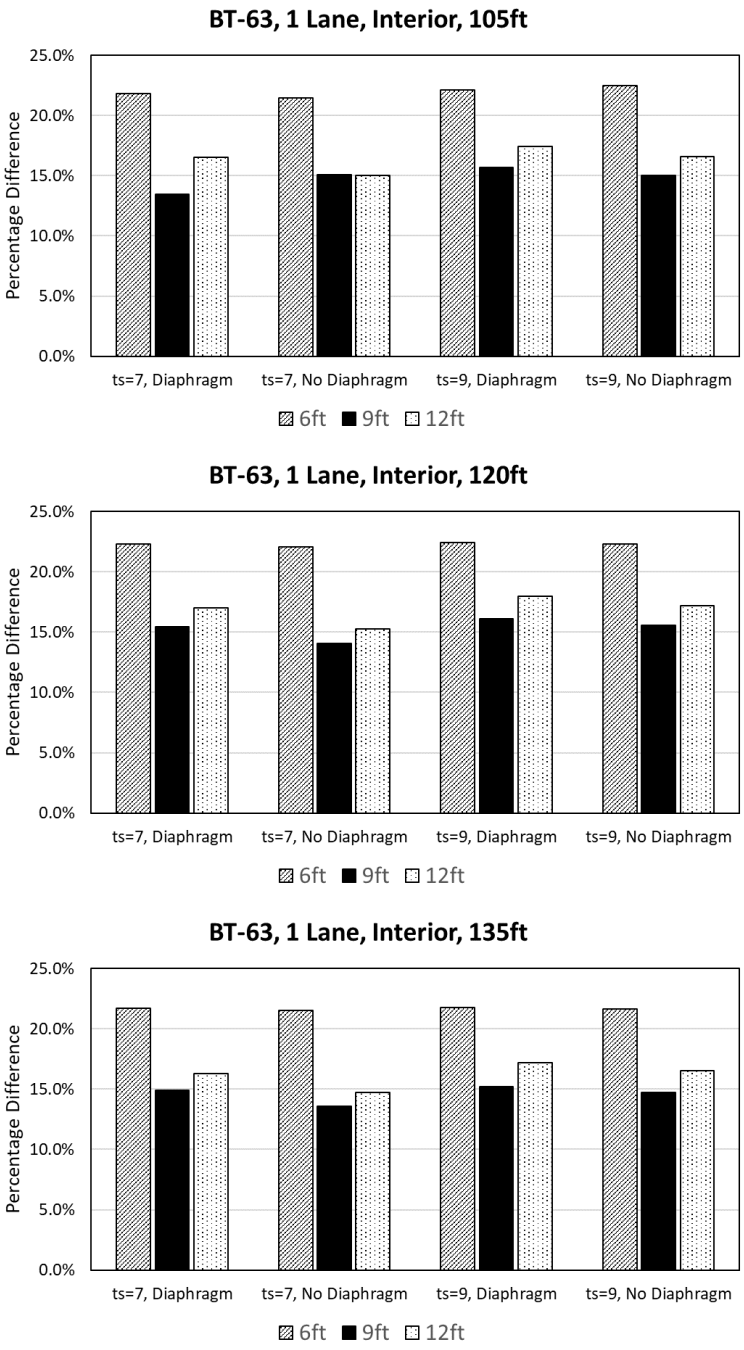

Figure 38. Percentage Difference Between AASHTO Equations and Grillage Models, for One Lane Loaded and Interior Girder, Type BT-63

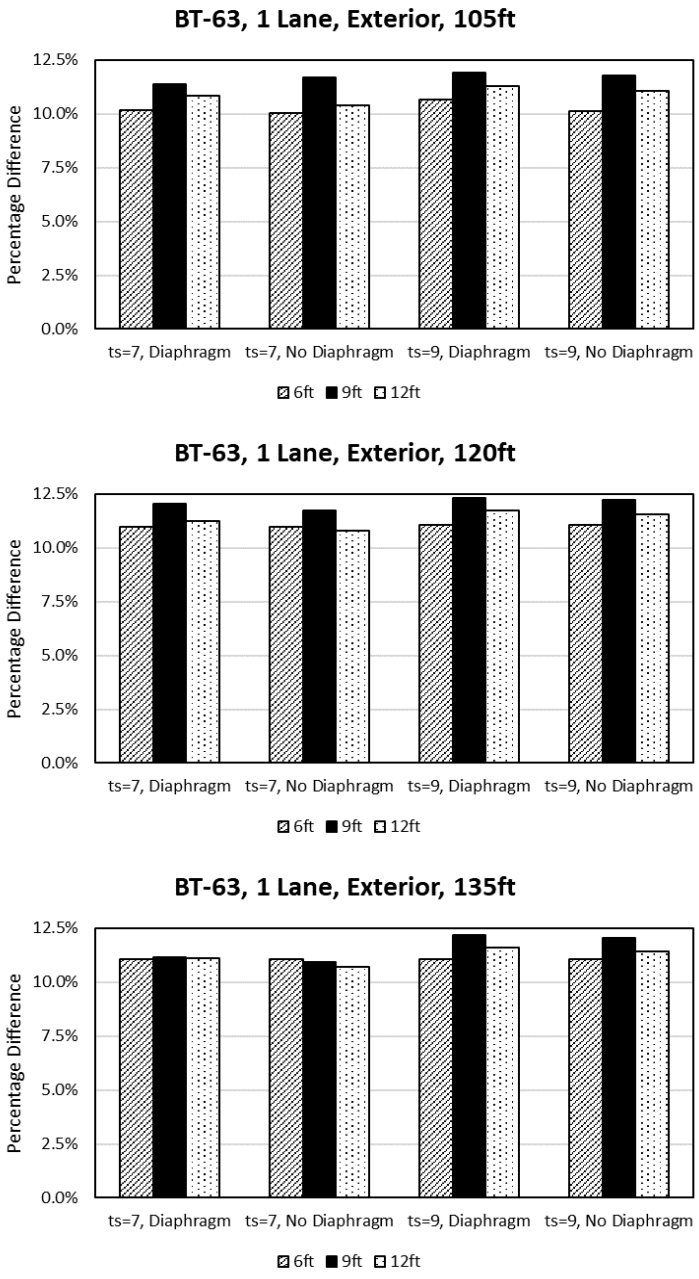

Figure 39. Percentage Difference Between AASHTO Equations and Grillage Models, for One Lane Loaded and Exterior Girder, Type BT63

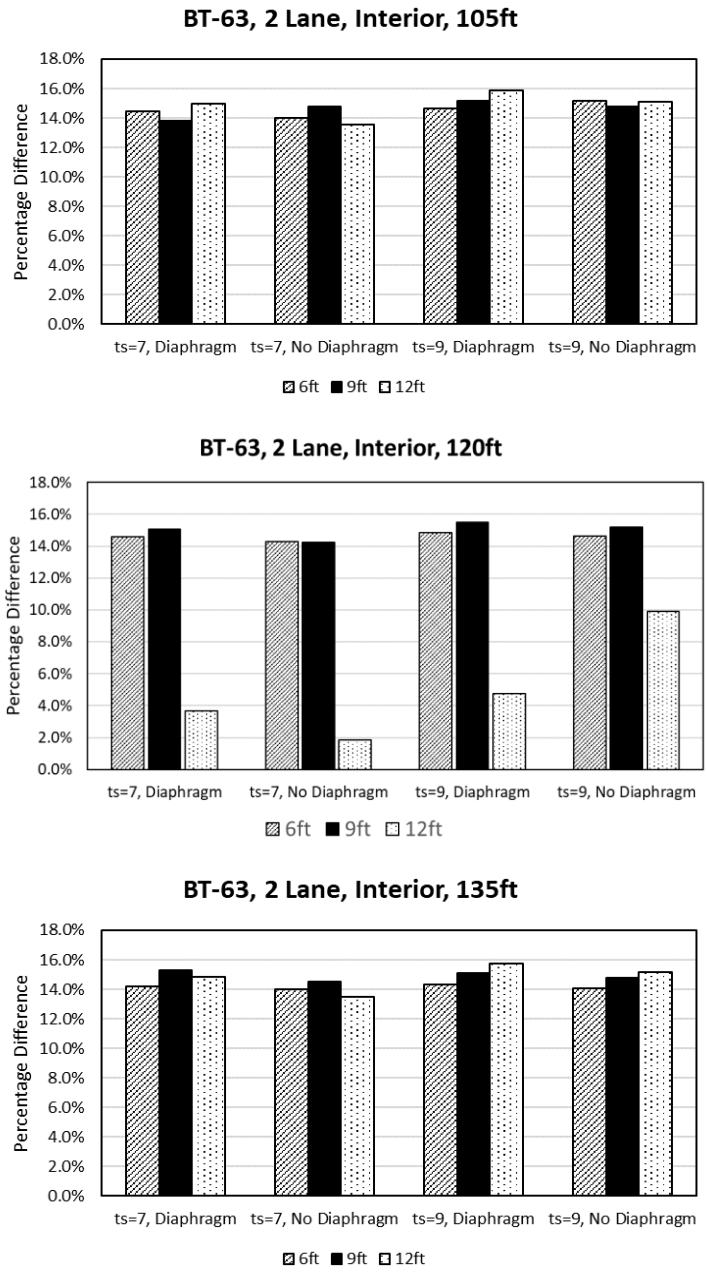

Figure 40. Percentage Difference Between AASHTO Equations and Grillage Models, for Two Lanes Loaded and Interior Girder, Type BT-63

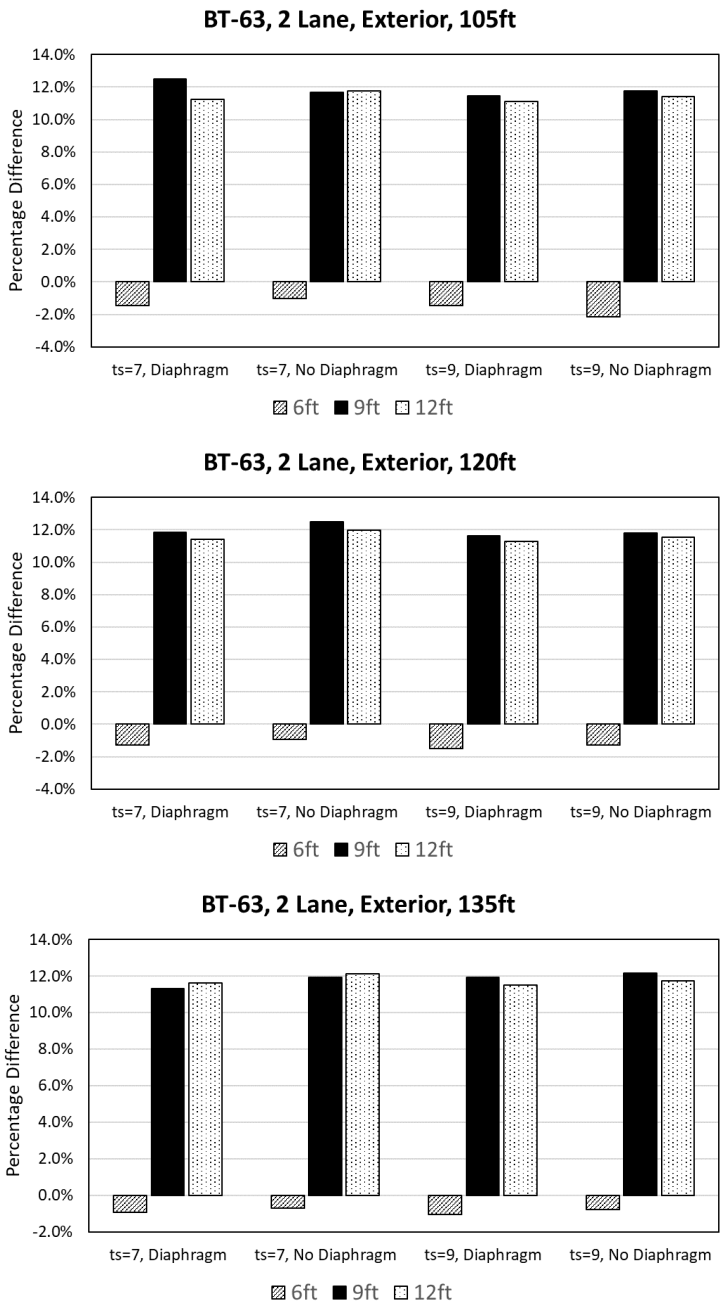

Figure 41. Percentage Difference Between AASHTO Equations and Grillage Models, for Two Lanes Loaded and Exterior Girder, Type BT-63

4.4.5: Quantitative Comparison of Load Distribution Factors

Figures 42 and 43 show linear trendlines for distribution factors determined for all BT-63 girder cases examined relative to girder spacing. Discussion on the use of a linear trendline for the quadratic AASHTO equation is provided in Section 4.2.5. For all cases, the results of grillage models were fit quite well with linear equations having coefficient of determination greater than 0.97. For all of the cases grillage model gave less steep trendlines than the AASHTO LRFD equations. The maximum percentage difference in slope was found for the two lanes loaded exterior girder case which was 28.1% and the minimum percentage difference was found for the one lane loaded interior girder case (2.7%). These results indicate that girder spacing had a large impact on load distribution factors and that the effect was less for grillage models than for the AASHTO equations.

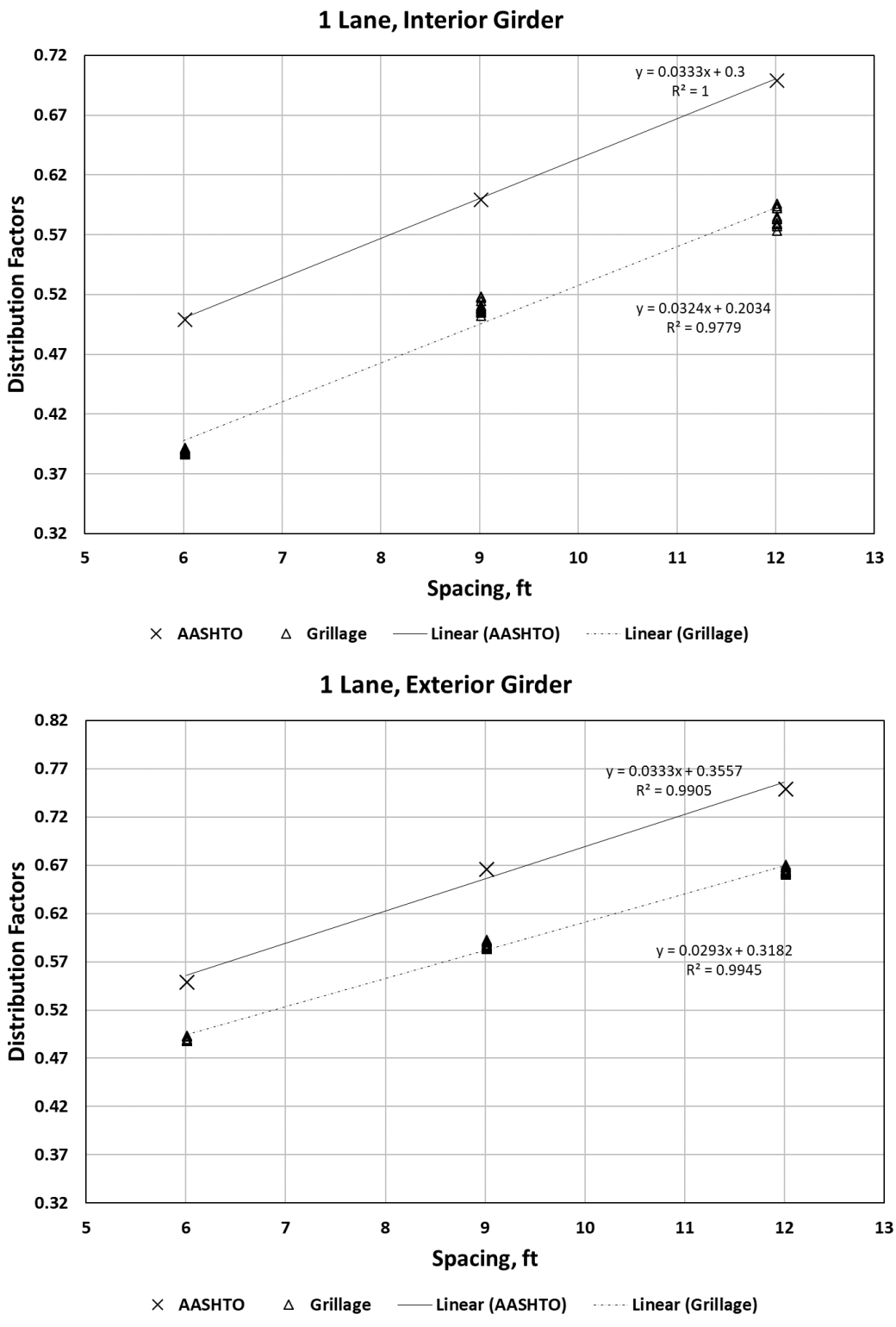

Figure 42: Linear Trendlines for Effect of Girder Spacing on Distribution Factors for BT-63 Girders, One Lane Loaded Case

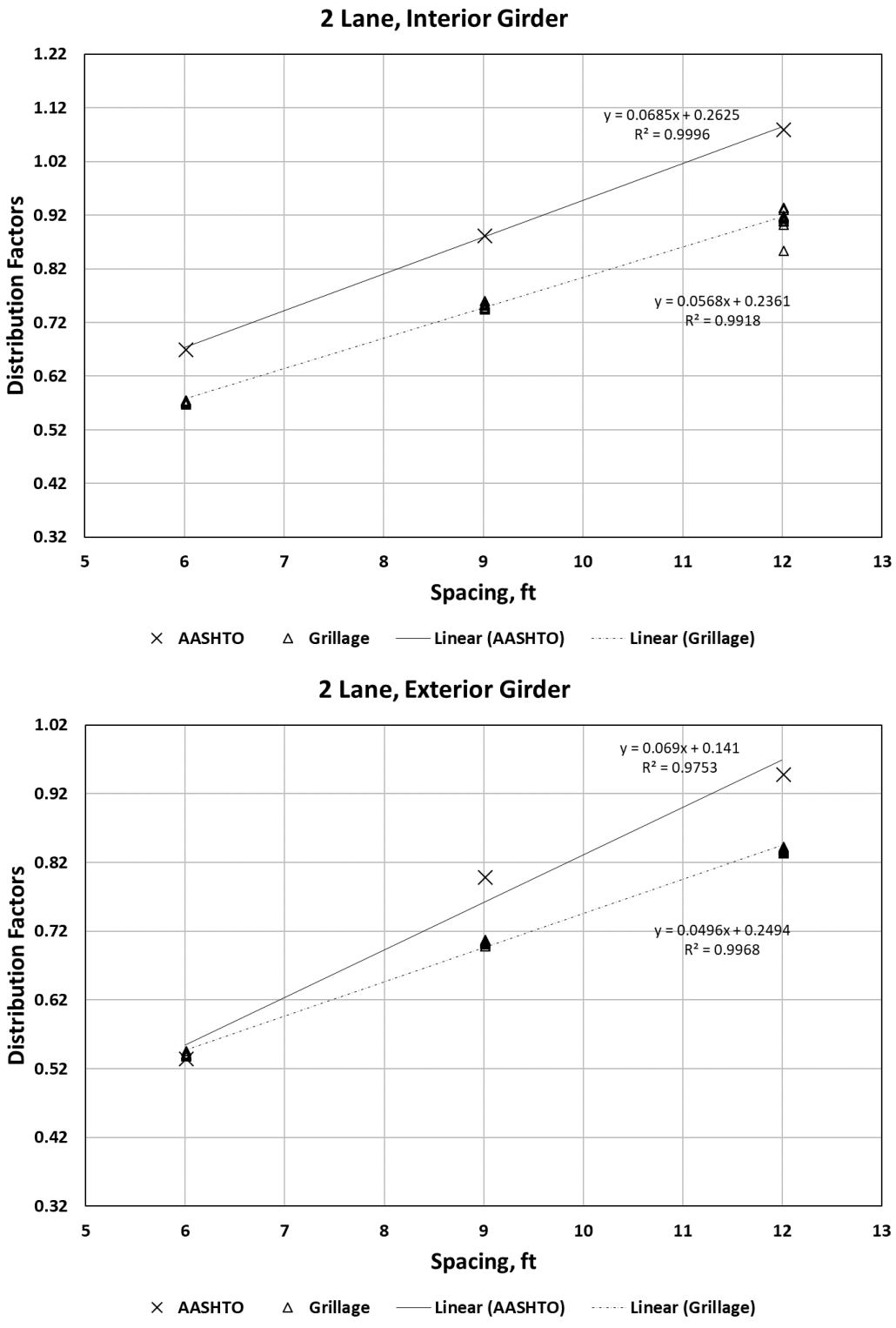

Figure 43: Linear Trendlines for Effect of Girder Spacing on Distribution Factors for BT-63 Girders, Two Lanes Loaded Case

4.5: BT-72 Girders

4.5.1: Effects of Girder Spacing

The distribution factors calculated using the AASHTO LRFD equations and from the grillage models for BT-72 girders are shown in Figures 44, 45, 46 and 47. The trends of change in distribution factor relative to girder spacing are very consistent between girder BT-63 and BT-72 girders. Even the percentage difference between AASHTO and grillage model distribution factors for BT-72 girders are quite close to those for BT-63 girders which can be seen from comparing Figures 38, 39, 40, and 41 and Figures 46, 47, 48, and 49.

4.5.2: Effects of Diaphragms

The effects of diaphragms on distribution factors for BT-72 girders are similar to those for all the other girders discussed previously. A difference of about 1% to 2% is observed when the percentage differences between AASHTO and grillage model factors for diaphragm and no diaphragm cases are compared as shown in Figures 48, 49, 50, and 51.

4.5.3: Effects of Deck Thickness

Similar to the Type-III, Type-IV and BT-63 girders, the effects of deck thickness are not remarkable. The change in deck thickness makes a very small impact of about 1% to2% on the difference between AASHTO and grillage model factors as shown in Figures 48, 49, 50, and 51.

4.5.4: Effects of Span Length

The percentage differences between AASHTO and grillage model factors shown in Figures 48, 49, 50, and 51 suggest only a 1% to 4% change in the percentage difference when the same configuration of bridge is compared with different span lengths.

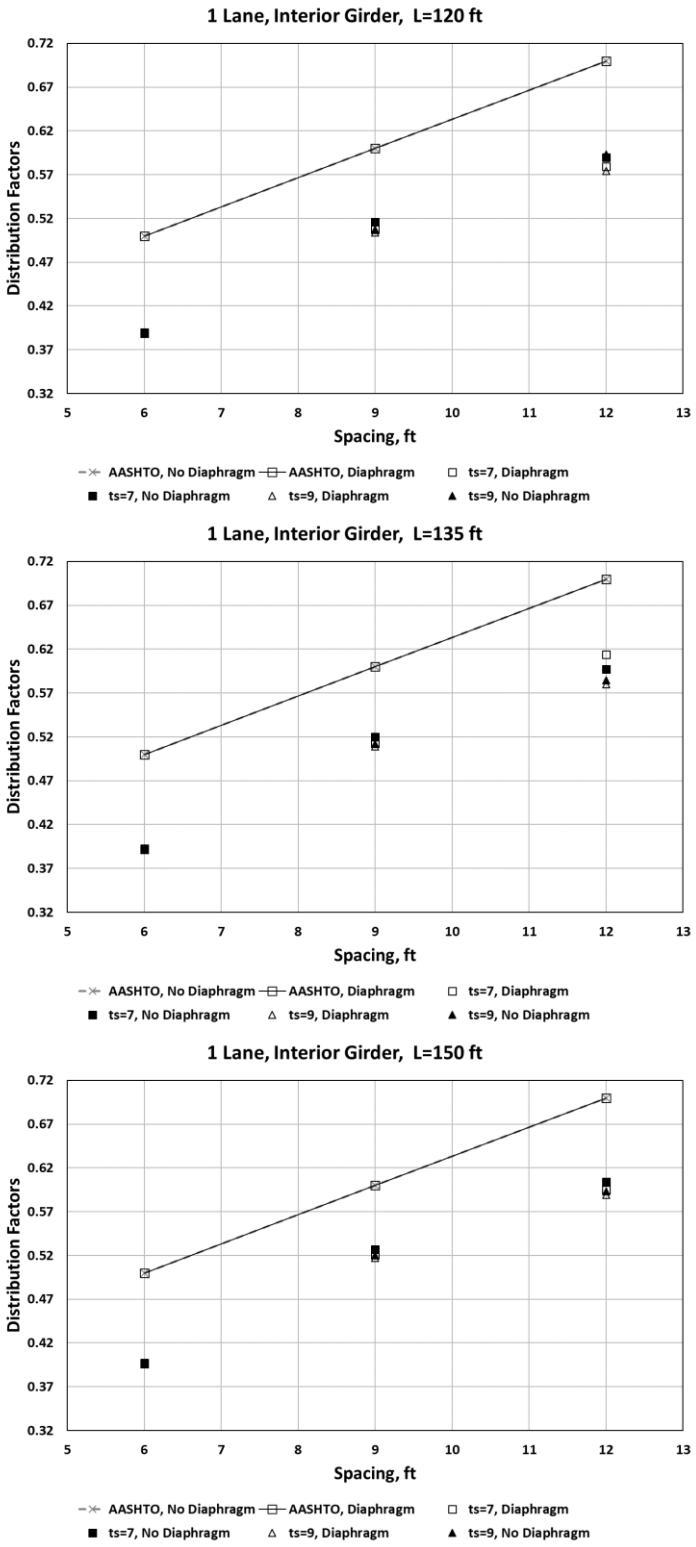

Figure 44. Distribution Factors for the Interior Girders, One Lane Loaded Versus Girder Spacing, BT-72

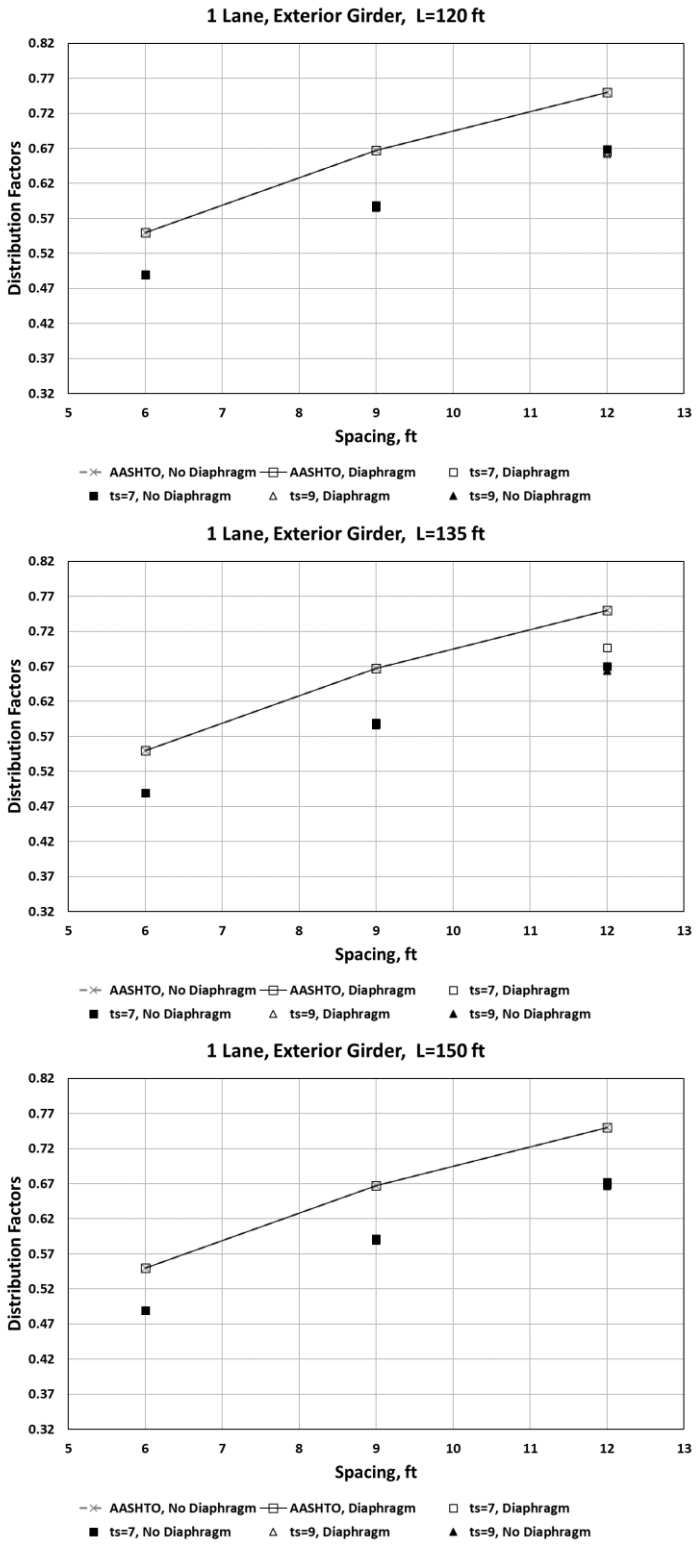

Figure 45. Distribution Factors for the Exterior Girders, One Lane Loaded Versus Girder Spacing, BT-72

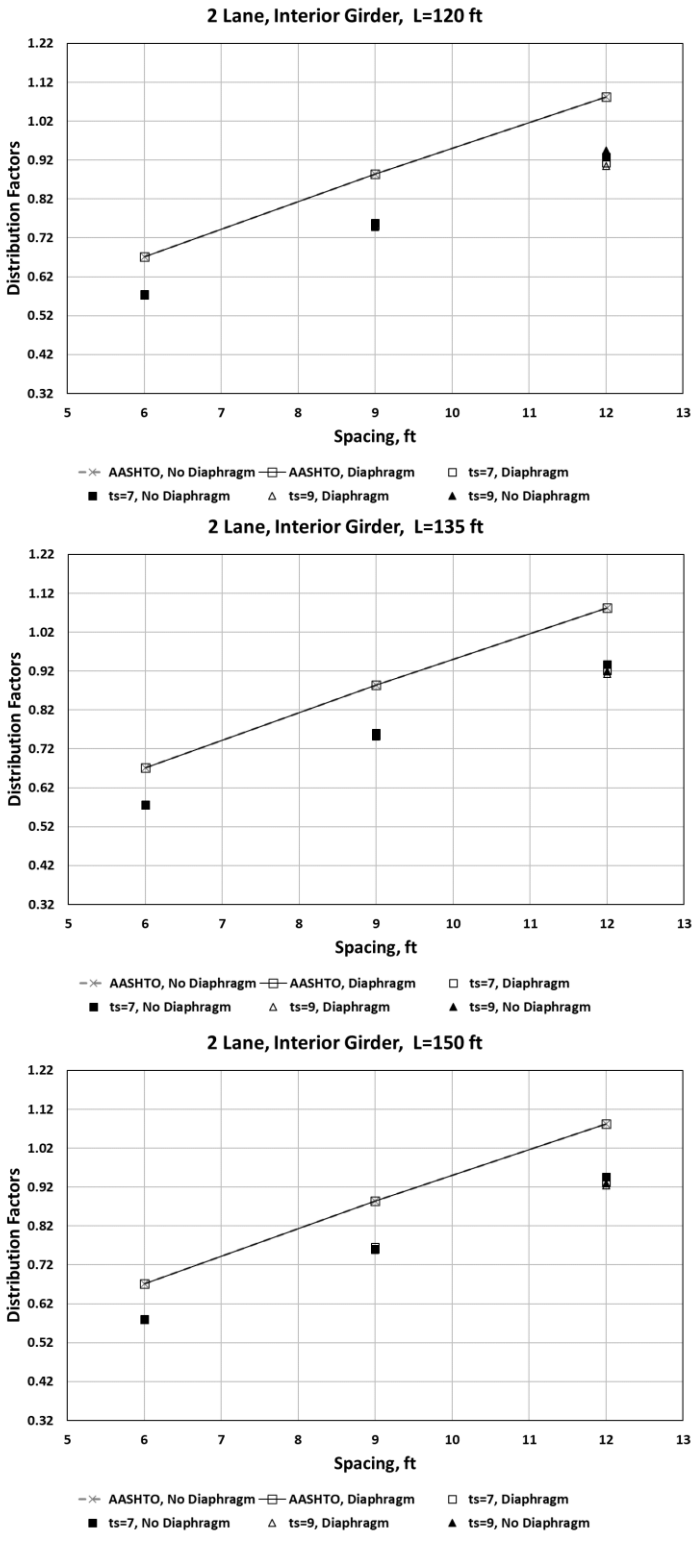

Figure 46. Distribution Factors for the Interior Girders, Two Lanes Loaded Versus Girder Spacing, BT-72

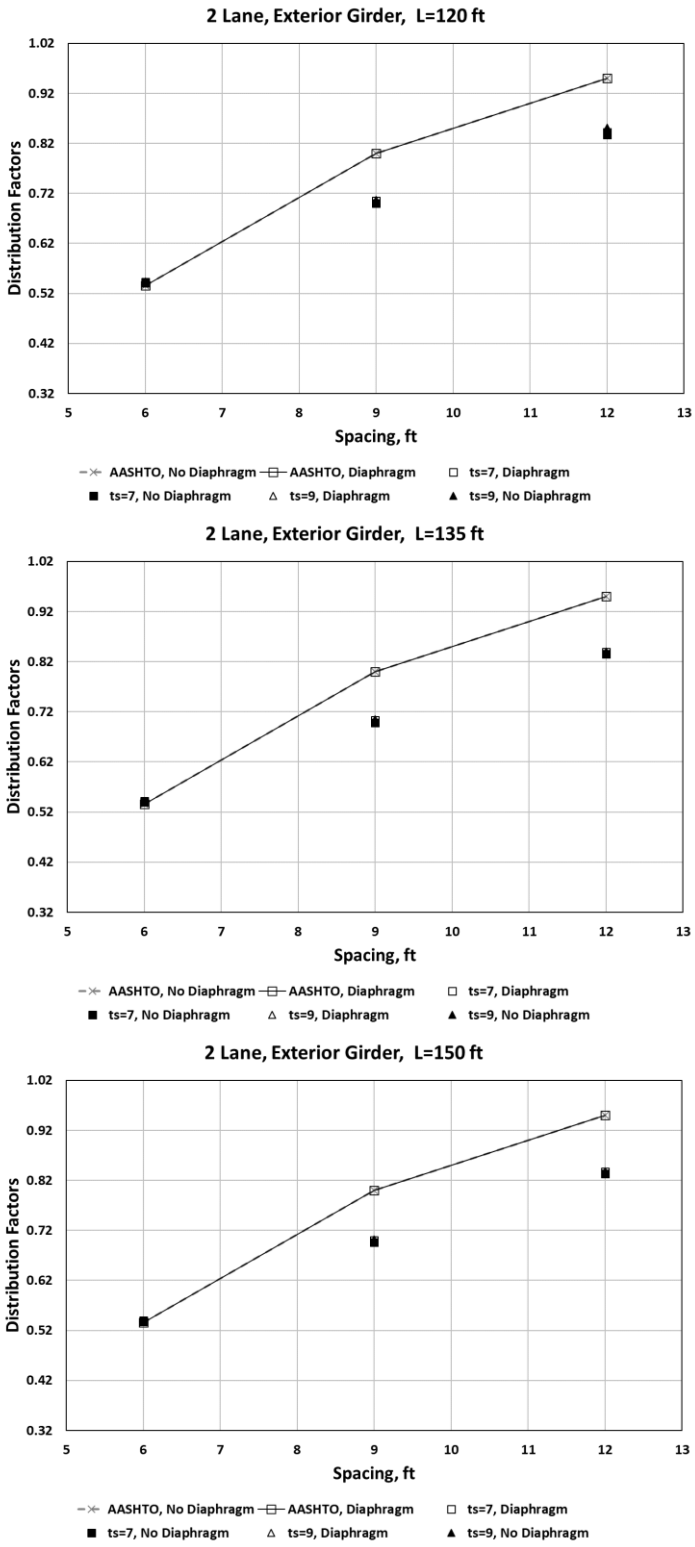

Figure 47. Distribution Factors for the Exterior Girders, Two Lanes Loaded Versus Girder Spacing, BT-72

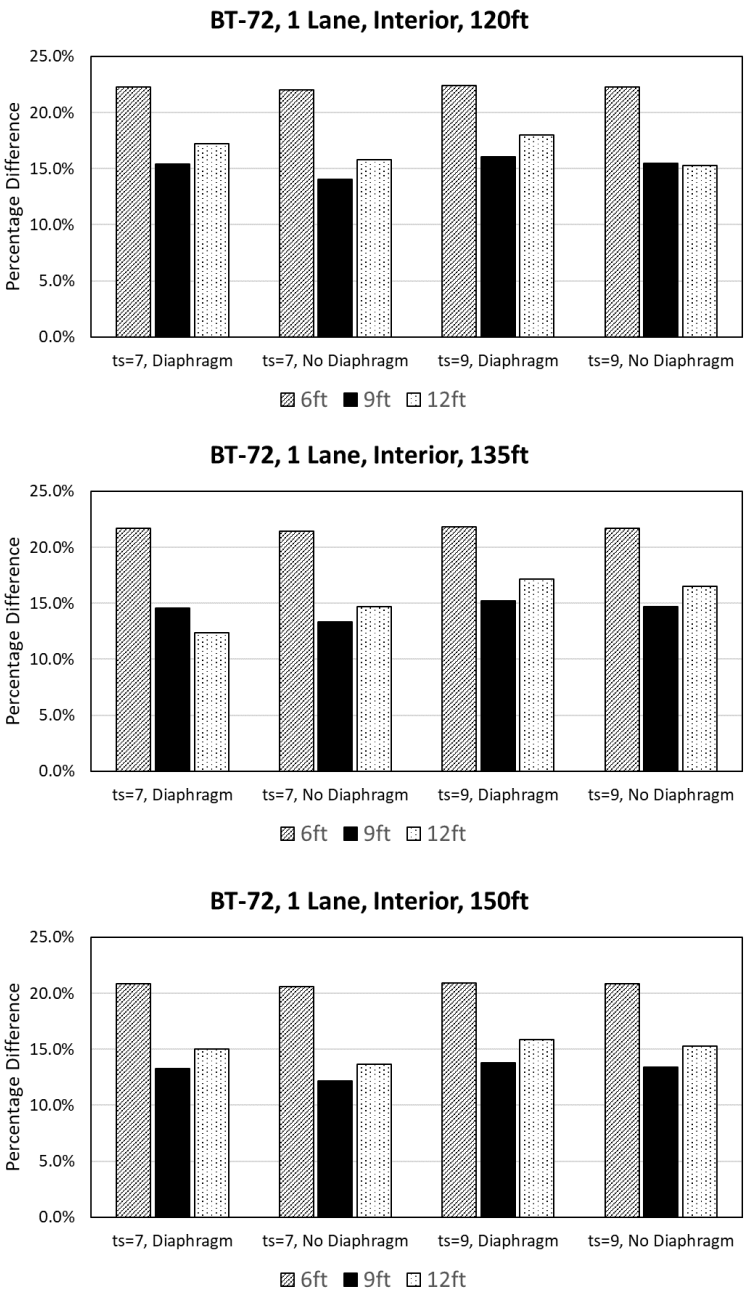

Figure 48. Percentage Difference Between AASHTO Equations and Grillage Models, for One Lane Loaded and Interior Girder, BT-72

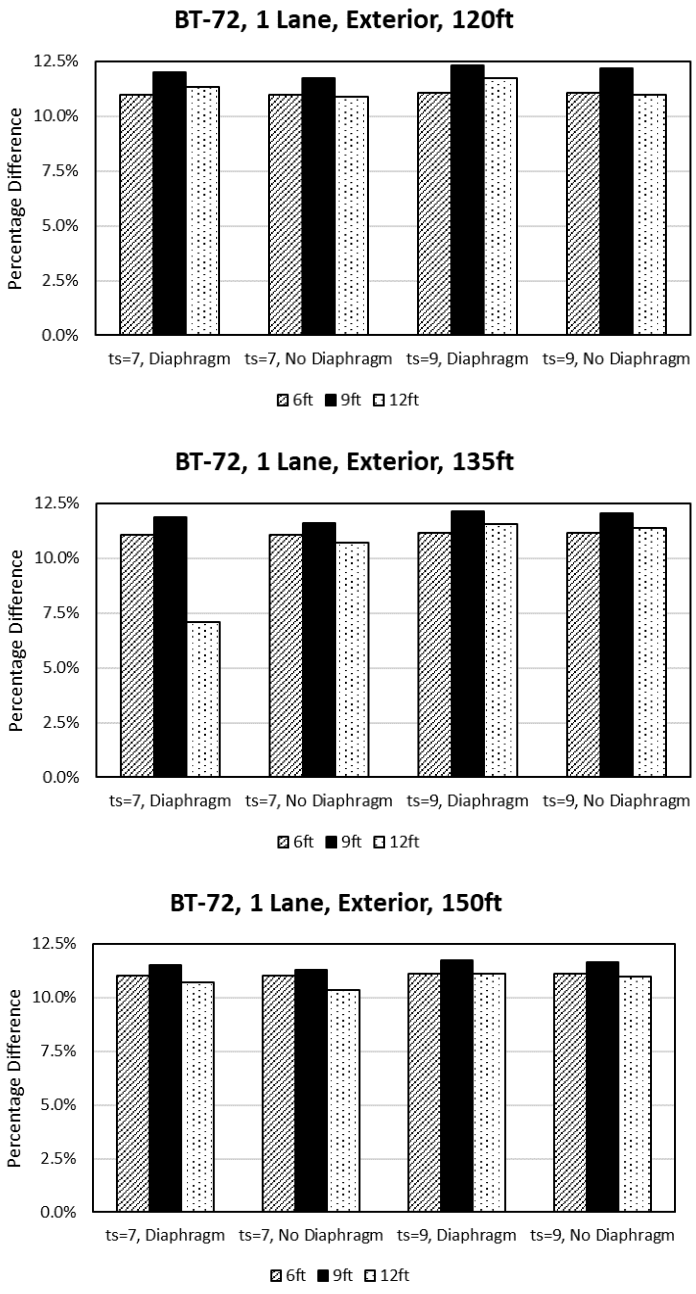

Figure 49. Percentage Difference Between AASHTO Equations and Grillage Models, for One Lane Loaded and Exterior Girder, BT-72

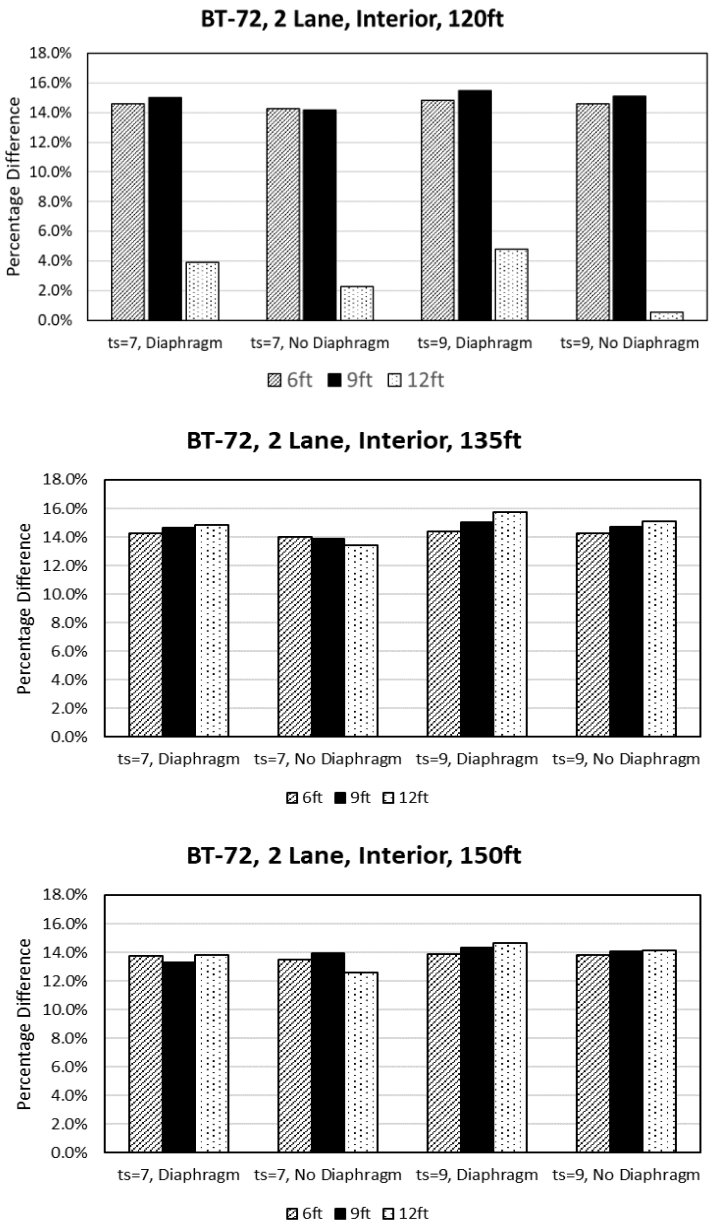

Figure 50. Percentage Difference Between AASHTO Equations and Grillage Models, for Two Lane Loaded and Interior Girder, BT-72

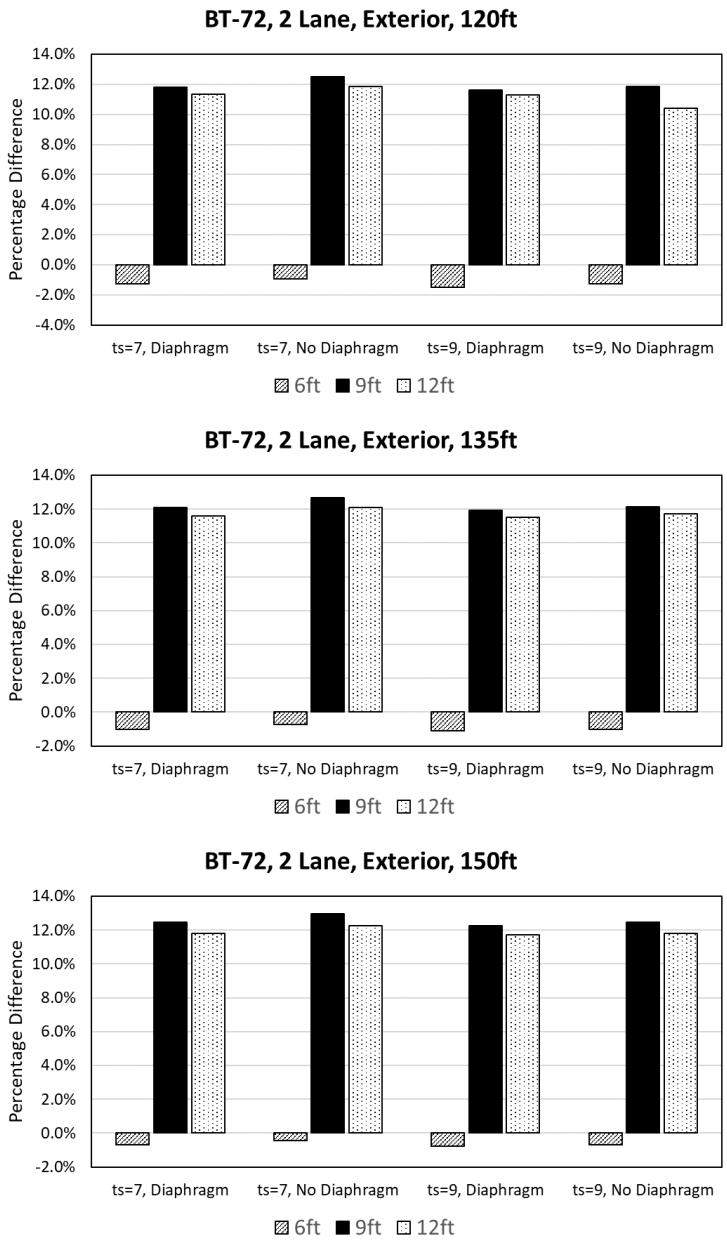

Figure 51. Percentage Difference Between AASHTO Equations and Grillage Models, for Two Lane Loaded and Exterior Girder, BT-72

4.5.5: Quantitative Comparison of Load Distribution Factors

Figures 52 and 53 show linear trendlines for BT-72 girder distribution factors determined from AASHTO LRFD and grillage models relative to girder spacing. Discussion on the use of a linear trendline for the quadratic AASHTO equation is provided in Section 4.2.5. Similar to results for BT-63 girders, the BT-72 load distribution factors determined from grillage models were fitted very well with linear equations with minimum coefficient of determination as 0.9751. For all of the cases, the trendlines from grillage model derived factors were less steep than the AASHTO LRFD equations. These results indicate that girder spacing had a large impact on load distribution factors and that the effect was less for grillage models than for the AASHTO equations.

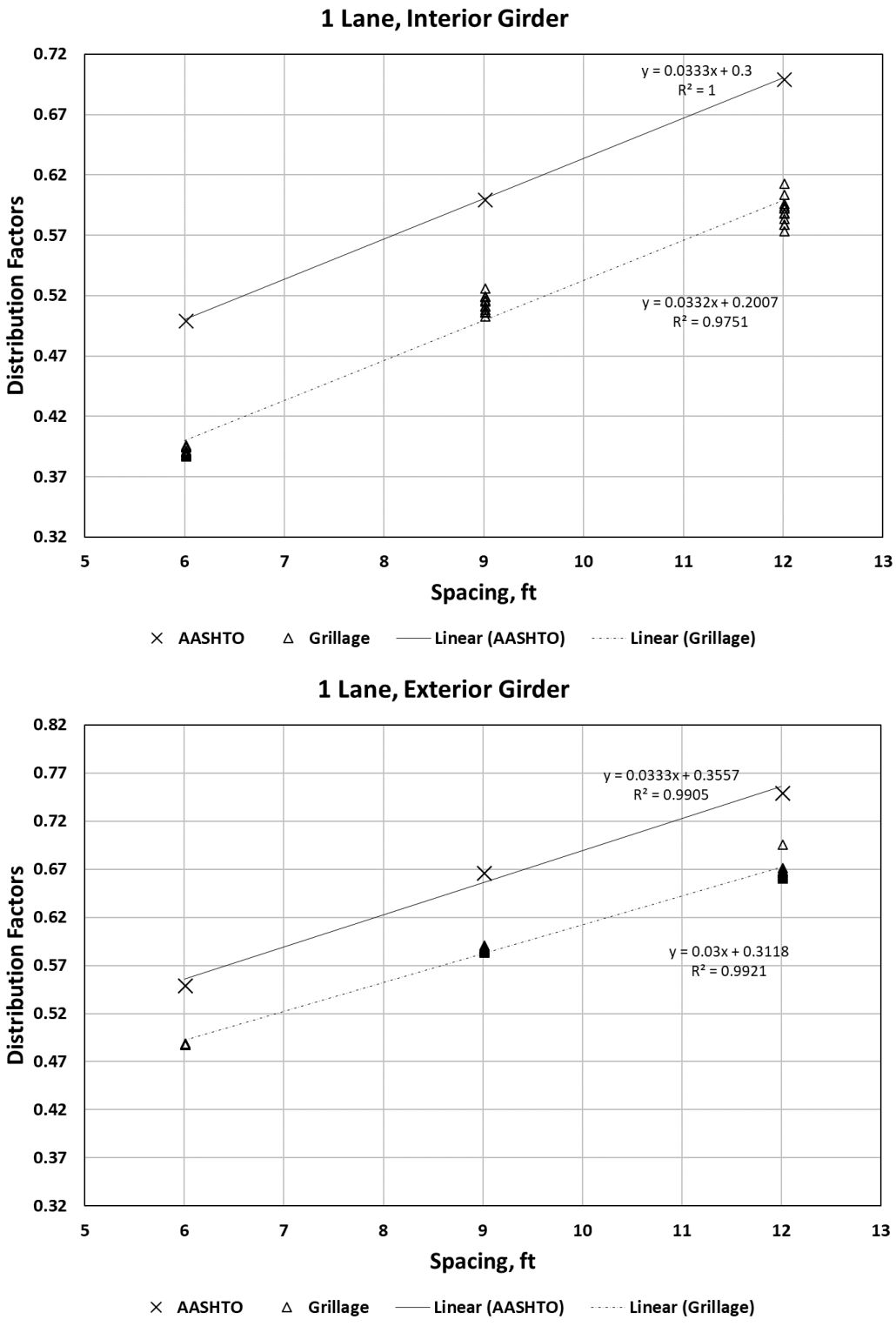

Figure 52: Linear Trendlines for Effect of Girder Spacing on Distribution Factors for BT-72 Girders, One Lane Loaded Case

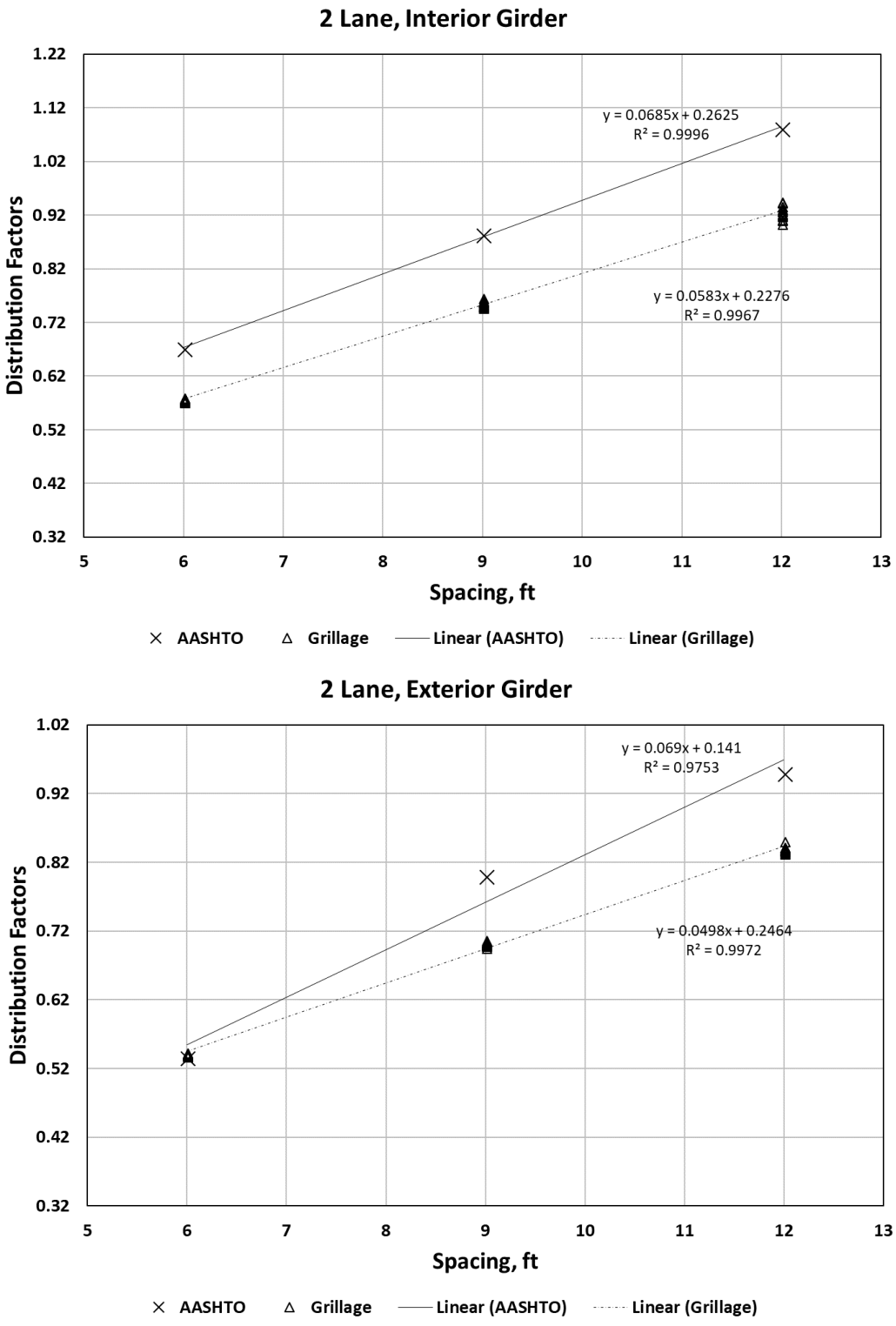

Figure 53: Linear Trendlines for Effect of Girder Spacing on Distribution Factors for BT-72 Girders, Two Lanes Loaded Case

4.6: Summary of Difference Between AASHTO Equations and Grillage Models

Table 4 presents a summary of the ranges of difference between the AASHTO LRFD distribution factors and the grillage model derived factors for all the configurations considered in this study. The major variable that controls the load distribution factor is the girder spacing, which is why Table 1 is organized based on different spacings. This table can be interpreted using for example when one lane loaded case is considered with a 6 ft spacing and interior girder the range of difference between the AASHTO LRFD and grillage mode load distribution factors is 16.3% to 21.0%. It should be noted that this range includes the effects of variations in the other three parameters considered, i.e. deck thickness, span length, and presence of diaphragms. Table 5 summarizes the slopes of trendlines of distribution factors relative to girder spacing plotted for AASHTO LRFD equations and the grillage models. For all of the cases the AASHTO LRFD equations produce a steeper slope than grillage models except for the one lane loaded interior girder case of Type-III girders. The largest deviation among slopes can be observed for the two lanes loaded exterior case for all of the girder types. The comparison of slopes indicates that the effect of girder spacing on distribution factors determined using grillage models was generally similar to or less than for the AASHTO equations.

Table 4: Ranges of Difference Between AASHTO and Grillage Load Distribution Factors (%)

		TYPE-III					
		6ft		9ft		12ft	
		Min	Max	Min	Max	Min	Max
Interior	One Lane	16.3	21.0	3.8	14.0	4.4	15.5
	Two Lane	11.9	14.2	3.4	13.5	2.7	13.6
Exterior	One Lane	4.9	5.3	5.7	11.2	5.8	7.5
	Two Lane	-0.4	-3.6	7.6	17.2	8.2	16.4
		TYPE-IV					
		6ft		9ft		12ft	
		Min	Max	Min	Max	Min	Max
Interior	One Lane	18.2	21.6	9.6	21.4	8.6	16.0
	Two Lane	12.3	14.7	10.9	13.9	7.0	14.0
Exterior	One Lane	5.3	6.4	6.4	7.3	6.4	7.8
	Two Lane	-0.6	-3.2	8.0	10.7	7.7	11.3
		BT-63					
		6ft		9ft		12ft	
		Min	Max	Min	Max	Min	Max
Interior	One Lane	21.5	22.5	13.5	16.1	14.7	18.0
	Two Lane	14.0	15.1	13.8	15.5	1.9	15.9
Exterior	One Lane	10.0	11.1	10.9	12.3	10.4	11.8
	Two Lane	-0.7	-2.2	11.3	12.5	11.1	12.1
		BT-72					
		6ft		9ft		12ft	
		Min	Max	Min	Max	Min	Max
Interior	One Lane	20.6	22.4	12.2	16.1	12.3	18.0
	Two Lane	13.5	14.8	13.3	15.5	12.6	15.7
Exterior	One Lane	11.0	11.1	11.3	12.3	7.1	11.8
	Two Lane	-0.4	-1.5	11.6	12.9	10.4	12.2

Table 5: Summary of Trendline Slopes

			AASHTO	Grillage Models	% Difference
Type-III	One Lane	Interior	0.0333	0.0371	-11.4
		Exterior	0.0333	0.0295	11.4
	Two Lanes	Interior	0.0685	0.0656	4.2
		Exterior	0.0690	0.0487	29.4
Type-IV	One Lane	Interior	0.0333	0.0329	1.2
		Exterior	0.0333	0.0299	10.2
	Two Lanes	Interior	0.0685	0.0629	8.2
		Exterior	0.0690	0.0518	24.9
BT-63	One Lane	Interior	0.0333	0.0324	2.7
		Exterior	0.0333	0.0293	12.0
	Two Lanes	Interior	0.0685	0.0568	17.1
		Exterior	0.0690	0.0496	28.1
BT-72	One Lane	Interior	0.0333	0.0332	0.3
		Exterior	0.0333	0.0300	9.9
	Two Lanes	Interior	0.0685	0.0583	14.9
		Exterior	0.0690	0.0498	27.8

4.7: Validation of Plate Models

The grillage modeling method used in this study was compared with experimental results from a scaled bridge test by a former student (Murray, 2017). The results from the experimental study done by Dr. Murray (Murray, 2017) are also used in this thesis to compare with the results of the plate model to confirm the applicability of the plate modeling methods.

The reactions and deflections for the bridge test and grillage models in Table 5 are taken from Dr. Murray's work. The section and plan layout of the tested bridge used for comparison are shown in Figure 54 (Murray, 2017). There were two scenarios under which the bridge was tested. In the first case, a 40 kips load was applied on beam A5 and in the second case, a 30 kips load was applied on beam A4. A plate model was developed (described in Section 3.4) to compare results with the grillage model and

results from the tested bridge. The geometry of the bridge and applied loads in the plate model were same as used in the grillage model and tested bridge. The mesh size of plate was 2 in. x 3 in. for the plate model. The results from the plate model shown in Table 6 are quite close to those from grillage models. The principles of statics are proven by all the models. When the 40 kips load is applied 4.5 ft from one end of the bridge then the total reaction on the end of the bridge nearest the load will be 30 kips and on the other end 10 kips. The summation of support reactions on the end of the bridge nearest the load is 30 kips for both types of models. The summation of all the support reactions was 40 kips for the 40 kips load on beam A5 case and 30 kips when the load of 30 kips was applied on beam A4. The deflections and the support reactions from the plate models are comparable with the grillage model and tested bridge results which validates the applicability of the plate models used.

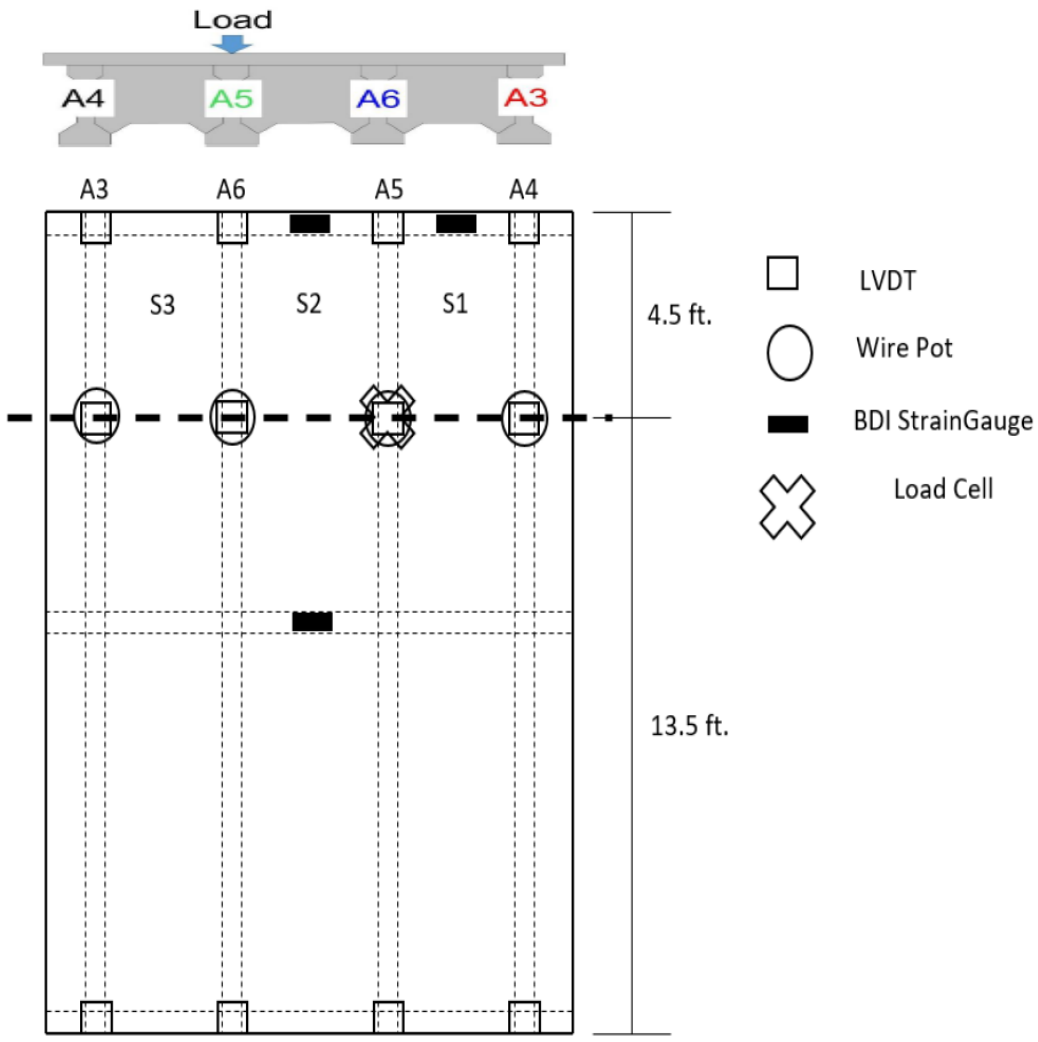

Figure 54. Section and plan of test bridge (Courtesy: Dr. Murray)

Table 6. Comparison of Bridge Test with Grillage and Plate Models

Load Position		From Bridge Test		From Grillage Model		From Plate Model	
		Support Deflection (in.)	Expressed as reaction force (kips)	Support Deflection (in.)	Expressed as reaction force (kips)	Support Deflection (in.)	Expressed as reaction force (kips)
A5 (40 kips)	A4	0.019	5.150	0.022	6.670	0.022	6.650
	A5	0.058	15.440	0.053	16.060	0.053	15.927
	A6	0.033	8.910	0.026	7.880	0.027	8.157
	A3	0.002	0.510	-0.002	-0.610	0.004	-0.737
	∑	0.113	30.000	0.099	30.000	0.106	30.000
A4 (20 kips)	A4	0.027	9.450	0.043	12.900	0.043	12.913
	A5	0.018	6.310	0.011	3.300	0.011	3.193
	A6	0.002	0.760	-0.001	-0.300	0.002	-0.344
	A3	-0.004	-1.520	-0.003	-0.900	0.003	-0.762
	∑	0.044	15.000	0.050	15.000	0.059	15.000

4.8: Comparison of Plate and Grillage Models

For the comparison of grillage models with plate models, only the extreme parameters were considered. Type-III and BT-72, the shallowest and deepest girders, respectively, considered in the study along with the smallest and largest girder spacing were considered for comparison. Even though the results for the grillage and plate models presented in Table 6 are almost identical and validate the modeling paradigm, they are still not conclusive because of the smaller size of the bridge. The differences can be analyzed in a better way by comparing models of real bridges. Table 7 summarizes the models considered for this comparison.

Table 7. Bridge plate models (deck thickness in in. on interior of table)

Girder	Spacing (ft)	Length (ft)				
		45		75		
Type-III	6	7	9	7	9	Diaphragm
		7	9	7	9	No Diaphragm
	12	7	9	7	9	Diaphragm
		7	9	7	9	No Diaphragm
Girder	**Spacing (ft)**	**Length (ft)**				
		120		150		
BT-72	6	7	9	7	9	Diaphragm
		7	9	7	9	No Diaphragm
	12	7	9	7	9	Diaphragm
		7	9	7	9	No Diaphragm

4.9: Discussion on Distribution Factors Calculated from Plate and Grillage Models

Figures 55 – 62 present comparisons of the load distribution factors determined using plate and grillage models. These figures not only compare the grillage and plate model results, but also show the impact of the diaphragms, girder spacing and deck thickness. It can be observed that when the Type-III and BT-72 girders are compared, the bars representing load distribution factors follow the same pattern for most cases. To simplify the situation, the comparisons are divided into eight sets of graphs. For the 12 ft spacing and two lanes loaded case, as shown in Figures 55 and 56, the plate model gives larger load distribution factors than grillage model for the exterior girder and vice versa for the interior girder. For the one lane loaded case and 12 ft spacing the behavior is opposite that of two lanes loaded case as shown in Figures 57 and 58.

When the spacing of the girders is 6 ft and two lanes are loaded, the pattern is the same as 12 ft spacing and two lanes loaded as shown in Figure 59 and 60. For the one lane loaded case with 6 ft spacing the pattern is different for the different types of girder. For

Type-III girders, plate models give greater load distribution factor for exterior girders and grillage models give greater load distribution factors

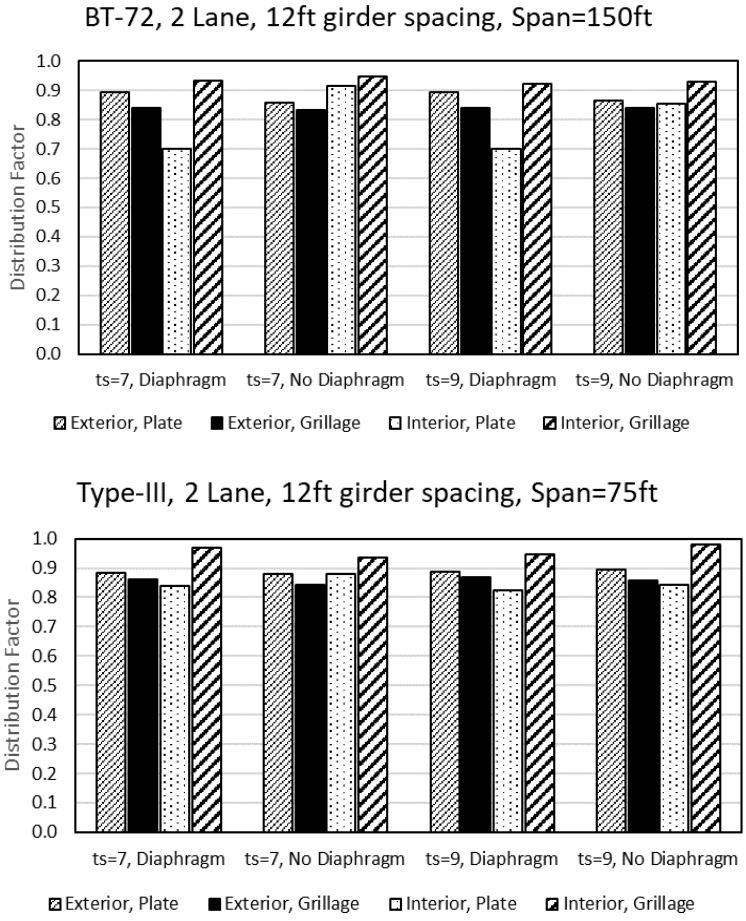

Figure 55. Comparison of Plate and Grillage Models for 12 ft Spacing and 2 Lanes Loaded Case with Larger Spans

for interior girders. The results are opposite in case of BT-72 girders as shown in Figures 61 and 62. The governing load cases should also be kept in mind (discussed in section 3.3) to better understand of these patterns because these graphs are based on multiple load cases. It can be observed from Figures 57 and 59 that diaphragms had a negligible impact on load distribution factor when grillage models were used for these configurations. The plate models, however, exhibited larger effects from the presence of

diaphragms. To determine the maximum load distribution factor for the interior beam, the center of the 6 ft wide HS-20 truck was placed over the interior beam

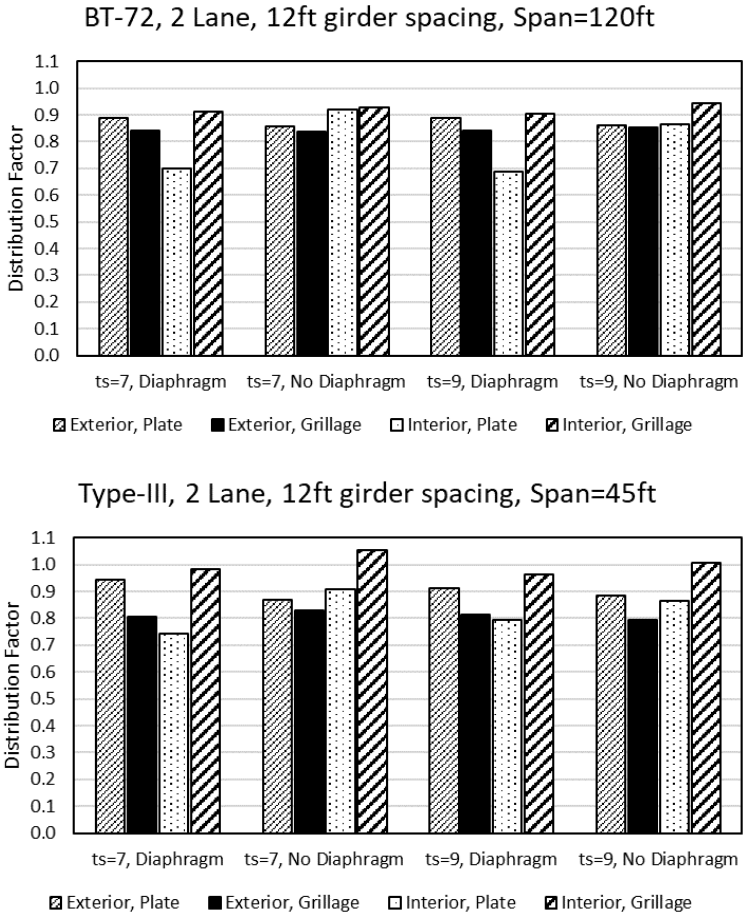

Figure 56. Comparison of Plate and Grillage Models for 12 ft Spacing and 2 Lanes Loaded Cases with Smaller Spans

(load cases are discussed in chapter 3). Since plate models have better lateral load distribution than the grillage models, the plate models always had a smaller load distribution factor for interior beams than the grillage models.

A variation in load distribution factor for interior and exterior girders is noticeable when diaphragm and no diaphragm cases are compared for plate models. This variation is not significant in grillage models. Figures 59 and 60 present the 2 lanes loaded case with 6

ft girder spacing. All the load distribution factors shown in Figures 51 and 52 are almost the same. Only four girders are used for all the models. Therefore, for a 6 ft

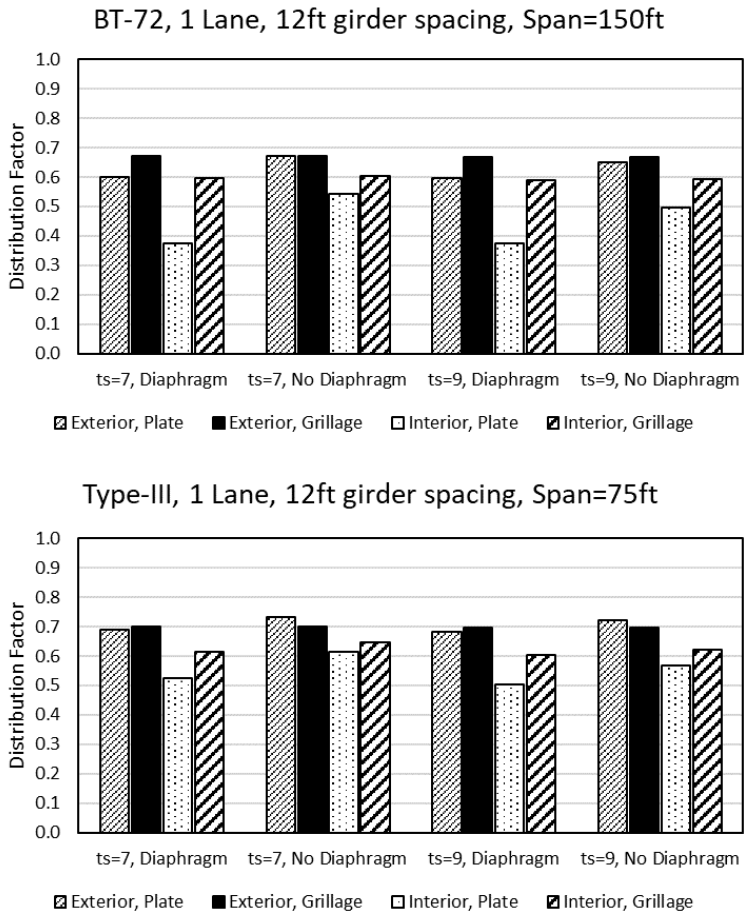

Figure 57. Comparison of Plate and Grillage Models for 12 ft Spacing and 1 Lane Loaded Case with Larger Spans

girder spacing, the width of the deck is 22 ft if a 2 ft overhang is included on each side and the distance from first girder to the last is 18 ft. When two HS-20 are placed on this bridge configuration, most of the bridge deck is loaded and it is difficult to determine the impact of different parameters, including the use of a plate for the deck. Figures 53 and 54 show the load distribution factors for the 6 ft girder spacing and one lane loaded case. In this case, there is not much impact visible from the diaphragms because of the

small girder spacing. The results show that diaphragms only impact the distribution factors when the spacing is much higher than 6 ft. It can be noticed that the load distribution factor for the Type-III exterior girder is higher than the load distribution factor for the BT-72 exterior girder. It could have been due to the span length, which changes the distance between end and intermediate diaphragms. When only the section properties of Type-III girder were changed to BT-72, the lateral distribution improved, and the exterior girder attracts less force thus resulting in a smaller load distribution factor. It can therefore be said that lateral distribution is better with the stiffer girders.

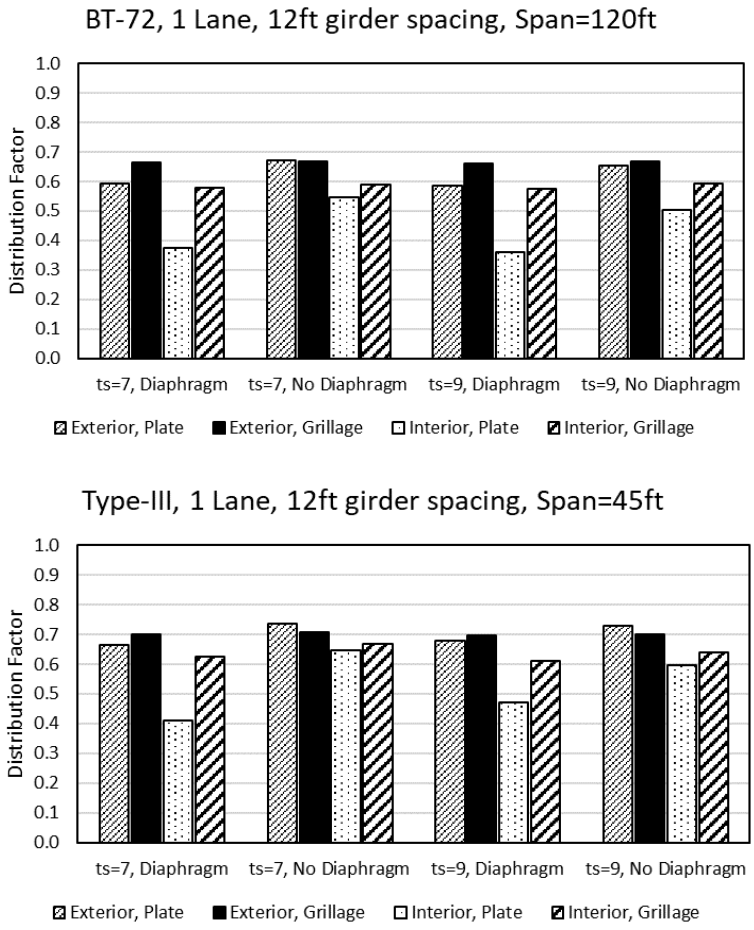

Figure 58. Comparison of Plate and Grillage Model for 12 ft Spacing and 1 Lane Loaded Case with Smaller Spans

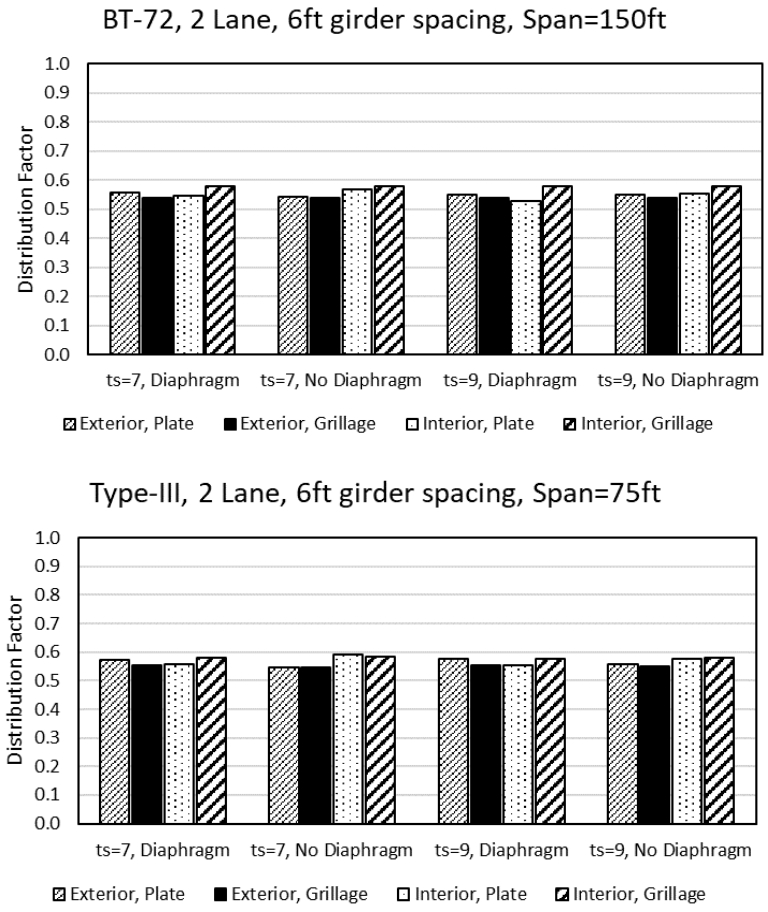

Figure 59. Comparison of Plate and Grillage Model for 6 ft Spacing and 2 Lanes Loaded Case with Larger Spans

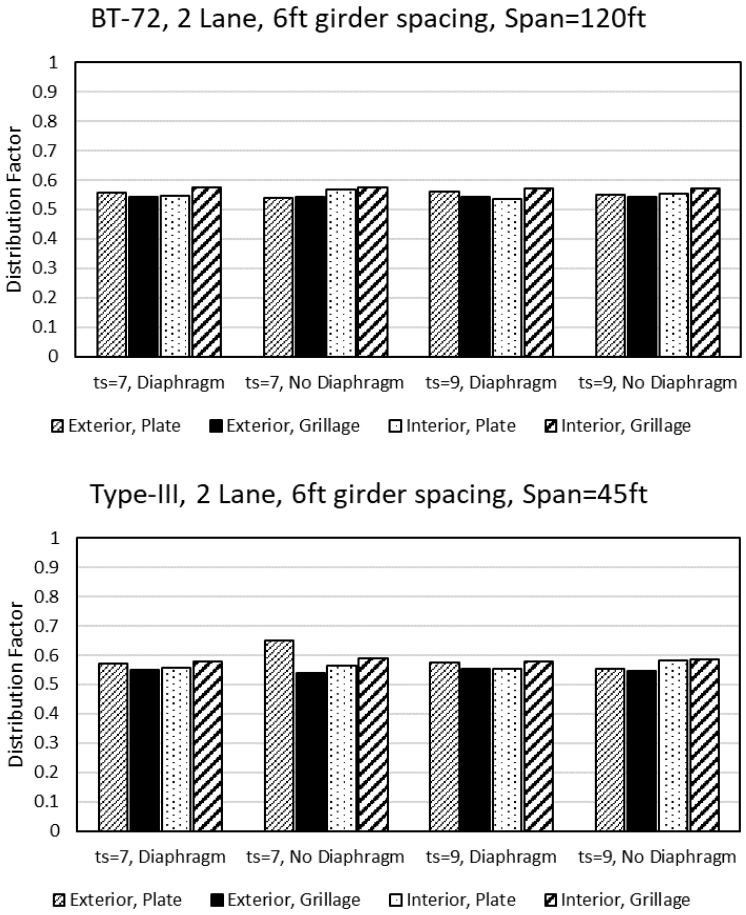

Figure 60. Comparison of Plate and Grillage Models for 6 ft Spacing and 2 Lanes Loaded Case with Smaller Spans

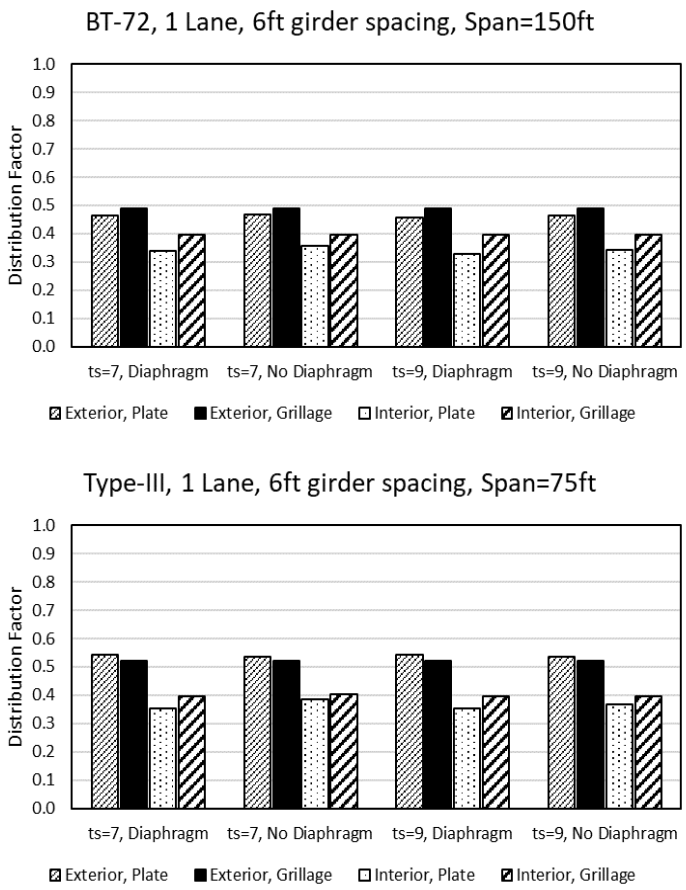

Figure 61. Comparison of Plate and Grillage Models for 6 ft Spacing and 1 Lane Loaded Case with Larger Spans

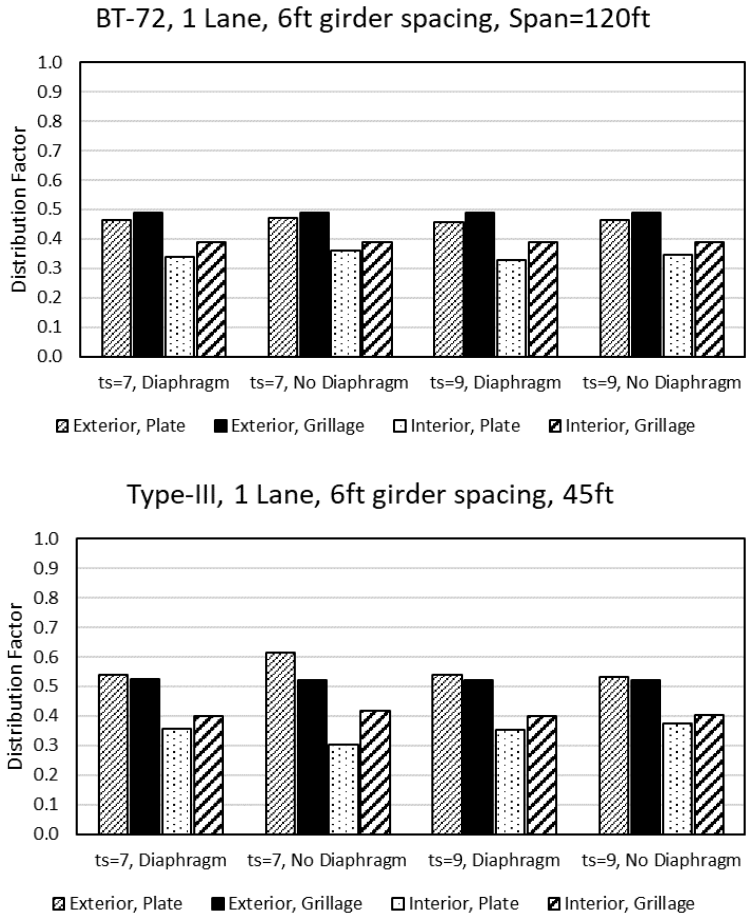

Figure 62. Comparison of Plate and Grillage Models for 6 ft Spacing and 1 Lane Loaded Case with Smaller Spans

Chapter 5: Summary, Conclusion and Recommendations

5.1 Summary

The bridge infrastructure in United States is aging. As bridges age and codes change it is important to have an accurate understanding of the capacity and demands on these bridges in order to load rate a bridge in the most effective manner. In some cases, it may be useful to utilize possible conservatism available in the AASHTO LRFD equations for load distribution to fulfill the need of accurately checking the bridge for adequacy. Different bridge modeling techniques are required to do so. In this study grillage models

with different variations of parameters were developed to make comparison with AASHTO LRFD equations. Grillage models have the potential to provide accurate results while still being relatively easy to implement by bridge engineers. The grillage modeling technique used in this research was previously compared with the scaled bridge tested by Dr. Murray (Murray 2017) and found to be reasonable. The same bridge configuration was developed using the plate modeling technique and results were not different from grillage model results and compared similarly to the scaled bridge results. The effects of girder spacing, diaphragms, deck thickness, and span length on shear load distribution factors were studied by developing 144 grillage models and 32 plate models of different bridge configurations. The different variables examined include the girder types Type-III, Type-IV, BT-63 and BT-72, the deck thicknesses of 7 in. and 9 in., and the girder spacings of 6 ft, 9 ft, and 12 ft. The effects of diaphragm are also studied by adding diaphragms to all the models and spans were varied as appropriate for the girder type.

5.2 Conclusions

The following specific conclusions can be drawn from the results of the work explained in this thesis and are only directly applicable to similar situations.

- The shear load distribution factor given by the AASHTO LRFD equations for interior girders increases linearly with an increase in girder spacing for the one lane loaded case, and it increases bilinearly for two lane loaded case. For the exterior girder one and two lanes loaded cases, the load distribution factor increases bilinearly for girder spacings used. The grillage model gives a bilinear

relationship for the shear load distribution factor in all four load cases for all girder types.

- All the shear load distribution factors calculated using the AASHTO LRFD equations were greater than grillage model results except for the two lanes loaded case for an exterior girder with 6 ft spacing for all girder types. For the one lane and two lanes loaded case for interior girders, the AASHTO LRFD equation shear load distribution factors were found to be 3.8% to 22.5% and 1.9% to 15.9%, respectively, greater than the corresponding grillage model derived factors. For the exterior girder one lane loaded case the AASHTO LRFD equation shear load distribution factors were 4.9% to 12.3% greater than those determined using the grillage model. For the exterior girder two lanes loaded case with 6 ft spacing the grillage models gave greater shear load distribution factors than the AASHTO LRFD equation by a maximum of 3.6% and for other spacings the distribution factors calculated using the AASHTO LRFD equation were greater than those derived from the grillage models by a maximum of 17.2%. It should be noted that the ranges given here include influence of all the parameters considered.
- The deck thickness did not substantially affect load distribution. The change in load distribution factors, determined using grillage model, when the deck thickness was changed from 7 in to 9 in for a given set of conditions was 0% to 6% for Type-III and Type-IV girders. The change was 0% to 3% for BT-63 and BT-72 girders for all the cases. In one odd case of BT-63 girder bridge configurations the percentage change was 8.1%.

- The effect of span length on shear load distribution reduces with increases in span length. A minimum span length of 45 ft and maximum of 150 ft were used in this study. When the models with span lengths of 45 ft and 60 ft were compared with all other remaining parameters remaining identical, the range of change in load distribution factor determined using grillage models was 0.2% to 7.6%. When the spans lengths of 135 ft and 150 ft were considered the percentage change was only 0% to 3.6%.
- When the results of Type-III grillage models were compared with Type-IV grillage models the maximum change in load distribution factors was 10.7%. This difference was reduced to maximum of 5.2% when models of Type-IV girders were compared with BT-63 girder models. Finally, maximum change in percentage is further reduced to a maximum of 4.0% when BT-63 grillage models were compared with BT-72 grillage models.
- The effect of intermediate diaphragms on shear load distribution reduces with increases in span length. It should be noted that there was only one intermediate diaphragm provided for each span length, therefore with an increase in span length the distance between end and intermediate diaphragms also increased. The maximum impact of diaphragm on percentage change in load distribution between cases when no diaphragm or diaphragm was included for the 45 ft span was 7.7% while it was 3.8% for the 90 ft span and only 2.7% for 135 ft span.
- The plate model and grillage model results were quite comparable. A deviation was observed when the spacing between the girders increased. The impact of

diaphragm on load distribution was more for plate models than grillage models particularly when the girder spacing is high.

- The effect of eccentricity in the plate models was more evident for large girder spacings. This effect was negligible for a small spacing such as 6 ft.

5.3 Recommendations

The following recommendations for future research and potential modification to methods used in this study are made based on analysis of the results of this study.

- Models with more than one intermediate diaphragm should be considered to study the effect on load distribution for longer spans.
- Reducing the spacing between the transverse elements of the grillage models to the maximum of 1.5 times the spacing of girders should be considered to examine the effect of transverse element spacing on the load distribution, especially for longer spans.
- Field tests of actual bridge should be carried out to obtain results for comparison with grillage and plate model results for full-scale bridges.
- Deck overhangs of different lengths should be considered to study the effect on exterior girders.
- Actual truck load data can be collected from Oklahoma Department of Transportation and used to calculate load distribution factor and reactions using plate or grillage models to make comparison with AASHTO equations.

References

AASHTO, L. Bridge Design Specifications, 1994, American Association of State Highway and Transportation Officials. *Inc.*, *CG*, *6*(1), 2-5.

AASHTO, LRFD (1998). Bridge design specifications.

AASHTO. (2014). "AASHTO LRFD Bridge Design Specifications". Washington, D.C.: American Association of State Highway and Transportation Officials.

ASCE. (2017). "Infrastructure Report Card". Retrieved from: https://www.infrastructurereportcard.org/cat-item/bridges/

Barr, P. J., Eberhard, M. O., and Stanton, J. F. (2001). "Live-load distribution factors in prestressed concrete girder bridges." J. Bridge Eng., 10.1061/(ASCE) 1084

Cai, C. S., Araujo, M., Chandolu, A., Avent, R. R., & Alaywan, W. (2007). Diaphragm effects of prestressed concrete girder bridges: Review and discussion. *Practice Periodical on Structural Design and Construction*, *12*(3), 161-167.

Cross, B., Vaughn, B., Panahshahi, N., Petermeier, D., Siow, Y. S., & Domagalski, T. (2009). "Analytical and experimental investigation of bridge girder shear distribution factors. Journal of Bridge Engineering", 14(3), 154-163.

Dicleli, M. and Erhan, S. (2009) "Live Load Distribution Formulas for Single-Span Prestressed Concrete Integral Abutment Bridge Girder" J. Bridge Eng., 10.1061/_ASCE_BE.1943-5592.0000007, 472-486

Eamon, D. C., Chehab, A. and Parra-Montesinos, G. (2016) "Field Test of Two Prestressed-Concrete Girder Bridges for Live-Load Distribution and Moment Continuity" J. Bridge Eng., 10.1061/(ASCE)BE.1943-5592.0000859, 1-12

Eby, C. C., Kulicki, J.M., and Kostem, C. N., (1973). "The evaluation of St. Venant torsional constant for prestressed concrete I-beam." Fritz Engineering Laboratory Rep. No. 400.12, Lehigh Univ., Bethleham, Pa.

Garcia, T. M. (1999, October). IDs for precast prestressed concrete bridges. In *Western Bridge Engineer's Seminar, Seattle, Washington*.

Ghali, A., & Neville, A. M. Structural analysis: a unified classical and matrix approach. 1997.

Hambly, E. C., (1991). "Bridge Deck Behaviour (2nd Ed.)". CRC Press.

LADOTD "Bridge Design Manual." Louisiana Department of Transportation and Development, Baton Rouge, LA, 2002.

Murray, C. D. (2017). "Understanding ultimate shear behavior of prestressed concrete girder bridges as a system through experimental testing and analytical methods". University of Oklahoma, Norman, OK.

National Cooperative Highway Research Program (NCHRP)., (1992). "Distribution of wheel loads on highway bridges." Rep. No., 12-26, Washington, D.C.

Nawy, E. G., (2009). "Prestressed Concrete: A Fundamental Approach (5th Ed.)". Prentice Hall.

ODOT. (2016). "Bridge Design Standards & Specifications". Retrieved from Oklahoma Department of Transportation: http://www.okladot.state.ok.us/bridge/2009-sb/brd_std_2009-lrfd-sb-index.php

Parke, G., & Hewson, N. (2008). ICE Manual of Bridge Engineering, 2nd edn. Institution of Civil Engineers, London.

Petersen-Gauthier, J. (2013). Application of the Grillage Methodology to Determine Load Distribution Factors for Spread Slab Beam Bridges (Doctoral dissertation).

Sozen, M. A., Zwoyer, E. M., Siess, C. P., (1959). "Strength in Shear of Beams without Web Reinforcement." Engineering Experiment Station Bulletin, No. 452, University of Illinois, 69 pp.

Suksawang, N., Nassif, H., & Su, D. (2013). "Verification of shear live-load distribution factor equations for I-girder bridges." KSCE Journal of Civil Engineering, 17(3), 550.

Swanson, J. A. and Miller, R. A. (2007), "AASHTO LRFD Bridge Design Specification". Retrieved from University of Cincinnati, Dept. of Civil and Environmental Engineering: https://www.inti.gob.ar/cirsoc/pdf/puentes_hormigon/16-AAC-Load%20Handout-Color.pdf

Turer, A. and Shahrooz, B. M. (2011) "Load rating of concrete-deck-on-steel-stringer bridges using field-calibrated 2D-grid models," Engineering Structures, 33: 1267-1276

TxDOT. (2015). "Bridge Design Manual – LRFD". Retrieved from Texas Department of Transportation: http://onlinemanuals.txdot.gov/txdotmanuals/lrf/lrf.pdf

Yousif, Z. and Hindi, R. (2007) "AASHTO-LRFD Live Load Distribution for Beam-and-Slab Bridges: Limitation and Applicability" J. Bridge Eng., 2007, 12(6): 765-773

Zokaie, T., (2000) “AASHTO-LRFD Live Load Distribution Specification.” J. Bridge Eng., 2000, 5(2): 131-138